CERTIFICATO DI FIRMA DIGITALE

Si certifica che questo documento informatico

phd_unisi_-076886.pdf

composto da n°136 pagine

È stato firmato digitalmente in data odierna con Firma Elettronica Qualificata (FEQ), avente l'efficacia e gli effetti giuridici equivalenti a quelli di una firma autografa, ai sensi dell'art. 2702 del Codice Civile e dell'art. 25 del Regolamento UE n. 910/2014 eIDAS (electronic IDentification Authentication and Signature).

PROCESSI INFORMATICI COMPLETATI

- **Apposizione di Firma Elettronica Qualificata Remota** emessa da Intesi Group S.p.A. in qualità di prestatore di servizi fiduciari qualificati autorizzato da AgID, per garantire con certezza l'autenticità, l'integrità, il non ripudio e l'immodificabilità del documento informatico e la sua riconducibilità in maniera manifesta e inequivoca all'autore, ai sensi dell'art. 20 comma 2 del CAD - D.lgs 82/2005.
- **Apposizione di Marca Temporale Qualificata** emessa da Intesi Group S.p.A. in qualità di prestatore di servizi fiduciari qualificati autorizzato da AgID, per attribuire una data e un orario opponibile a terzi, ai sensi dell'art. 20 comma 3 del CAD - D.lgs 82/2005 e per far sì che la Firma Elettronica Qualificata apposta su questo documento informatico, risulti comunque valida per i prossimi 20 anni a partire dalla data odierna, anche nel caso in cui il relativo certificato risultasse scaduto, sospeso o revocato.
- **Apposizione di Contrassegno Elettronico**, l'unica soluzione tecnologica che permette di prorogare la validità giuridica di un documento informatico sottoscritto con firma digitale e/o marcato temporalmente, rendendolo inalterabile, certo e non falsificabile, una volta stampato su supporto cartaceo, ai sensi dell'art. 23 del CAD - D.lgs 82/2005.

  Per risalire all'originale informatico è necessario scansionare il Contrassegno Elettronico, utilizzando l'applicazione HONOS, disponibile per dispositivi Android e iOS.

FIRMATO DIGITALMENTE DA:
Nome: ANGELA
Cognome: LEO
Data: 18 febbraio 2021

UNIVERSITÀ
DI SIENA
1240

Università degli Studi di Siena

Department of Biotechnology, Chemistry and Pharmacy

Research Doctorate in Biochemistry and Molecular Biology
BIBIM2.0

Cycle XXXIII

Coordinator: Prof. Lorenza Trabalzini

The study of cell motility and plasticity in cancer: the role of the crosstalk between BM-MSCs and tumor in osteosarcoma progression and Claisened Hexafluoro as potential inhibitor of amoeboid motility in metastatic melanoma

Scientific-disciplinary sector: BIO/10

PhD student: **Angela Leo**

Supervisor: **Prof. Maria Letizia Taddei**

Academic year 2019/2020

Table of contents

1. Abstract 1

2. Introduction 3

2.1 Hallmarks of Cancer 3

2.2 Cancer metabolism 3

2.2.1 The major metabolic pathways 7

2.2.2 Metabolic oncogenes 9

2.2.3 Reactive oxygen species (ROS) 13

2.2.4 AMP-activated protein kinase (AMPK) signaling 17

2.3 Cell motility and plasticity 18

2.3.1 Mesenchymal motility 22

2.3.2 Amoeboid motility 23

2.3.3 Tumor cell plasticity 24

2.4 Metastatic dissemination 26

2.4.1 Local infiltration and detachment from the primary tumor mass 27

2.4.2 Dissemination (intravasation) 29

2.4.3 Circulation survival (resistance to anoikis) 29

2.4.4 Adhesion to the endothelium and trans-endothelial migration (extravasation) 32

2.4.5 Survival at the new site and development of metastasis 32

3. Part 1 34

3.1 Osteosarcoma 34

3.1.1 Bone marrow-mesenchymal stem cells (BM-MSCs) 36

3.1.2 Role of BM-MSCs in neoplastic progression 37

3.2 Aim of the project 39

3.3 Results 40

3.3.1 BM-MSCs show significant tropism for OS cells-derived conditional medium and strongly affect the metastatic potential of cancer cells. 40

3.3.2 BM-MSCs acquire a CAF-like phenotype after contact with OS cells. 42

3.3.3 The crosstalk between BM-MSCs and OS leads OS cells towards an amoeboid motility. 45

3.3.4 GRO-a, IL-6, IL-8 and MCP-1 produced by BM-MSCs determine the migration plasticity of OS cells 50

3.4 Discussion 53

4. Part 2 56

4.1 Malignant melanoma 56

4.2 Honokiol (HNK) 59

4.2.1 A Honokiol analogue: Claisened Hexafluoro 62

4.3 Aim of the project 63

4.4 Results 65

4.4.1 Claisened Hexafluoro inhibits amoeboid motility and invasion ability 65

4.4.2 Claisened Hexafluoro decreases adhesion ability and trans-endothelium migration of A375M6 cells 67

4.4.3 Claisened Hexafluoro inhibits the stemness features of A375M6 cells 69

4.4.4 Claisened Hexafluoro inhibits the mitochondrial activity and ATP production 70

4.4.5 Claisened Hexafluoro affects AMPK signalling 73

4.4.6 Claisened Hexafluoro decreases the in vivo lung metastasis formation *74*

4.5 Discussion **76**

5. Materials and Methods **79**

5.1 Materials **79**

5.1.1 Isolation and culture cell *79*

5.1.2 Preparation of conditioned media (CM) *79*

5.2.2 3D invasion assay *82*

5.2.3 Western blotting *82*

5.2.4 RhoA and Rac1 activity assays *83*

5.2.2 Confocal analysis *83*

5.2.3 Flow Cytometric Analysis *84*

5.2.4 ELISA and cytokine antibody array *84*

5.2.5 RT-qPCR *85*

5.2.6 Cell migration in three-dimensional collagen matrices *85*

5.2.7 Cell viability assay *86*

5.2.8 Adhesion assay *86*

5.2.9 Melanospheres formation *86*

5.2.10 Seahorse XFe96 Metabolic Assays *87*

5.2.11 Lactate quantification assay *87*

5.2.12 ADP/ATP quantification assay *87*

5.2.13 Lung colonization assay *87*

5.2.14 Statistical analysis *88*

6. References **89**

1. Abstract

Part 1

Growing evidence suggest that bone marrow-derived mesenchymal stem cells (BM-MSCs) are key players in tumor stroma. Here, we investigated the cross-talk between BM-MSCs and osteosarcoma (OS) cells in tumor progression.

We revealed a strong tropism of BM-MSCs towards these tumor cells and identified monocyte chemoattractant protein (MCP)-1, growth-regulated oncogene (GRO)-α and transforming growth factor (TGF)-β1 as pivotal factors for BM-MSC chemotaxis. Once in contact with OS cells, BM-MSCs trans-differentiate into cancer-associated fibroblasts, further increasing MCP-1, GRO-α, interleukin (IL)-6 and IL-8 levels in the tumor microenvironment. These cytokines promote mesenchymal to amoeboid transition (MAT), driven by activation of the small GTPase RhoA, in OS cells, as illustrated by the *in vitro* assay and live imaging.

The outcome is a significant increase of aggressiveness in OS cells in terms of motility, invasiveness and trans-endothelial migration. In keeping with their enhanced trans-endothelial migration abilities, OS cells stimulated by BM-MSCs also sustain migration and invasion. Thus, BM-MSC recruitment to the OS site and the consequent cytokine-induced MAT are crucial events in OS malignancy.

Part 2

Metastatic melanoma is one of the most aggressive and lethal malignancies with a poor prognosis. Melanoma cells are able to migrate using different types of cell motility such as the rounded/amoeboid-type motility and the elongated/mesenchymal-type motility thanks to their high plasticity. Really several data underline the crucial role of amoeboid motility in the dissemination process of highly metastatic melanoma cells. Thus, targeting this process could be a promising strategy to prevent the metastatic spreading of melanoma cells.

Claisened Hexafluoro is a chemical analog of Honokiol (HKL), a biphenolic compound derived from *Magnolia officinalis* which has antitumoral and antimetastatic effect in numerous cancers, including melanoma.

Starting from these evidence, here we tested Claisened Hexafluoro on human metastatic melanoma cells, as an inhibitor of amoeboid motility. Data here reported demonstrate that Claisened Hexafluoro, impairing mitochondrial activity and affecting AMP-activated protein kinase (AMPK) signaling, strongly inhibits amoeboid motility and many steps of the disseminating process *in vitro* as well as *in vivo,* confirming its possible future application to fight metastatic spreading of melanoma cells.

2. Introduction

2.1 Hallmarks of Cancer

Cancer is a generic term for a large group of diseases that are characterized by cells endowed with abnormal growth and the potential to invade and spread to other parts of the body. Cancer is the second cause of death worldwide, after cardiovascular diseases, accounting for 8.2 million deaths in 2015 [1].

Carcinogenesis is a progressive process during which successive genetic alterations induce a sequence of cellular and molecular events that promote the transformation of a normal cell into a cancer cell. These events consist in the acquisition of specific features summarized by Hanahan and Weinberg as the "Hallmarks of cancer" [2]. Nowadays, the acknowledged hallmarks are ten: self-sufficiency in growth, insensitivity to growth-inhibitory signals, evasion of programmed cell death (*apoptosis*), limitless replicative potential, sustained angiogenesis, and tissue invasion and metastasis, genomic instability and mutations (necessary for the acquisition of such traits), tumor promotion inflammation, avoid immune destruction and reprogramming of energy metabolism [3].

Among these, one of the hallmarks that has become of great interest for studying the mechanisms of tumor survival, growth and resistance to therapies, is the cancer metabolism. Multiple molecular mechanisms that converge to alter core cellular metabolism, providing support for the basic needs of dividing cells. Moreover, growing evidence indicates that several of mentioned hallmarks are under metabolic control, suggesting the importance of metabolic characterization for the development of new therapeutic approaches against cancer [4].

2.2 Cancer metabolism

Since1920s Warburg demonstrated that tumor cells convert large amount of glucose in lactate, even in presence of oxygen. This metabolic phenotype, observed in tumor cells, consists in a shift from oxidative phosphorylation (OXPHOS) to glycolysis to generate adenosine triphosphate (ATP), nowadays it is known as the "Warburg effect" or "aerobic glycolysis" [5]. Although ATP production by glycolysis can be faster than by OXPHOS, ATP generated per unit of glucose is significantly lower. Indeed, each molecule of glucose,

through lactate fermentation pathway, produces only 2 ATPs, whereas OXPHOS generates up to 36 ATP. The glycolytic switch therefore needs that tumor cells increase glucose uptake in order to respond to their energetic, biosynthetic and redox requirements.

This apparent waste of energy in proliferating cancer cells using glycolysis preferentially to OXPHOS, even in the presence of oxygen, led Warburg to hypothesize that increased aerobic glycolysis in tumor cells was due to defects in mitochondrial respiration function, and that aerobic glycolysis was a necessary adaptation to the lack of ATP [6]. However, subsequent studies demonstrated that the mitochondrial functionality is not impaired in most tumor cells [7] (Fig. 1).

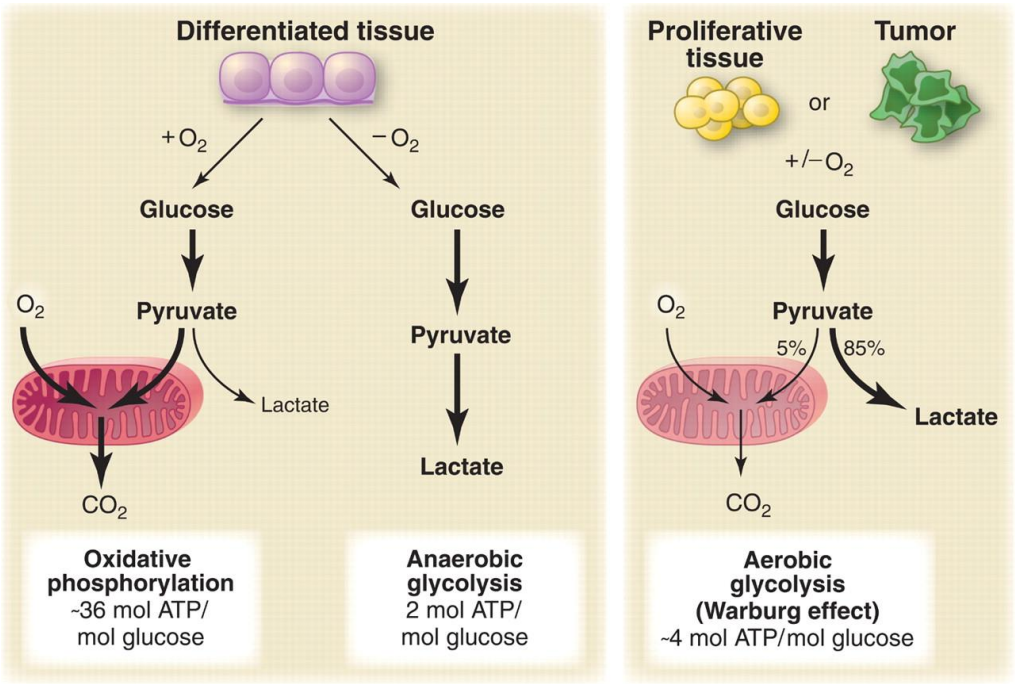

Figure 1. The differences between oxidative phosphorylation, anaerobic glycolysis, and the Warburg effect (Vander Heiden MG, Cantley LC, and Thompson CB, Science, 2009).

This phenomenon raises the question of why a less efficient metabolism, at least in term of ATP production, would be selected in tumor cells.

There are several explanations for the glycolytic switch: first of all, tumor cells must respond to important metabolic requirements that go beyond simple ATP demand. Indeed, they need nucleotides, amino acids and lipids to maintain their high proliferative rate. Thus, metabolic reprogramming can be exploited to support the biosynthesis of these macromolecules. Second, glucose and glutamine are main metabolic requirements for

cancer cells, as they supply most of the carbon, nitrogen, free energy and the reduced form equivalent necessary to support cell growth and division [8]. Therefore, in proliferating cells, glucose is not fully oxidized to CO_2 via OXPHOS, rather, glucose is mainly driven to the synthesis of macromolecular precursors, such as acetyl-coA for fatty acids, glycolytic intermediates for nonessential amino acids and ribose for nucleotides. Thus, although ATP hydrolysis provides free energy for some of the biochemical reactions responsible for replication of the biomass, cells cannot use glucose only for ATP production during growth and cell division since they have to generate intermediates for biosynthesis and biomass. In addition, in the case a high rate glycolysis would serve only to produce ATP, the increase in the ATP/adenosine diphosphate (ADP) ratio would severely impair the flux through glycolytic intermediates, limiting the production of acetyl-CoA and nicotinamide adenine dinucleotide phosphate hydrogen (NADPH) required for macromolecular synthesis. Excessive lactate production, that accompanies the Warburg effect, would appear as an inefficient use of cellular resources and a waste of three carbons that might otherwise be utilized for ATP production or macromolecular biosynthesis. A possible explanation of this phenomenon is that the release of lactate allows faster incorporation of carbon into biomass, which facilitates a quick turnover of the cells [9] (Fig.2).

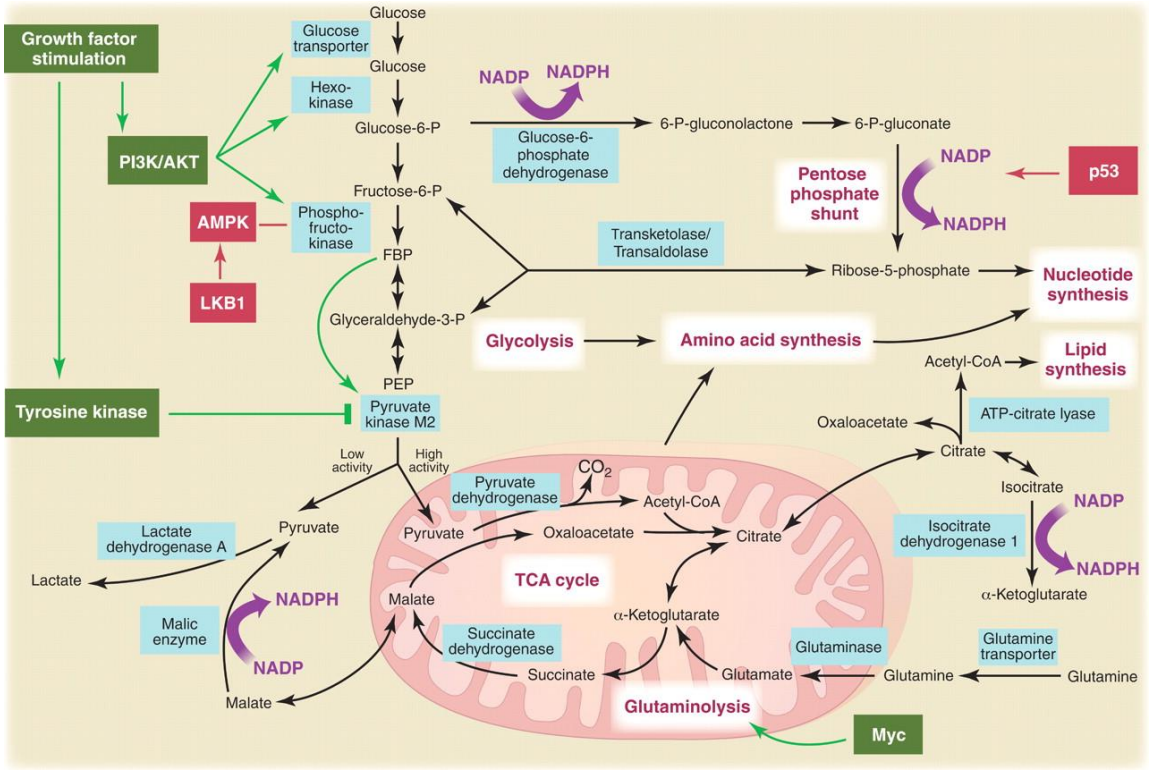

Figure 2. Glycolysis, oxidative phosphorylation, the pentose phosphate pathway, and glutamine metabolism in proliferating cells (Vander Heiden MG, Cantley LC, and Thompson CB, Science, 2009.

Although the traditional view of cancer metabolism is that cancer cells are dependent on aerobic glycolysis, it has been shown that they have a broad spectrum of bioenergetic states, ranging from a predominance of aerobic glycolysis to a predominance of OXPHOS to adapt to rapidly changing microenvironments. As already mentioned, the Warburg effect plays a vital role in cancer cell proliferation and survival [9]. A good example of this metabolic flexibility inhabits in the concept of "metabolic symbiosis" between cancer cells. *Sonveaux et al*. in 2008 showed that in the tumor *milieu* exists different populations of cancer cells that adapt to the relative abundance of oxygen and nutrients [10]. Properly oxygenated cancer cells at the tumor edge rely on OXPHOS for energy production. They use lactate produced from hypoxic cells resident in the tumor core, instead of glucose, as a main metabolic fuel, so sparing glucose for the hypoxic core. On the contrary, lactate produced by the hypoxic population of cells is used as an oxidative fuel by well-oxygenated cells. The expression of different lactate transporters defines this symbiosis, and it has been reported that glycolytic cancer cells normally express lactate transporter monocarboxylate transporter 4 (MCT4) (optimized for lactic acid extrusion) [11], whereas

oxidative cancer cells mostly express monocarboxylate transporter 1 (MCT1), which is optimized for lactate uptake [12].

Accordingly, *Lisanti* and colleagues in 2009 proposed a complementary model. Cancer-associated fibroblasts (CAFs) can also employ aerobic glycolysis. It is induced by cancer cells that produce reactive oxygen species (ROS), and results in the production of energy-rich metabolites (such as lactate and ketone bodies) that can be taken from the cancer cells and can be fuel the tricarboxylic acid (TCA) cycle, resulting in high ATP production via OXPHOS. Basically, the stromal fibroblasts are forced to feed cancer cells via the transfer of high-energy metabolites. This interplay between CAFs and cancer cells is termed "The Reverse Warburg Effect" [13] and includes a mutual metabolic reprogramming. CAFs acquire a Warburg metabolism and undergo mitochondrial stress as a result of contact with cancer cells. Intracellular contact activates CAFs, triggering increased expression of glucose transporter 1 (GLUT1), lactate production and extrusion of lactate by *de novo* expressed MCT4. Contrariwise, cancer cells, upon contact with CAFs, are reprogrammed toward an aerobic metabolism, with a decrease of GLUT1 expression and an increase in lactate uptake *via* MCT1. Metabolic reprogramming of both stromal and cancer cells is under the stringent control of hypoxia inducible factor-1 (HIF-1) [14,15]. The theory suggests that cancer cells induce oxidative stress in adjacent fibroblasts, which in turn induces the autophagic program via the activation of HIF-1 and nuclear factor kappa-light-chain-enhancer of activated B cells (NF-kB). During autophagy, the cellular components are destroyed by lysosomal degradation, leading to the production of recycled nutrients to feed cancer cells. Mitophagy further promotes aerobic glycolysis in CAFs [16].

2.2.1 The major metabolic pathways

Cancer cells must activate or enhance metabolic pathways in order to achieve and sustain the proliferative capacity [17]. The major metabolic pathways involved in cancer cell anabolism, maintenance and biosynthesis will be described below.

Glucose

As described above, the cancer cells drive glucose catabolism through Warburg metabolism, promoting lactate production. Lactate is carried out of cells by MCT4, which is target for cancer therapy, since it is essential to sustain glycolysis in cancer cells [18].

Moreover, pyruvate, derived from glucose, contributes to the synthesis of the aspartate and asparagine and the synthesis of acetyl-CoA, involved in fatty acid, cholesterol and lipid synthesis. By oxidative action of glucose 6 phosphate dehydrogenate (G6PD), glucose became glucose 6-phosphate (G6P) first metabolite of the pentose phosphate pathway (PPP), which generates the ribose groups for the synthesis of nucleotides. The PPP is also a major pathway for NADPH generation, most important in the redox pathway [19]. Finally, 3-phosphoglycerate (3PG) is the branching point for the synthesis of the amino acid serine (discussed deeply below). Serine donates one-carbon units to the folate cycle, producing glycine. Glycine, in turn, acts as a precursor for the synthesis of purine and glutathione (GSH), essential for redox pathway [20].

Glutamine

Glutamine is the most abundant circulating amino acid in humans [21]. The anaplerotic role of glutamine has been shown to sustain the anabolic metabolism of cultured cancer cells derived from various tissues, as well as glutaminases (GLS) is identified as a potential therapeutic target for tumors addicted to glutamine [22,23]. A high percentage of glutamine is generally deaminated and released into the medium as glutamate [21,24]. Glutamate is converted into α-ketoglutarate (αKG), by glutamate dehydrogenase (GDH) or transaminases, that contributes to the replenishing of TCA cycle, both oxidatively (to succinyl- CoA) and reductively (to citrate). Moreover, citrate derived from αKG through reductive carboxylation has been reported to be crucial for growth of cancer cells with mitochondrial defects [25].

One-carbon metabolism

Serine is a non-essential amino acid most consumed by cancer cells [21,26]. The first step of its biosynthesis is catalyzed by 3PG dehydrogenase (PHGDH), this enzyme is found genetically amplified in breast cancers [27] and melanoma [28]. Serine is mostly converted into glycine [29,30] through serine hydro methyltransferases (SHMT1 and SHMT2), releasing a one-carbon unit to the one-carbon pool. Also the glycine could contribute to the one-carbon pool, but, in cancer cells, serine is the major donor [31]. The one-carbon unit donated by serine is utilized in the biosynthesis of thymidine monophosphate (dTMP) and purines. The one-carbon stock for dTMP synthesis is generated in the cytosol in a cyclical pathway involving SHMT1, thymidylate synthase (TYMS) and the co-enzyme folate in the form of dihydrofolate (DHF) and tetrahydrofolate (THF) [32]. Instead, for purine synthesis, the one-

carbons are generated in the mitochondria via SHMT2 [33]. High SHMT2 drive cancer cell growth [34,35]. In conclusion one-carbon metabolism could be a new target for anticancer therapy.

ROS. It will be discussed deeply below.

2.2.2 Metabolic oncogenes

The metabolic phenotype of cancer cells is controlled by intrinsic genetic mutations and the crosstalk with the tumor environment. Oncogenic signaling pathways are activated by the loss of activity of tumor suppressors or the unregulated activation of oncoproteins. These altered signals modify cellular metabolism to reach the requirements for cell division [4]. Therefore, it is not surprising that several known oncogenes also modify the metabolic activity of cancer cells. The most frequent mutations occur in the following genes:

- **p53**.The transcription factor and tumor suppressor p53 is known for its role in the response to DNA damage and apoptosis, but it also plays an important role as regulator of cell metabolism. In over 50% of human tumors, p53 is mutated, mostly for a loss of function. The expression of mutant p53 increased glucose uptake, glycolytic rate and lactate production [36–38]. P53 is involved in the regulation of both glycolysis and oxidative phosphorylation. It can intervene on several genes and mechanism: p53 inhibits the expression of the glucose transporters GLUT1 and GLUT4 [39]; decreases the levels of phosphoglycerate mutase (PGM) [40] while increases the expression of TP53-induced glycolysis and apoptosis regulator (TIGAR), an enzyme that decreases the levels of glycolytic activator fructose-2,6-bisphoshate and thus reduces glycolysis and diverts glucose catabolism to the PPP [41]. *Zhang et al.* showed that p53 mutant forms, in lung carcinoma, promote GLUT1 and GLUT4 translocation on the cell membrane through RhoA/Rho-associated protein kinase (Rock) activation. While, the inhibition of the RhoA/Rock/GLUT1 axis abolished Warburg effect mediated by mutant p53 [42].

  Moreover, p53 modulating the nuclear factor-κb (NF-κb) pathway can also indirectly regulates glycolysis [43], it limits the activity of Iκb kinase-α (IKKα) and IKKβ, decreasing the activation of NF-κb and thereby the expression of glycolysis-

promoting genes such as GLUT3 [44]. *Matoba et al*., in 2006, have been reported that, even if p53 activates the expression of hexokinase 2 (HK2), it inhibits the glycolytic pathway by upregulating the expression of TIGAR [45]. p53 supports the expression of phosphatase and tensin homolog (PTEN) by binding to PTEN promoter [46], which inhibits the phosphatidylinositol 3-kinase (PI3K) pathway, thereby decrease glycolysis. Recently, *Wang L. et al*. have demonstrated that in prostate cancer cells the loss of p53 and PTEN determines an increase of HK2 expression, contributing to aerobic glycolysis [47]. Additionally, p53 affects energy metabolism by regulating AMP-activated protein kinase (AMPK), kinase mammalian target of rapamycin (mTOR), PTEN and insulin-like growth factor binding protein 3 (IGFBP3) [48]. Furthermore, p53 suppresses the transcription of MCT1 to inhibit the carriage of lactate out of cancer cells. Higher expression of MCT1 in p53-deficient cancer cells adapts these cells to metabolic needs by facilitating lactate export or import depending on the glucose availability [49].

- **AMPK**. It will be discussed deeply below.
- **c-MYC**. MYC proteins are a small family of oncoproteins, among these, c-MYC, N-MYC, L-MYC have been involved in the genesis of several human tumors [50,51]. Their expression, in normal cells, is strictly controlled by growth factor-dependent signals; whereas in tumor cells is deregulated and enhanced through many mechanisms. Numerous evidence demonstrate clearly that enhanced MYC expression is a major driving force of tumorigenesis [52–55]. c-MYC has several important effects on cell metabolism. Oncogenic levels of c-Myc, both in Burkitt's lymphoma [56,57] and in liver carcinoma [58] promote high consumption of glucose. Indeed Myc controls cell growth and proliferation and collaborate with HIF-1 for the activation of several glucose transporters and glycolytic enzymes, including GLUT1, HK2, phosphofructokinase (PFK), enolase, lactate dehydrogenase A (LDHA) and pyruvate dehydrogenase kinase 1 (PDK1) [59]. c-MYC also promotes, through the upregulation of glutamine transporters SLC5A1 and SLC7A1, the use of glutamine in cancer cells [60]. Aerobic glycolysis is regulated by pyruvate kinase isoform M2 (PKM2), which is expressed almost in all tumors [61]. In glioma cells, has been demonstrated that MYC enhances expression of PKM2 by promoting the expression of hnRNP splicing factors [62,63]. Moreover, nicotinamide adenine

dinucleotide (NAD^+) is reduced to nicotinamide adenine dinucleotide hydrogen (NADH) + H^+ during glycolysis, and cells need to regenerate NAD^+ to maintain the glycolytic flux. LDHA utilizes pyruvate as substrate derived from both the glycolytic and the glutaminolytic pathway and converts it into lactate generating NAD^+ [64,65]. Overexpressing of MYC increases LDHA expression and typically results in extracellular acidification due to the increased production of lactate [64,66–68]. MYC also promotes the secretion of lactate through the expression of MCT1 [69]; lactate, in turn, has several and well known oncogenic effects [70].

- **PI3K**. The PI3K pathway is often modified in cancer cells. This pathway is activated by mutations of tumor suppressor genes (such as PTEN), and its activation provides strong growth, survival signals and alteration in cell metabolism. Protein kinase B (PKB or AKT1) is the most studied downstream effector of PI3K. It stimulates glycolysis activating key glycolytic enzymes, such HK and PFK2, and increasing the expression of glucose transporters. AKT1 signaling inhibits Forkhead box protein O1 (FOXO1) transcription factor resulting in an increased cells glycolytic capacity [71] and stimulates mTOR. Activation of mTOR induces protein and lipid synthesis and cell growth in response to nutrient and energy availability [72], and activates transcriptional factors, such as HIF-1, even under normoxic conditions.
- **HIF-1**. HIF-1 is a heterodimeric transcription factor that consists of 2 subunits: HIF-1α, that is O2-regulated and HIF-1β, constitutively expressed. HIF-1, through the activation of transcription of genes encoding for glucose transporters and glycolytic enzymes, plays a key role in reprogramming cancer metabolism. In normoxic conditions, HIF-1α is hydroxylated by prolyl hydroxylase domain protein 2 (PHD2), which uses O_2 and αKG as substrates. Then, von Hippel-Lindau tumor suppressor protein (VHL) binds prolyl-hydroxylated HIF-1α and recruits an E3-ubiquitin ligase that marks HIF-1α for proteasomal degradation. Under hypoxic conditions, prolyl-hydroxylation reactions are inhibited by O_2 deprivation and by the mitochondrial generation of ROS; thus, HIF-1α is rescued from degradation and can migrate into the cell nucleus where it binds to HIF-1β to activate the transcription of its target genes that possess a hypoxia-responsive element (HRE) in their promoter sequence [73,74]. Once activated, HIF-1 promotes the expression of

most glycolytic enzymes and transporters, such us GLUT1 and GLUT3, HK2 (which converts glucose to G6P), LDHA (which converts pyruvate to lactate), MCT4 (which transports lactate out of the cell), PDK (which phosphorylates and inactivates the catalytic domain of pyruvate dehydrogenase) [73]. It is considered to be a main promoter of glycolysis in tumors [75]. HIF-1α can also be activated under normoxic conditions by oncogenes, including PI3K, and by mutations that inactivate tumor suppressor genes, such as VHL, succinate dehydrogenase (SDH) and fumarate hydratase (FH) [76–78]. Accumulation of succinate or fumarate directly inhibits PHD2 activity, thus contributing to normoxic HIF-1α stabilization. The interplay between HIF-1 and metabolism is reciprocal, as it has been shown that lactate itself can directly stabilize HIF-1α in normoxia by inhibiting PHD2 [79].

- **Rat sarcoma (Ras) family**. Ras mutations are important in cancer initiation and progression. K-Ras, the most commonly mutated oncogenic Ras in pancreatic cancer, has been shown to affect the shape and function of mitochondria during fibroblast transformation [80]. Further studies showed that fibroblasts transformed by K-Ras attenuate OXPHOS by suppressing the activity of respiratory complex I, with a corresponding decrease in the expression level of complex I proteins [81]. Similarly, H-Ras-transformed mouse fibroblasts exhibit low mitochondrial respiration and an increased dependency on glycolysis, a sensitivity to glycolytic inhibitors and an insensitivity to OXPHOS inhibitors [82].

  Mutations of Ras pathway was observed in almost 30% of cancers, these alterations leads to a constitutively expression of Ras proteins [83]. Indeed, mutations in KRAS or BRAF play important roles in regulating metabolic reprogramming in several type of cancers such us pancreatic cancer, adenocarcinoma, melanoma and others [84–87]. The colorectal cancer cell lines DLD-1 and RKO, which are mutated respectively in KRAS and BRAF, show increased expression of GLUT1 and exhibit a Warburg effect phenotype [84]. As well as, pancreatic ductal adenocarcinomas, characterized by a KRAS G12D mutation, exhibit increased glucose utilization drove in the PPP [88] and are highly dependent upon glutamine metabolism for tumor growth [85]. Moreover, BRAF V600E mutation in melanoma cells decreased expression of TCA cycle enzymes and mitochondrial oxidative phosphorylation effects reversed by selective kinase inhibitors of BRAF V600E [89].

2.2.3 Reactive oxygen species (ROS)

ROS include a large group of oxygen-derived small molecules that comprises radicals and non-radical species. Radicals such as superoxide ($O_2^{\cdot -}$), the hydroxyl anion ($OH^{\cdot}$) and peroxyls ($RO_2^{\cdot}$) are short-lived, highly electrophilic and reactive molecules with an unpaired electron in their external shell. Non-radical ROS include hypochlorous acid (HOCl), ozone (O_3), singlet oxygen ($^1O_2$) and hydrogen peroxide (H_2O_2). During aerobic metabolism, ROS are constantly generated from oxygen. Mitochondria consumes about 80% of O_2 available during oxidative phosphorylation, contributing the maximum in the generation of ROS ⁵[5,90].

The first step in the formation of these molecules is the transfer of one electron to O_2 to form the anion $O_2^{\cdot -}$, which can then be transformed into H_2O_2 spontaneously or by the activity of SODs. Supplementary steps in the cascade of ROS production include the reaction of $O_2^{\cdot -}$ with nitric oxide (NO) to form peroxynitrite ($ONOO^-$), the peroxidase-catalyzed formation of HOCl from H_2O_2, and the iron-catalyzed Fenton reaction leading to the generation of $OH^{\cdot}$ [91]. Mitochondria and the family of NADPH oxidases (NOXs) are the two main sources of ROS. The three best-characterized sites in the mitochondria are complexes I, II and III. These complexes generate $O_2^{\cdot -}$ by the one-electron reduction of molecular oxygen [92]. In normal cells ROS homeostasis is required for proper cell signaling and cellular fitness. Low doses of ROS indeed promote cell survival, growth, proliferation and angiogenesis. However, higher ROS levels can be toxic to the cells, inducing cell proliferation arrest and even cell death [93]. Thus, the availability of ROS results from the balance between its production from various sources and its clearance by enzymatic and non-enzymatic antioxidants [94]. This equilibrium is allowed by several types of antioxidants which play important roles in ROS homeostasis, such as endogenous molecules (e.g. glutathione, α-lipoic acid, ferritin, coenzyme Q, bilirubin, uric acid); antioxidant enzymes (e.g. catalases [CATs], glutathione peroxidases [GPXs], SODs, glutathione reductase [Gr], Trx and Prx) and dietary natural antioxidants (e.g. β-carotene, tocopherol, ascorbic acid, selenium and polyphenol metabolites) [95].

Cancer cells show a persistent metabolic oxidative stress (a hallmark of many cancers) compared with normal cells, which is mainly due to mitochondrial dysfunction. Indeed,

they are usually subjected to high levels of ROS and aberrant antioxidant levels [93,96]. It is well known that although many cancer cells exhibit high glycolysis rates, they still conserve some mitochondrial oxidative phosphorylation activity [97]. Nowadays, it is well demonstrated that cancer cells use the oxidation of glucose, glutamine and other nutrients coupled to the electron transport chain (ETC) to satisfy part of their energy demand [98,99], with O_2 as the final electron acceptor. Moreover, tumor cells periodically could go under hypoxic conditions which results in increased glycolysis and, correspondingly, decreased oxidative phosphorylation that is caused either directly, or indirectly, by the activation of HIF1α [100,101]. Moreover, oxidative stress in tumor microenvironment, in particular in CAFs, determine the amplification of ROS production feeds back upon cancer cells, inducing DNA damage and aneuploidy, which are characteristic of genomic instability. Therefore, ROS production in the stroma could fuel cancer cell evolution via a process of random mutagenesis [102]. Cancer cells increase rate of ROS production to promote proliferation and aggressiveness. On the other hand, tumor cells produced higher levels of antioxidant proteins to survive [103]. Antioxidant systems in cancer cells are regulated by several factors including nuclear factor erythroid-2-related factor 2 (Nrf2), forkhead homeobox type O family (FoxOs) ataxia telangiectasia mutated (ATM) and apurinic/apyrimidinic endonuclease1/redox factor-1 (APE1/Ref-1). It has been reported in melanoma that cells to sustain metastatic process must have reversible metabolic changes by GSH regeneration in order to endure increased oxidative stress [104]. In castration-resistant prostate cancer (CRPC) increase of antioxidants like Trx1 has been associated with tumor progression. Whereas the Trx1 inhibition determines an increase in tumor suppressor p53 levels and cell death due to higher ROS levels [105].

Thus, the role of ROS in cancer is bilateral: moderate levels of ROS contribute to cancer initiation, progression and spreading through the activation and maintenance of signaling pathways that regulate cellular proliferation, survival, angiogenesis and metastasis [93], altering different signaling pathway such us p53 loss [106] and constitutive activation of RAS down streaming (PI3K/AKT/mTOR) [48,107]. However, excessive levels of ROS can also induce cell cycle arrest, cell death signaling and senescence [93], as well as mitochondrial DNA damage and mutations and alterations of the mitochondrial genomic functions that seem to be implicated in the process of carcinogenesis [108]. In order to survive under stress conditions, cancer cells adapt and acquire different mechanisms to maintain ROS levels as

close as possible to their pro-tumorigenic concentration. More specifically, the increased rate of ROS production in cancer cells promotes the acquisition of various hallmarks of cancer: sustained proliferation, increased cell survival and disruption of cell death signaling, epithelial to mesenchymal transition (EMT), angiogenesis and metastasis [109].
Several biological features of cancer cells are affected by ROS, including:

- *Cell proliferation*. ROS promote cancer cell proliferation by increasing proliferative signaling pathways like PI3K/AKT/mTOR and mitogen-activated protein kinases/extracellular signal–regulated kinases (MAPK/ERK) cascades [110]. H_2O_2 oxidizes and inactivates phosphatases, such as protein tyrosine phosphatase 1B (PTP1B) and PTEN, which both inhibit the PI3K/AKT pathway [111,112]. Moreover, ROS also inactivate phosphatases inhibiting MAPK, thus resulting in the activation of mitogen signaling [113].

- *Cell survival*. Hyper-activation of the PI3K/AKT pathway by ROS can promote cancer cell survival through inhibition of PTEN [114]. ROS can also activate and stabilize antioxidant regulator Nrf2, protecting cells against oxidative stress, cell death and senescence [115].

- *Anoikis resistance.* Cancer cells often enter in the bloodstream, but only few of them are able to survive without anchorage-dependent prosurvival signaling, and then, to induce metastatic spread; this particular skill is called "*anoikis resistance*". During the invasive process, cancer cells are exposed to different stresses, such as a loss of interaction with their environment, that can trigger *anoikis*. Mechanisms adopted by cancer cells, to overcome *anoikis* include: (i) overexpression of neurotrophin receptor TrkB [116] which can be upregulated directly by HIF-1 [117] and can regulate vascular endothelial growth factor (VEGF) expression via HIF1 [118]; (ii) c-Met signaling, which supports anchorage independence [119]; (iii) HIF signaling, that increases the metastatic potential of cancer cells by promoting cell survival in the bloodstream and in metastatic colonies [117]; (iv) Src family kinases, critically involved in the control of cytoskeletal organization and in the generation of integrin-dependent signaling that is triggered by cell attachment to the ECM [120]; moreover, Src has been described as playing a key role in *anoikis* resistance, and its redox sensitivity has an essential role in this function [121]. Indeed, in metastatic

prostate carcinoma cells undergoing a constitutively deregulated production of ROS, Src kinase is constitutively oxidized and activated in the absence of adhesion. This allows a constitutive, Src-dependent and ligand-dependent, transphosphorylation of epidermal growth factor receptor (EGFR), activating the ERK- and AKT-mediated pro-survival pathways. Antioxidant treatment of prostatic cancer cells totally abolishes the ligand-independent activation of EGFR and reestablishes the pro-apoptotic *stimuli*. Contrariwise, addition of H_2O_2 physiological doses to normal epithelial cells allows them to escape from *anoikis*, confirming the central role of ROS in *anoikis* resistance [122].

- *Metastasis.* Mithochondrial- (mt) ROS have been shown to promote metastasis formation by upregulating several redox-sensitive pathways, including proline-rich tyrosine kinase 2 (Pyk2), two members of the transforming growth factor β (TGFβ) signaling pathway [123]. Furthermore, ROS further induce HIF-1α stabilization, which in turn is related to various key steps of the metastatic cascade and selects for metastatic modifications [124].

- *Angiogenesis*. Angiogenesis is important for tumor development insofar as it provides nutrients and oxygen for continuous tumor growth. ROS induce HIF-1α stabilization through inhibition of PHDs, which leads to increased VEGF expression and subsequent angiogenesis and tumor progression [125].

- *Epigenetics*. In addition to genetic mutations, also epigenetic changes are involved in tumor progression and metastasis. For instance, hypermethylation of CpG islands in promoter regions of tumor suppressor genes is frequently seen in cancer cells [126,127]. *Lim et al*. confirmed that prolonged ROS stress induces the methylation of the E-cadherin promoter via a Snail-dependent pathway. Remarkably, redox stress seems to be associated with Snail upregulation, methylation of the E-cadherin promoter and its downregulation [128].

2.2.4 AMP-activated protein kinase (AMPK) signaling

AMPK is a serine/threonine protein kinase consisting in a heterotrimeric complex containing one catalytic α-subunit and two regulatory β- and γ-subunits [129]. In mammals, AMPK α- and β-subunits have two isoforms each, whereas the γ-subunit has three isoforms. Suggesting several AMPK active isoforms, all regulated differently under different physiological conditions [130,131]. AMPK is regulated allosterically and by post-translational modifications. Mainly, AMPK activation is regulated both by phosphorylation on threonine residue (Thr-172) of the α-subunit and by adenosine monophosphate (AMP) and/or ADP binding to γ-subunit [132]. The binding of AMP and ADP to the γ-subunit is competitively inhibited by ATP, thus, resulting in AMPK as a sensor of AMP/ATP or ADP/ATP ratios. Phosphorylation in Thr-172 of the AMPK α-subunit is regulated by three kinases: calcium-/calmodulin-dependent kinase kinase 2 (CaMKK2); TGFβ-activated kinase 1 (TAK1); liver kinase B1 (LKB1); and by three phosphatases: protein phosphatase 2C (PP2C); protein phosphatase 2A (PP2A) and Mg2+-/Mn2+-dependent protein phosphatase 1E (PPM1E) [133–140].

AMPK is active when is phosphorylated by upstream kinases at Thr-172 in response to cellular stresses that reduce cellular energy levels [141]. AMPK is activated under situations in which the cellular level of ATP is depleted (such as hypoxia and tissue ischemia), and the level of AMP is increased (with subsequently increase of the AMP/ATP ratio) such as those triggered by glucose deprivation, hypoxia, oxidative stress, hyperosmotic stress, tissue ischemia and muscle contraction/exercise [142,143]. Indeed, high levels of AMP and ADP bind CBS3, a region on the γ-subunit, which avoids the access to Thr-172 to phosphatases, increasing its phosphorylation. Furthermore, AMP could bind to CBS3, stimulating LKB1-mediated phosphorylation, which requires myristylation of the AMPK β-subunit [144]. Moreover, the binding of AMP, but not of ADP, to the CBS1, γ-subunit segment, increases intrinsic AMPK activity by causing its allosteric activation. Finally, intracellular calcium through CaMKK2-mediated phosphorylation and TAK1, a MAPKKK family member (MAP3K7) also phosphorylate and activate AMPK; although, the physiological conditions under which the TAK1–AMPK pathway operates remain to be clarified [145,146]. Once activated, AMPK reestablishes cellular energy levels by stimulating catabolic pathways, such as glucose uptake, glycolysis and fatty acid oxidation [147] and

limits ATP-consuming cellular events including synthesis of protein, cholesterol and fatty acids [148,149].

Certainly, AMPK acts as a crucial sensor of the cellular energy balance in mammalian cells, regulates glucose and lipid metabolism by contrasting the effect of AKT1 and functions as a potent inhibitor of mTOR [150,151]. Moreover, recent studies have implicated AMPK as an important factor in cancer cell growth and migration [152,153]. Cancer cells must overcome this checkpoint in order to proliferate in response to activated growth signaling pathways, even in periods of energetic stress. Several oncogenic mutations can suppress AMPK signaling, allowing cancer cells to respond to inappropriate and aberrant growth signals. In particular, loss of AMPK signaling promotes the activation of mTOR and HIF-1 and might therefore also support the glycolytic shift [151].

2.3 Cell motility and plasticity

Cell migration is a universal process that involves different mechanisms based on the type of cell and the characteristics of the microenvironment in which it happens. These phenomena not only occur during the processes of invasion and metastasis of tumor cells, but also is important during physiological processes such as embryo-morphogenesis, wounds repair, angiogenesis as well as during immune responses, moreover with mechanisms similar to those used by cancer cells [154]. For many cells, including epithelial, stromal, and neuronal cells, migration occurs only in some phases of cellular differentiation, during morphogenesis or tissue regeneration. On the other hand, for other cell types, such as leukocytes, migration is an integral part of their functionality and they maintain this ability throughout lifelong [155].

There are several migration strategies, principally divided into two main groups: single cell motility (mesenchymal or amoeboid) and collective motility as multicellular groups. Then it is possible to classify migration on the basis of cell morphology, adhesion [156–158] and contractility ability [159,160], Rho-family GTPase signalling activity [161,162], cytoskeletal organization, composition and rigidity of extracellular matrix (ECM) [163,164] and the types of cell-ECM and cell-cell interaction [155]. Changes in some of these factors can induce switches in style of migration. This plasticity allows the cells to continue to migrate in response to changes in their environment.

Collective motility

Collective motility occurs in fundamental physiological processes such as the formation of embryonic sheets and glandular epithelia [154].

Several studies have demonstrated that collective movement could be considered as the movement of a single functional unit in which cells remain adherent each other thanks to the establishment of cortical actin junctions that allow the formation of a single contractile body [165]. Thus, cells could form groups in which they are held together by cadherins, molecules of the immunoglobulin superfamily and connexins through gap junctions [154,166,167] (Fig 3B).

The cellular complex moves through the formation of pseudopods that generate traction forces and push forward, degrading the matrix with the production of matrix metalloproteases (MMPs), especially MMP 1 and 2, and co-localizing clusters of integrins α1β3 adhered to collagen fibers to "stick" to the ECM and to perform the movement [168].

Single cell motility

The single-cell migration outcomes from five interdependent molecular steps that alter shape and position of the cells as well as the tissue structure towards which they migrate and are valid in many types of cell movement for both normal and neoplastic single cells [155,169,170]. During the first step, thanks to the actin polymerization, the cytoskeleton polarizes and forms a leading protrusion at the opposite end of a ‘‘pre-uropod’’ region, which characterizes the constitutive rear end of the cell [171,172]. In the second step, it is coupled the extracellular adhesion to the force generation at the leading-edge protrusion through engagement of extracellular substrates, followed by the recruitment and adhesion of cell surface receptors that form focalized clusters [173]. In the third step, cell surface proteases bind extracellular scaffold proteins and induce locally proteolysis [155]. Proteolysis modifies the molecular and mechanical properties of the tissue and leaves space for the movement of the cell [173]. In the fourth step, the small GTPase Rho activates myosin II, and the contraction, mediated by actomyosin, generates tension inside the cell. Finally, in the last step, after the contraction, there is a gradual turnover of adhesion bonds at the trailing edge, which slides forward while the leading edge further protrudes [173] (Fig. 3A).

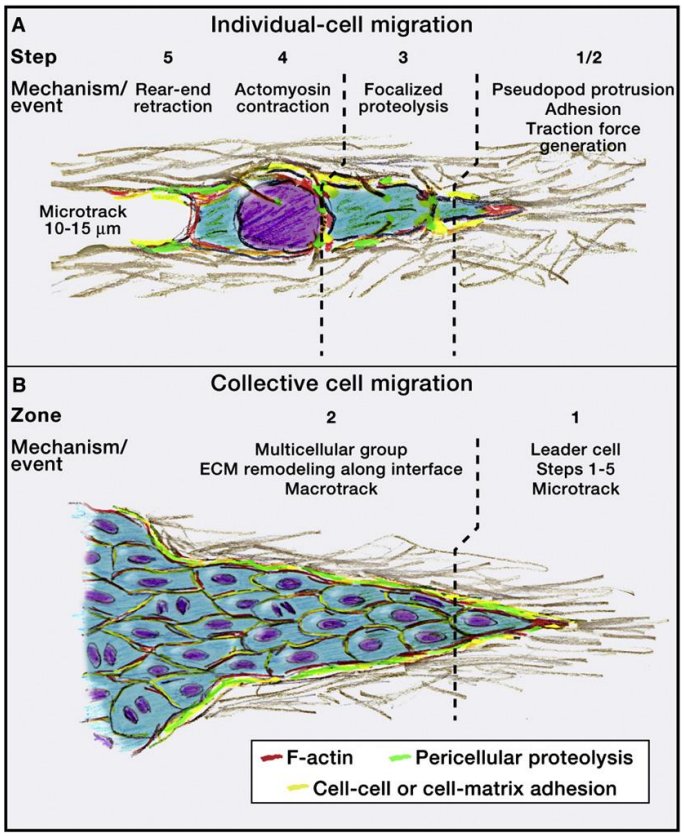

Figure 3. (A) The five molecular steps involved in single cell migration. (B) Collectively migration. *From Friedl P and Alexander S, Cell, 2011*

The protein–protein interactions and signaling events that cause shape modification and control cell migration are linked to the events of adhesion, actomyosin polymerization and contraction [169,174,175]. Adhesion to ECM, leading by pseudopods, are mediated by integrin binding, which are transmembrane receptors family. Integrins, coupled to the actin cytoskeleton, cluster and develop into an initial small focal complex, which can become focal contact. In each focal contact different pattern of integrins could be involved, according to differences in ECM substrate and cell type. These include α5β1 integrin, which binds fibronectin [176]; αvβ3 which binds fibronectin or vitronectin [177], α2β1, which binds collagen [178] and α6β1 or α6β4, which bind laminin [179]. Additional, non-integrin receptors also interact with ECM such as CD44, discoidin receptors, CD26, immunoglobulin superfamily receptors, and surface proteoglycans. In the meanwhile, the actin filaments locally assemble, through the action of crosslinking proteins such as α-actinin and myosin II [175,180]. The arrangement of actin below the inner part of the plasma membrane is called cortical actin, whereas cytoplasmic bundles of actin filaments are

nominated stress fibers [180]. The assembly and contraction of the stress-fibers are controlled by myosin II, mainly induced by Rho and its important downstream kinase, ROCK [181,182]. While, the cortical actin network is controlled by the myosin light-chain kinase (MLCK), but not by Rho [183–185]. This allows the cell to separately control cortical actin dynamics from contractions in inner regions. Actomyosin contraction promotes the shortening of the cells length axis and generates inner tension towards focal contacts that are located at external edges [154,186]. The number and size of focal contacts can change from cell to cell in response to different environments, and the speed generated by the migration cycle is limited from the turnover rates of the adhesion events [169], causing an inverse relationship between migration rates and focal contact strength. Stabilization of focal contacts increases attachment, reduces detachment and impairs migration rates, whereas weakening of adhesion strength, forces migration [169,187,188].

The single-cell motility described below is effective for normal cells as well as for cancer cells. Indeed, integrin signaling, focal-contact formation and actomyosin-dependent contractility are involved in tumor cells motility [178,179,189–191]. Moreover, frequently, in tumor cells ECM-degrading enzymes, such as cathepsins and MMPs, are overexpressed [192,193], and simplify migration *in vitro* [194–196], as well as metastasis *in vivo* [197,198]. Likewise, the upregulation or activation of the GTPases Rac and Rho and their downstream effector ROCK or MLCK have been demonstrated to be correlated with *in vitro* tumor cell migration and *in vivo* invasion and progression [199–202]. Single-cell motility of tumor cells typically initiates from the interstitial stroma or bone-marrow. Indeed, cells originate from a multicellular compartment, such as epithelium, lose their cell contacts and migrate as individual cells through the adjacent connective tissue [203]. The migration of cancer cells seems to be activated by an imbalance between pro-migratory and anti-migratory signals [204,205], and this allows cancer cells to increase their invasiveness towards tumor metastasis. There are multiple factors that can regulate cancer motility: chemokines and growth factors sustain migration by pro-migratory signals transduction via PI3K, Rac and Rho signalling; matrix proteases generate chemotactic ECM fragments as well as pro-migratory neoepitopes that engage specific sets of integrins [205,206]; insulin-like growth-factor-1 (IGF1) and the epidermal growth factor (EGF), that also promotes cell proliferation and survival [207].

Single cell motility is characterized by two subtypes: mesenchymal motility and amoeboid motility, in which cells assume completely different phenotypic, morphological and molecular characteristics (Fig.4).

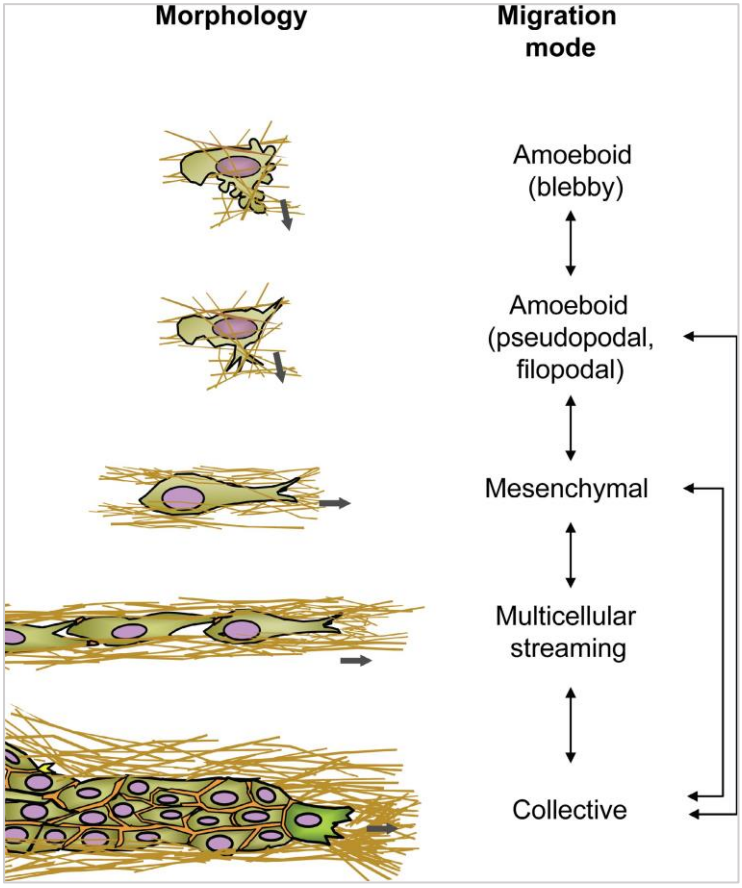

Figure 4. Cell morphologies, migration modes, and transitions. From Friedl and Wolf, 2010

2.3.1 Mesenchymal motility

Mesenchymal-like motility predominates in connective tissue tumors such as fibrosarcoma, glial cell tumors, and myoblastomas [154]. Cells that moves with mesenchymal motility have a typically elongated morphology and lack polarity, both functional and morphological. This type of motility depends on the proteolysis of the ECM mediated by an intense secretion of MMPs. The cells stably adhere to the ECM thanks to focal contacts, where the integrin receptors cluster and firmly anchor the cell to the substrate. The activation of integrin signaling stimulates the secretion of MMPs which, by degrading the matrix, generate the space necessary for cell movement. The actin cytoskeleton is organized in stress fibers connecting several focal adhesions. Cell movement is driven by membrane

portion on the leading edge [208,209]. Different cell types generate different cytoplasmic protrusions: lamellipodia, filipodia and pseudopodia or invadopodia [154]. These membrane structures are formed by bundles of actin filaments and lined with integrin receptors [154,179,192,210,211]. At the molecular level, mesenchymal motility is driven by GTPases Rac and Cdc42, which are essential for the formation of cytoplasmic protrusions [175,212].

2.3.2 Amoeboid motility

Different kinds of amoeboid movement have been described in the last 10 years [155,213], and in most of the cases, there are not described adhesion regions which mediate interaction with substrate [157]. One type of non-adhesive amoeboid movement is characterized by the formation of membrane blebs. The amoeboid motility was described for the first time during embryonic development [214–216] and it was observed in the amoeba *Dictyostelium discoideum*, which is able to move quickly in a few seconds by alternating cycles of expansion and contraction of the cell body [217,218]. This type of motility has also been observed in leukocytes, in hematopoietic stem cells and in some cancer cells such as leukemia, breast cancer, small cell lung cancer and metastatic melanoma [154,219]. *Lorentzen et al.,* showed that melanoma cells with increased metastatic potential, contain a higher proportion of cells (90%) which move through squeezing amoeboid motility [219]. Moreover, rounded cells predominate in the invasive front of melanoma, confirming the relevance of amoeboid motility in the invasive process [220]. For lymphocytes and neutrophils migration, integrin-mediates adhesion within connective tissue is not entirely necessary, both *in vitro* and *in vivo* [156,221,222]. Indeed, this type of migration is completely independent of cell adhesion to the substrate and ECM proteolysis. The cells show a rounded morphology and pass through the tissues by "squeezing" rapidly between the fibers of the ECM in the absence of proteolytic enzymes due to their lack of focal contacts allowing them to move at 10-30 fold higher velocities then cells that use mesenchymal migration mechanism [223,224]. This ability depends on the rapid changes in morphology promoted by the contraction of the actin filaments organized to form cortical rings [218]. Cells with blebbing amoeboid movement are characterized by a lack of apparent polarization and high actomyosin contractility [155,213] regulated by the GTPase RhoA inhibiting p190RhoGap [225] or engaging of ephrin A2 (EphA2, an indirect Rho activator) [226] . Blebbing starts by the

disassembly of the submembrane actin cortex [227]. Cytoplasm is hard up through such ruptures to form membrane blebs [228,229] that grow until actin-binding proteins, such as those of the ezrin radixin moesin (ERM) family, are assembled in the blebs, which in turn recruit actin and actin-bundling proteins to the bleb membrane to form a new cortex. Finally, myosin II is recruited and drives retraction of the blebs [230]. The position of blebs formation determines the direction of cell movement [231]. However, some cells, such as A375 melanoma cells, form multiple blebs over the membrane and therefore they would not be able to move directionally, while they are able to invade into a collagen matrix and move both *in vitro* and *in vivo* [232,233]. Amoeboid dissemination allows cancer cells to undergo early metastatic spread from a small primary tumor [234].

2.3.3 Tumor cell plasticity

Different cell types preferably use a different migration style, for example leukocytes use amoeboid migration, stromal cells move with a mesenchymal mode, epithelial cells with collective movement [235]. However, in recent years, it has become clear that some modifications induced by the environment or by the cells themselves, can cause an adaptation that alters the style of migration [155]. Cancer cells, during growth and neoplastic progression, are able to shift from one to another type of motility, adapting to the modification in the microenvironment depending on the differences in ECM or on the cellular components. This ability is defined as “migratory plasticity” and often correlates with highly invasive and metastatic phenotypes in cancer cells [154,235,236] (Fig.5).

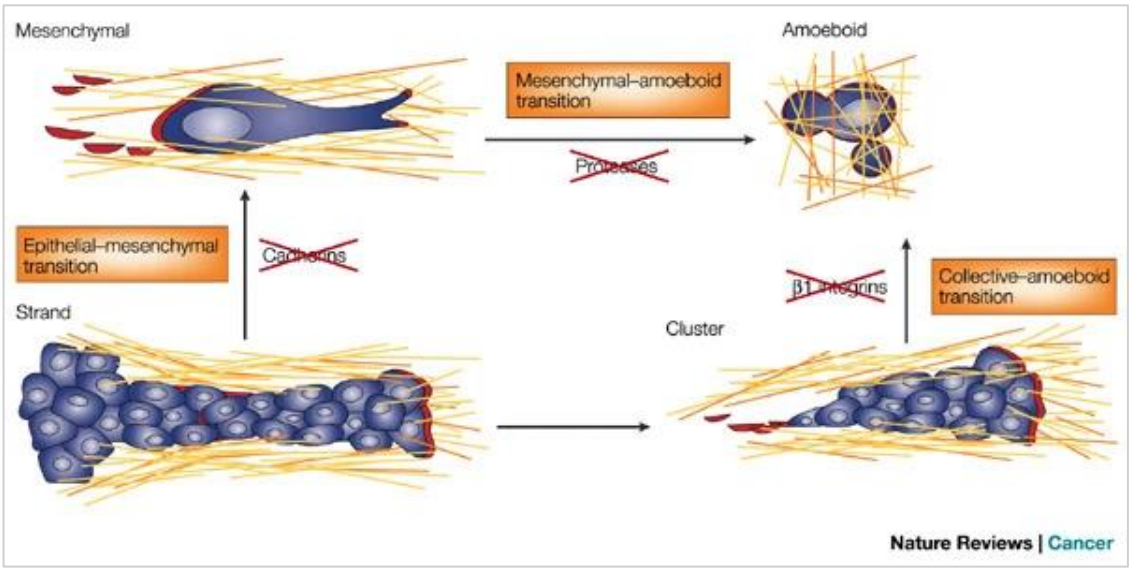

Figure 5 The migratory plasticity of cancer cells. The ability of tumor cells to switch from one migration style to another (From Friedl and Wolf, Nature Reviews, 2003)

Epithelium-mesenchymal transition (EMT)

EMT is an epigenetic transcriptional program that leads to a profound reprogramming of epithelial cells, which lose their phenotype and acquire the mesenchymal characteristics necessary to migrate from the primary site [235,237]. The EMT program firstly determines the loss of cell-cell and cell-ECM contacts followed by the loss of functional polarity typical of epithelial cells, and by a deep reorganization of the cytoskeleton. The induction of EMT is determined by *stimuli* induced from the tumor microenvironment. The main activator of this transcriptional program is TGF-β, but also hypoxia, ROS and paracrine signals released by the cellular components of the tumor stroma [238,239]. The crucial events during EMT are both the loss of E-cadherin, which leads to the destruction of cell-cell junctions, and the increased expression of MMPs [240]. In addition, cells that undergo EMT show an increased expression of some mesenchymal markers such as vimentin, fibronectin, α-smooth muscle actin (SMA) and N-cadherin. There are many transcription factors involved in this process; among the most specific, Snail-1, Twist, Slug, ZEB1 and 2, and SIP1 [237,241–243].

Mesenchymal-amoeboid transition (MAT)

During the mesenchymal-amoeboid transition (MAT), a motile cell acquires a more rounded morphology and becomes completely independent of adhesion to the substrate. Indeed, this type of transition is associated with an increased ability to overcome the *anoikis* conferring further benefits to cancer cells during the last stages of the metastatic cascade [218,244,245]. Numerous studies have shown that using integrin and/or protease inhibitors, typically in mesenchymal cells such as HT1080 fibrosarcoma cells, or MDA-MB-231 breast cancer cells, cells shift from mesenchymal to amoeboid motility [246]. In prostate cancer it also been demonstrated that CAFs, in a synergistic way with endothelial cells recruited *in situ,* lead cancer cells to undergo MAT via Eph1/EphA2 signaling [247]. Moreover, in melanoma cells, MAT is associated with the acquisition of a stem-like phenotype which sustains tumor progression [248].

This shift induces not only a change in morphology (from elongated to rounded), but also a redistribution of the integrin receptors (from focused to dispersed on the membrane), a reorganization of the actin cytoskeleton (the membrane protrusions), as well as changes in the molecular strategy used to overcome the anatomical barriers that prevent cell spread (from protease-dependent to protease-independent). Consequently, the main molecular markers of this transition are represented by a drastic decrease of MMPs expression and GTPases Rac1 and Cdc42 activation and by a strong increase in the expression and/or activation of RhoA and its downstream effector ROCK [246].

2.4 Metastatic dissemination

Most of cancer deaths, statistically up to 90%, are due to the development of metastases [249,250].

Metastasis is the process by which a primary tumor spreads to distant organs and develops a second cancerous lesion [251]. It is an adaptive process, characterized by a series of critical steps (Fig.6), including:

1. Local infiltration and detachment from the primary tumor mass (EMT)
2. Dissemination (intravasation);
3. Resistance to *anoikis*;
4. Adhesion to the endothelium and trans-endothelial migration (extravasation);

5. Survival in the bloodstream, arrival in the new site and development of metastasis [252,253].

It has now been widely demonstrated that genetic mutations in cancer cells alone are not enough to explain tumor growth and progression. Both *stimuli*, from the microenvironment and epigenetic alterations of tumor cells, play a leading role during the various phases of the metastatic cascade [254,255].

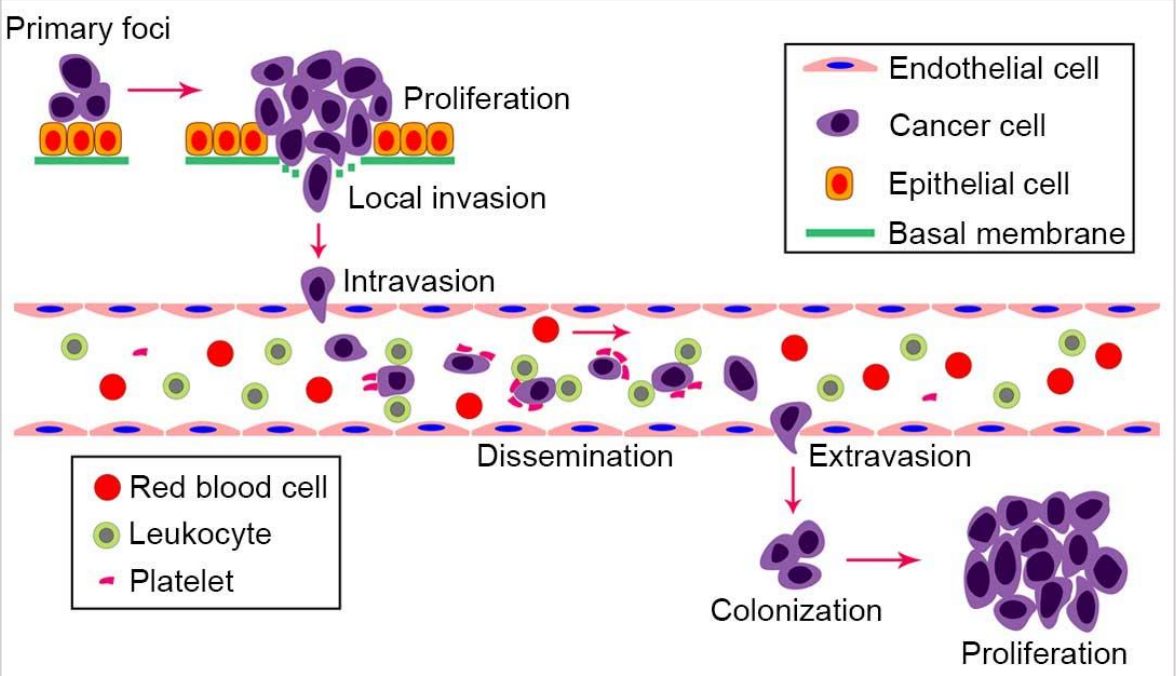

Figure 6. The five successive steps of the metastatic process. *(From Ding D. et al, Oncology Letter, 2016)*

2.4.1 Local infiltration and detachment from the primary tumor mass

In the primary site, the tumor, thanks also to the microenvironmental factors, grows and spreads, modifying its structure. However, the tumor mass, without blood circulation, grows up to 1-2 mm^3 in diameter. Since 1971, several studies have been demonstrated that the absence of neo-vascularization causes a stop in tumor growth [256,257]. Therefore, the establishment of new blood vessels that provide to the tumor growth factors and nutrients is necessary. Indeed, angiogenesis, one of the hallmarks of cancer, is essential for growth and especially for metastasis formation. Angiogenesis allows the spread from the primary site to distant organs of the metastasizing cancer cells, representing the so-called "*escape route*" [256,257]. The term "tumor angiogenesis" has been coined since 1968 by Greenblatte Shubik to describe the vascularization associated with tumor growth. Tumor angiogenesis

can occur through various mechanisms; in addition to sprouting angiogenesis and vasculogenesis, it has recently been described a third modality of tumor angiogenesis: the "*vascular mimicry*". It was defined as the ability of tumor cells, and of some stromal components, to acquire functional capabilities typical of endothelial cells, therefore "*mimicry*". It was described for the first time in melanoma [258] and then in other types of tumors such as glioblastoma, breast, ovarian and hepatocellular carcinoma [259]. Tumor endothelial cells (TECs) are irregular in shape and size with poorly defined margins compared to the normal endothelial cells, with long cytoplasmic protrusions extending and crossing the vessel lumen. At the top of these cytoplasmic protrusions there are intercellular gaps that create micro pores in the vessel wall, increasing its permeability [260]. The blood flow in these vessels is heterogeneous and it can go both in an antegrade and retrograde direction [261].

The main causes of induction of vascular mimicry are vascular endothelial (VE) -cadherin, endothelial (E) -selectin, CD34, EphA2, tyrosine kinase receptor (TKR) -1, and neuropilin 1. Furthermore, a leading role in the development of tumor angiogenesis is played by hypoxia and by HIF1 and HIF2. These factors not only support angiogenesis but can also induce and select tumor cells with a more invasive and metastatic phenotype [262]. Hypoxia can also induce the transcription of pro-angiogenic factors, including VEGF, and can inhibit the signals that normally control the stability and integrity of the vessels. Given the importance of tumor angiogenesis in the tumor mass progression, targets to inhibit this process have been identified. Bevacizumab, or Avastin, is a humanized monoclonal antibody directed against VEGFA. It was the first anti-angiogenic drug to be used, in 2004, for colorectal cancer; currently, it is used in combination with other drugs such as 5-fluorouracil, because it has proved to be ineffective, sometimes also capable to select more aggressive clones determining the formation of secondary tumors [263,264].

Once neovascularized, the tumor uses the new vessels not only as a source of nutrients, but also to spread and metastasize. Tumor cells must escape from the primary mass and thus acquire motile and invasive abilities; in epithelial carcinomas this process is called EMT (already described above).

2.4.2 Dissemination (intravasation)

On this step cancer cells enter into blood or lymphatic vessels (intravasation), first through the invasion into the basal lamina of the endothelium, then, moving between the endothelial cells that structure the capillaries and, finally, entering into the bloodstream [249,265–267]. To achieve the intravasation step, cancer cells need to break the cadherin-dependent bonds, present between endothelial cells, and form new cell-to-cell contacts [268]. Furthermore, the cancer cells undergo several morphological changes that allow them to rapidly penetrate into the vessel, such as a significant increase in cytoplasmic plasticity [269–271]. In this phase, the effect exerted on the endothelial cells is also central, indeed they must reduce the tight junctions that keep the vessel layer compact.

Key factors of the intravasation process are:

- T-α, produced mainly by tumor-associated macrophages (TAMs), is essential for increasing vessel permeability and promoting interactions between tumor cells and the endothelium;
- Interleukin (IL) -1 and IL-6, produced by leukocytes and monocytes infiltrated in the tumor site, activate different MMPs, and Urokinase-Type plasminogen activator (uPA);
- Hypoxia. It represents one of the most effective inducers of VEGF secretion by tumor cells. A high concentration of VEGF is in turn essential to inhibit the tight junctions between endothelial cells [272].

2.4.3 Circulation survival (resistance to anoikis)

In physiological conditions, in the absence of adhesion to the ECM, the cells undergo a particular type of apoptosis called *anoikis*. The execution of *anoikis* can be mediated by both apoptotic pathways: the intrinsic and the extrinsic pathway. Both pathways end with the activation and translocation in the nucleus of caspases, cytoplasmic endonucleases that fragment DNA inducing cell death [273,274].

The Bcl-2 family of proteins plays a key role in both pathways. It can be divided into 3 different protein groups:

- Anti-apoptotic proteins such as Bcl-2, Bcl-XL and Mcl-1;
- The pro-apoptotic multi-domain proteins Bax, Bak and Bok;

- Pro-apoptotic proteins BH3-only Bid, Bad, Bim, Bik, Bmf, Noxa, Pumae Hrk [275].

The intrinsic pathway

The intrinsic, or mitochondrial, pathway is activated in response to a series of intracellular signals that include DNA damage, growth factors deprivation, radiation, or endoplasmic reticulum stress. In response to death signals, the pro-apoptotic proteins, Bax and Bak, translocate from the cytosol to the outer mitochondrial membrane (OMM), where form oligomers creating channels in the membrane and causing permeabilization of the mitochondria and the release of cytochrome c [276]. The release of cytochrome c determines the formation of the apoptosome, composed of caspase 9, a cofactor of apoptosis, Apaf, and cytochrome c itself, with the subsequent activation of caspase 3 and its translocation into the nucleus [277–279].

The extrinsic pathway

The extrinsic pathway begins with the binding from extracellular ligands to receptors of the tumor necrosis factor receptor (TNFR) family, such as fragment apoptosis stimulating (FAS) [280,281]. Briefly, FAS and FAS ligand (FASL) induce the establishment of the death inducing signaling complex (DISC); which interacts with fas-associated death domain (FADD), that recruits numerous pro-caspases 8 and promotes their activation. Caspases 8 activated and translocated into the cytoplasm, cut and activate caspases 3, 6, and 7 which induce cell death [280,281].

Alternatively, caspase 8 activates, through proteolytic cutting, Bid, that in its truncated form, t-Bid, promotes the release of cytochrome c by the mitochondria and induces the assembly of the apoptosome. At this point the intrinsic and extrinsic pathways converge [282] (Fig.7).

Epithelial cells are protected by *anoikis* when they adhere to ECM proteins. Integrin receptors play a key role in ensuring the adhesion of cells to the matrix and therefore protection from *anoikis*. In particular, the integrins α5β1, αvβ3, α1β1, α6β1. When these receptors permanently lose the link with the ECM, activate different intracellular pathways capable to trigger both the extrinsic and the mitochondrial pathways. Not only cell-matrix adhesion, but also cell-cell contacts are essential to ensure cell survival. Contacts between cells are mediated by cadherins, a family of membrane receptors that allow homotypic or heterotypic cell-to-cell calcium-mediated anchoring. It has been reported that the blocking

of the binding mediated by E-cadherin induces *anoikis* in epithelial cells [283,284], while the over-expression of β-catenin, a downstream target in the signaling of many cadherin receptors, induces resistance to *anoikis* [285]. EMT, metabolic shifts, autophagy and constitutive activation of survival pathways, are other mechanisms by which cancer cells implement resistance to *anoikis* [240]. The constitutive activation of the PI3K/Akt signaling pathway is the most common mechanism to induce *anoikis* resistance in cancer cells, and PTEN is the most important negative regulator. The prolonged activation of Akt can be induced by various pathways; for example through the over-expression of integrin receptors; the constitutive activation of Ras through mutations; the loss of phosphatase and PTEN activity through gene mutations such as deletion or methylation; alterations in PI3K activity; amplification or over-expression of the Akt gene [286,287]. Akt activation modulates the activity of transcription factors that control the expression of pro- and anti-apoptotic genes, such as IKKβ, Forkhead box proteinO1 (FKHR), Forkhead box proteinO3 (FKHRL1), and Forkhead box protein O4 (AFX), or through direct phosphorylation of pro-apoptotic proteins, such as Bad and procaspase-9, inhibiting their function [278,288–291]. Another important transcription factor that contributes to *anoikis* resistance is HIF-1. Activation of HIF-1 pathway triggers the transcriptional program of EMT, activating the transcription of specific factors such as Snail, Twist and NF-κB [292–296]. Furthermore, HIF-1 can induce resistance to *anoikis* through the increased expression of EGFR, the activation of MAPK and causing the degradation of pro-apoptotic proteins such as Bim and Bmf [297].

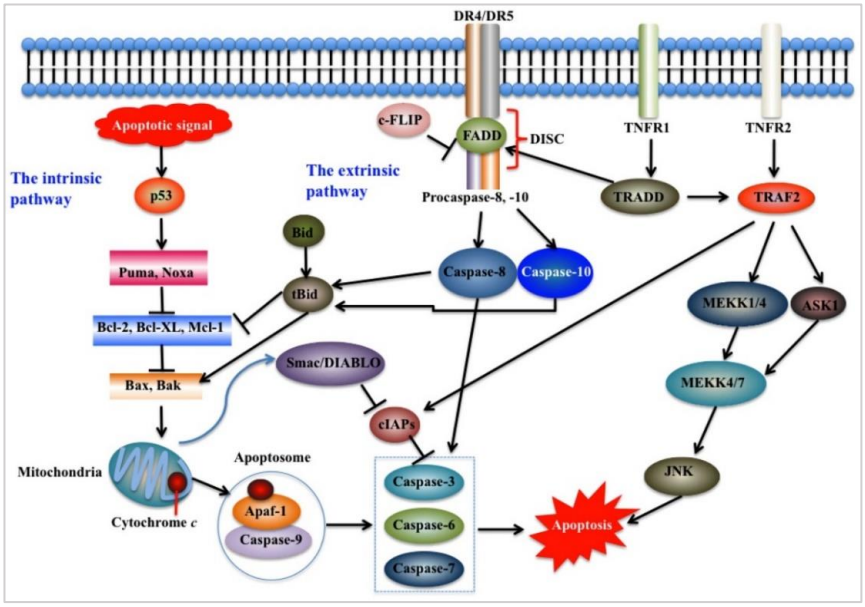

Figure 7. Intrinsic and extrinsic apoptosis pathways. *(From Zang F. et al., International Journal of Molecular Medicine, 2016)*

2.4.4 Adhesion to the endothelium and trans-endothelial migration (extravasation)

Extravasation is the process by which cancer cells migrate from the bloodstream, or from the lymphatic system to a secondary site. Cancer cells move passively or actively within the vessel [298] and respond to signals that derive from the vascular endothelium [299]. There are two possible theories that have been considered for the arrest of cancer cells at the level of the endothelial barrier and that can explain the formation of metastases with a greater frequency in certain organs. The first is Paget's "*seed and soil*" hypothesis, according to which the tumor (the seed) depends on the characteristics of the distant organ (the fertile soil) to spread [300]. Numerous studies, both *in vitro* and *in vivo*, have shown that cytokines and growth factors, as well as specific cell-cell interactions, play a crucial role in determining the metastasis of given types of cancer in specific organs and tissues. These molecules are called "*homing factors*" [301,302]. For example, breast cancer cells, which express high levels of CXCR4, preferentially metastasize into bone, recalled by a high concentration of its specific ligand, stromal-derived factor (SDF) -1. This gradient is also involved in the metastasis of leukemia and prostate cancer, while the chemokine (CC motif) ligand (CCL) -21 is the main homing factor for lungs and lymph nodes [303,304].

On the other hand, according to Ewing's hypothesis, tumor tropism is based exclusively on mechanical phenomena [305]. For example, tumor cells tend to aggregate to leukocytes and platelets forming heterogeneous aggregates, the so-called "*metastatic emboli*", which flow more slowly on the endothelial wall favoring the extravasation process [306,307].

Once firmly adhered to the vascular endothelium, the cancer cells migrate through the vessel wall, crossing the basement membrane and invade the new tissue.

2.4.5 Survival at the new site and development of metastasis

Once exceed the basement membrane of the vessel, the metastatic cells must survive, invade and proliferate in the new tissue. Numerous evidence have shown that metastatic tumors appear histologically less differentiated than the primary lesion and frequently express a stem-like phenotype. *Balic M. et al*. demonstrated for the first time that cancer cells from bone metastases derived from breast cancer expressed $CD133^{+}$, $CD44^{high}/CD24^{low}$ phenotype, typical of undifferentiated stem cells [308] . *Hermann et al.*

instead, by isolating $CD133^+$ cells from pancreatic carcinoma that showed a marked migratory capacity, demonstrated that the elimination of these cells abolishes the ability of the tumor to form metastases [309].

The growth of the metastatic lesion is characterized by the ability of tumor cells and microenvironment components to establish conditions that induce the formation of so-called "*metastatic niches*", created to provide the optimum microenvironment for the growth of metastatic cells in the secondary lesion [310–313]. Therefore, a cross-talk is established between tumor and stromal cells which supports tumor growth both recruiting endothelial cell progenitors for the formation of new vessels and by the secretion of numerous soluble molecules, such as growth factors, cytokines and chemokines, which influence the behavior of cancer cells, by each of the niche residents [314–316]. During the final steps of metastatic event the tumor cells acquire the possibility to shift towards an amoeboid phenotype undergo MAT. This transition is associated not only with an increase in the ability to overcome the *anoikis* but also with an enhance of stem-like phenotype, promoting spread of cancer cells and sustain tumor progression [235,245,248,265]. In particular, it has been demonstrated that 90% of metastatic melanoma cells move through squeezing amoeboid motility with respect to the less metastatic parental melanoma cell line [219].

However, not all tumor cells belonging to the primary site are able to acquire all the characteristics necessary to all the events that occur during the metastatic cascade, but this capacity remains limited to a small pool of tumor cells. This explains the sporadic nature of the metastatic event.

3. Part 1

3.1 Osteosarcoma

Osteosarcoma (OS) is the most common primary bone cancer, characterized by high aggression and rapid metastatization mainly to the lung, which is associated with reduced survival [317,318]. OS shows high tumor heterogeneity, a feature common to various solid tumors. There are two general models of tumor heterogeneity. In the "*genetic mutations*" model, the neoplastic transformation occurs in a single cell, from which the primary lesion will be originated. In the "*cell of origin*" model, instead, the tumor derives by oncogenic events which are sustained simultaneously by different cell populations [319]. The histological heterogeneity of OS, indeed, is due to a cell of multipotent origin, which is identified in the mesenchymal stem cell (MSCs) during the osteoblastic differentiation process. The mutations which trigger the disease are still unknown, mainly because it is characterized by high genetic instability. Cytogenetic studies have shown various complex changes involving some chromosomes without a specific pattern. Two genes - an hereditary retinoblastoma mutation and an autosomal recessive mutation of p53 in Li Fraumeni syndrome - located at 13q14 and 17p13 respectively, seems to be involved in a gradual accumulation of genomic defects [320]. More recently, *Gambera S et al.,* demonstrated that the overexpression of c-JUN and c-JUN/c-FOS in immortalized hMSC was sufficient to induce cell transformation and OS formation [321].

Understanding the origin and etiology of OS is therefore complicated due to numerous factors such as genomic rearrangements, marked histological heterogeneity, and the high genetic instability that prevents the identification of the main genes [322].

Localization

Bone is a very complex connective tissue, composed of various cell types, including osteoblasts, osteoclasts, chondrocytes, endothelial cells, hematopoietic stem cells (the progenitors of blood cells) and MSCs [323].

Primary OS can develop in any bone, but it forms mainly in the long bones at the level of the metaphysis (90%). Particularly, bones of the knee (50%), distal femur (30%), proximal tibia (15%), and pelvic [323–325]. In addition, several cases have also been documented in the skeleton axial (10%) [326].

Epidemiology

OS is classified as a rare tumor, with a European incidence of 3/100,000 patients in 1 year [327]. Although it represents less than 1% of all cancers, it is the third most common cancer in adolescents, less frequent only than lymphomas and brain tumors in this age group [328]. The highest incidence of cases (70%) was found in children and adolescents aged between 10 and 16 years, or in more adult patients, in 30% of cases, over 40 years of age [317]. It is extremely rare in children under 5 years [329]. It has been shown that the location of the primary tumor is a determining factor in the outcome of the disease. For example, the survival for patients who develop the primary lesion in the pelvis has been estimated from 27% to 47% at 5 years from the onset; between 10-38 months instead, for patients with a primary tumor at the level of the vertebral column. Overall, axial localization was associated with a worse prognosis. To date, about 10-20% of patients have macroscopic metastases, the most common (90%) in the lung, which develop within 2-3 years of onset, but may also be present in the bones (8-10%) and in the lymph nodes. However, 80-90% of patients also have micro-metastases that are subclinical [320].

Etiology

The etiology is unknown, although there is an increase in the incidence of primary OS in many genetic diseases such as Li Fraumeni syndrome, Rothmund Thomsone's hereditary retinoblastoma [323] . Physical agents such as radiation, even if not in young patients, and chemical agents such as beryllium oxide, asbestos, and chromium salts may also be involved in the etiology of this tumor [330,331].

Numerous studies show that the use of radiotherapy on children for the treatment of other types of solid tumors leads, in 5.4% of these, to the development of a secondary tumor and 25% of these are sarcomas [332].

The rapid growth that occurs from puberty to adulthood associated with tumor predisposing factors could be responsible for the preponderance of cases in a young age. This is confirmed by the research of *Gelberg et al.*, who noted an association between the tumor and stature one year before the diagnosis, also compared with other factors, such as size and body mass index [333]. Furthermore, despite a male: female ratio, that is of 1.5: 1, the disease occurs at an earlier age in females than in males, which is believed to be due to earlier development in females than in males [334].

Current therapy

Nowadays, surgery combined with chemotherapy is the first-line treatment for most OS cases. Almost all patients, as initial treatment (8-10 weeks before surgery), receive combined neoadjuvant chemotherapy intravenously (doxorubicin and cisplatin with or without methotrexate and Ifosfamide), and after surgery for another 12-29 weeks [335,336].

Although it is considered a tumor resistant to radiation therapy, this could be an option for local treatment for inoperable OS, following resection or as a palliative for symptomatic metastases [337].

With modern therapy, in patients without metastases, survival at 5 years after surgery is about of 60-70%. In patients with metastases or relapse, survival at 3-5 years has remained at 10-30% since 1980 [320], highlighting the necessity for a better understanding of the disease and therefore the development of new therapies [338].

3.1.1 Bone marrow-mesenchymal stem cells (BM-MSCs)

MSCs are a heterogeneous group of multipotent progenitors capable of self-renewal and resident in some tissues such as: umbilical cord, adipose tissue (in Wharton's Jelly), peripheral blood, liver, lungs, placenta and amniotic fluid. In these tissues, their resident pool is maintained through self-renewal and migration of bone marrow-mesenchymal stem cells (BM-MSCs) [339–341].

After *ex vivo* expansion, BM-MSCs isolated from different tissues have similar properties but are able of exerting different effects in different biological contexts [342]. Phenotypically, they express several membrane antigens such as CD29, CD44, CD49, CD73, CD90, CD105, CD106, CD140b, CD166 and STRO-1, with negativity for CD34, CD45, HDA-DR, CD14 or CD11b, CD79a, or CD19 [343,344]. They also express numerous adhesion molecules for binding ECM components, such as integrin receptors α5β1, αvβ1 and αvβ3; for the binding to fibronectin, α1β1 and α2β1; for the binding to collagen, α3β1 and α6β1 for the laminin binding [345]. Genotypically, they derive from different tissues and therefore express different levels of transcription factors associated with pluripotent stem cells such as NANOG, OCT-4 and/or SOX-2. But, the functional contribution to the proliferation and differentiation of MSCs of these transcription factors is still under investigation [346].

MSCs are cells that normally participate in the structural and functional homeostatic maintenance of the connective tissue in normal conditions. Their activities include the

regulation of vital processes such as hematopoiesis and the preservation of the integrity of blood vessels and bones. Crucially, also their role in cases of wound healing and tissue repair, indeed, in response to systemic factors released from damaged tissue, MSCs exit from their niches in the bone marrow and are recruited into the injury site to restore normal homeostasis [346].

BM-MSCs mainly differentiate towards the mesodermal lineage: osteoblasts, chondrocytes, adipocytes and stromal cells (fibroblasts and pericytes). Nevertheless, their ability to differentiate into cells of endo- and ectodermal origin, such as myoblasts, neurons and epithelial cells, has recently been demonstrated [347,348].

The differentiation of BM-MSCs is controlled by several factors present in the microenvironment including cell-to-cell and cell-to-ECM contact, cytokines, chemokines, growth factors, and by numerous transcription factors, such as RUNX-2 and OSTERIX that trigger the differentiation towards the osteoblastic phenotype [348,349].

3.1.2 Role of BM-MSCs in neoplastic progression

Several studies, both *in vivo* and *in vitro*, have demonstrated the high tropism of BM-MSCs for different types of epithelial carcinomas. This migration is driven by a chemotactic gradient of cytokines and growth factors released by the tumor cells [350]. For example, EGF and platelet-derived growth factor (PDGF) are responsible for the chemotaxis of BM-MSCs in pancreatic cancer [351], while the VEGF, mediates the recruitment of BM-MSCs in models of murine glioma [352]. Monocytes chemoattractant protein (MCP) -1 and IL-6 are responsible for the migration of BM-MSCs in breast cancer [353], uPA and its receptor (uPAR), determines a consistent migration of BM-MSCs in lung cancer [354]. Finally, as regards OS, some authors have recently reported the involvement of SDF-1 in the recruitment of BM-MSCs towards the primary lesion site [355].

Once the BM-MSCs have migrated within the tumor stroma, they can promote neoplastic growth and progression through different mechanisms:

- They exert their activity on cancer cells through the paracrine secretion of various molecules such as cytokines and growth factors which influence the proliferation and metastatic spread of cancer cells [356],
- They can induce tumor vascularization through neo-angiogenesis, thanks to the production of pro-angiogenic factors such as VEGF, angiopoietin, TGF-β, PDGF

and fibroblast growth factor (FGF) -7; or by differentiating themselves into endothelial cells and pericytes [357,358];

- They act as immunomodulators capable of suppressing both the innate and the acquired immune response against the tumor [346];
- MSCs are able to trans-differentiate into other stromal components such as TAMs [359], and CAFs, both crucial modulators of the neoplastic progression process [346,360].

While we have described the pro-tumor role of MSCs, there is also evidence showing an anti-tumor activity. *Khakoo et at*. described an intrinsic capacity of anti-tumor BM-MSCs since they induce the inactivation of Akt signaling (a constitutively active pathway in cancer cells) in Kaposi's sarcoma cells [361]. Furthermore, *Barcellos-de-Souza P. et al*., demonstrated that BM-MSCs, through the secretion of oncostatin-M, a cytokine that exerts an anti-proliferative effect in several types of cancer, inhibit *in vitro* proliferation, migration and invasion and *in vivo* tumor growth of lung adenocarcinoma cells [362].

Therefore, to date the role of MSCs in tumor progression is controversial and still under investigation. To understand it better, it would be required to define the complex network of interactions that takes place among tumor cells, BM-MSCs and the other stromal components. Thus, once integrated into the tumor stroma, the equilibrium between the pro- and anti-tumor effects exerted by the BM-MSCs is determined by the changes in the microenvironment where they are resident [362].

3.2 Aim of the project

Several studies, both *in vitro* and *in vivo*, have documented the high tropism of BM-MSCs for different types of primary tumors. Numerous cytokines and growth factors, have been found involved in recruiting MSCs from their niche in the bone marrow of different types of epithelial carcinoma, such as melanoma, breast, prostatic, hepatic, and ovarian cancer [350–355]. Once recruited in the tumor stroma, BM-MSCs can actively promote tumor growth and progression, on the other hand, it has been described in literature their anti-tumorigenic abilities [362]. Consequently, the role played by BM-MSCs in tumor progression remains an open question and object of study.

The purpose of this project was to evaluate the effects induced by the cross-talk between BM-MSCs and tumor cells, in the progression of osteosarcoma, a tumor with mesenchymal origin. Given the high heterogenicity of this tumor, in our studies we used three different cell lines: HOS, Saos-2 and MG-63, which differ in proliferative rate, migratory and invasive capacity, resistance to *anoikis* and tumorigenicity *in vivo* [363]. HOS show a more aggressive phenotype than MG-63 and Saos-2, which have an intermediate phenotype, both in terms of migratory capacity and *in vitro* proliferation. We used BM-MSCs isolated from the bone marrow of 4 different healthy donors. These cells were characterized by the Immunohematology Unit of the Meyer Hospital, directed by Dr. Franco Bambi, for their ability to differentiate *in vitro* into osteoblasts, chondrocytes and adipocytes, as well as for the expression of specific surface markers (CD73 ++; CD90 ++; CD105 ++; CD34 -; CD45 -; CD19 -; CD14).

3.3 Results

3.3.1 BM-MSCs show significant tropism for OS cells-derived conditional medium and strongly affect the metastatic potential of cancer cells.

Accordingly with data from the literature that described a strong homing properties of BM-MSCs for several tumors, including OS [355,364–366], we confirmed a significant chemotaxis of BM-MSCs toward conditional medium (CM) obtained from the three OS cell lines (SaOS-2, MG-63 and HOS), with a 2- to 2.5-fold increase in migration compared with control (St Med, Fig. 1A). It has been reported that SDF-1 is a key factor to promote BM-MSCs homing to CM from SaOS-2 cells [355]. Nevertheless, by performing chemotaxis experiments with blocking antibodies against CXCR4 (Fig. 1B) we excluded the involvement of the CXCR4/SDF-1 axis. Consequently, to identify the soluble factors involved in the BM-MSC chemotaxis toward OS cells, CM derived from MG-63, that disclosed the highest chemoattractant skills, was analyzed by ELISA. We quantified cytokines and growth factors already known to be involved in BM-MSC migration in other cancer models [352,362] (Fig. 1C). Among these, we focused on those with the highest levels of secretion: GRO-α (542 pg/mL^{-1} ± 70), MCP-1 (359.9 pg/mL^{-1} ± 65) and TGF-β1 (1161.7 pg/mL^{-1} ± 81), a pattern of cytokine expression common to other OS cell lines, as reported in several studies [367–370]. The role of these chemokines in BM-MSC recruitment, were validated performing transwell migration assays with the specific inhibitors: neutralizing antibodies against MCP-1 (αMCP-1), a TGF-β receptor blocker (TbR blk) and a pharmacological inhibitor of the GRO-α receptor, SB225002 [371]. The treatment of MG-63-derived CM with anti-MCP-1 antibodies, or the incubation of BM-MSCs with SB225002 and TbR blk, significantly reduces BM-MSC migration compared with untreated MG-63-derived CM (Fig. 1D), Moreover, the combined treatment of all the compounds further reinforces this effect, confirming the key role of these cytokines in BM-MSC chemotaxis toward CM.

Almost 50% of OS patients develop lung metastasis, the primary cause of death for this tumor [372,373]. We investigated whether the conditioning of OS cells by BM-MSCs could affect the metastatic potential of cancer cells. OS cells were incubated for 48 h with CM derived from BM-MSCs, and their invasion and intravasation abilities were analyzed by transwell migration assays. We demonstrated that the treatment of OS cells with CM from

BM-MSCs significantly increases tumor cell migration through either a Matrigel-coated membrane (Fig. 1E) or a monolayer of human umbilical vein endothelial cells (HUVECs) (Fig. 1F), thus suggesting the positive role of BM-MSCs in promoting the invasive properties of OS cells.

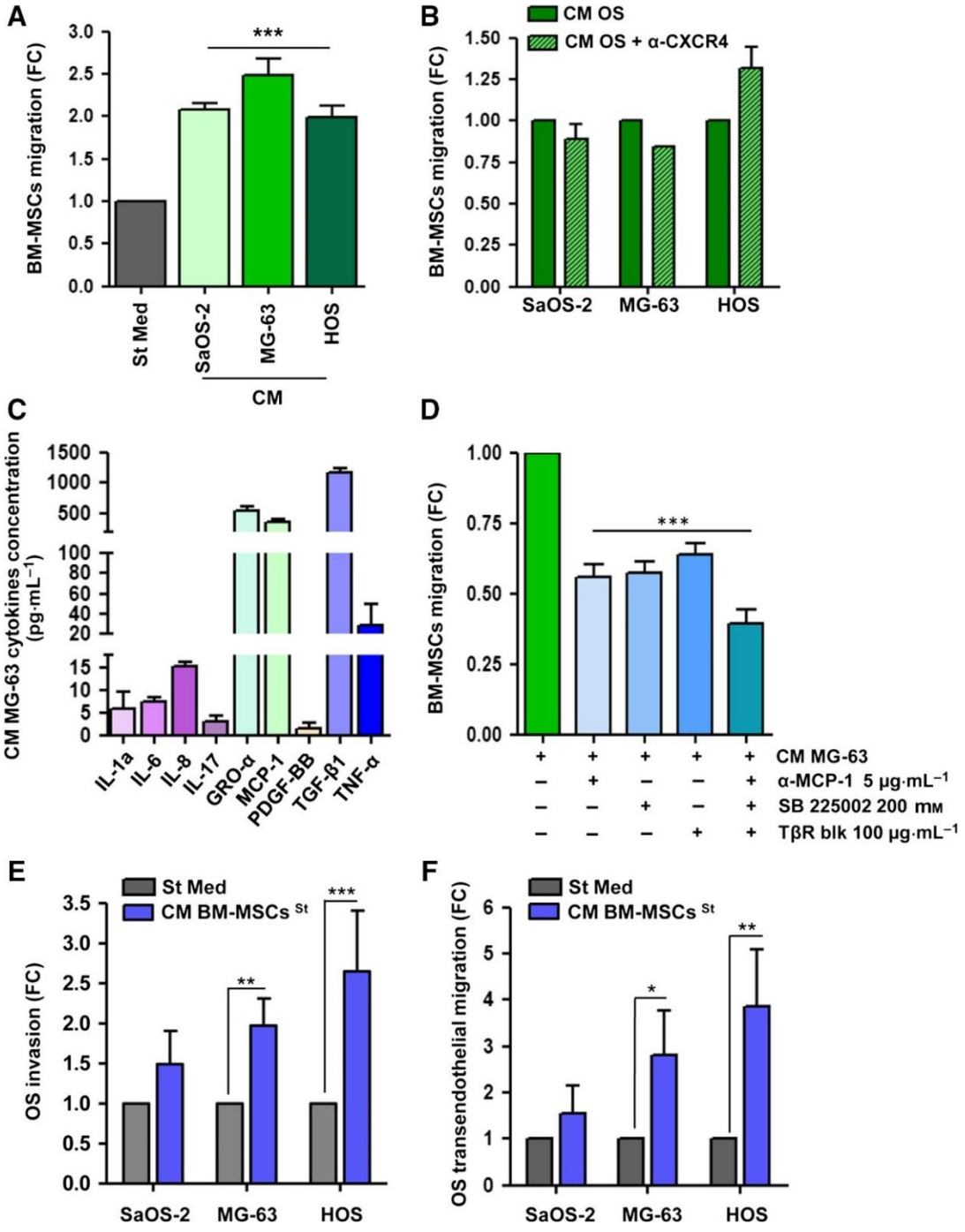

Figure 1. BM-MSCs migrate toward CM from OS cells and affect the invasive behavior of tumor cells. (A) BM-MSCs were let to migrate overnight toward CM from OS cells (SaOS-2, MG-63 and HOS). Starvation medium (St Med) was used control. (B) BM-MSCs starved for 24 h in the presence or absence of neutralizing antibodies against CXCR4 (20 μg/mL^{-1}) were allowed to migrate toward CM from OS cells. (C) ELISA of cytokines and growth factors in CM derived from MG-63 starved for 48. (D) BM-MSC migration toward CM from MG-63 with neutralizing antibodies against MCP-1 (5 μg/mL^{-1}, a-MCP-1), blocking of GRO-a receptor (200 nM, SB 225002) and TGF-b1 receptor (100 μg/mL^{-1}, TbR blk). (E) OS cells were maintained for 48 h in St Med or CM obtained from BM-MSCs starved for 48 h. Cells were then allowed to invade or (F) transmigrate toward complete medium (FBS 10%). *Results are presented as mean ± SEM of three biological replicates; * P < 0.05; ** P < 0.01; *** P < 0.005 vs. St Med*.

3.3.2 BM-MSCs acquire a CAF-like phenotype after contact with OS cells.

Once engrafted into the tumor microenvironment, BM-MSCs can promote tumor growth and progression through different mechanisms: i) direct effect on cancer cells; ii) stimulation of the neo-angiogenesis process; iii) trans-differentiation into other components of the tumor stroma, such as CAFs; iv) immunomodulation. Furthermore, the establishment of the crosstalk with tumor cells could promote the trans-differentiation of BM-MSCs towards different tumor stromal cells, such as CAFs, pericytes and endothelial cells [364,374]. BM-MSCs were incubated for 48h with OS CM-derived. To determine which kind of soluble factors produced by OS cells could stimulate their trans-differentiation, the expression of established markers of endothelial cells and pericytes were analyzed through flow cytometry, respectively: CD31 and neural/glial antigen 2 (NG2). As shown in Fig. 2A, following the treatment of BM-MSCs with CMs, the levels of CD31 and NG2 are undetectable. Furthermore, to analyze a possible trans-differentiation into CAF-like cells, we measured the expression of α-SMA and collagen I-α1 in tumor-activated BM-MSCs through Western Blot analysis. We found that the levels of both proteins significantly increase after CM from OS exposure (Fig.2B). Notable, according with our results, the contraction capacities of BM-MSCs are potentiated after conditioning with CM from HOS cells (Fig. 2C). All together these data confirm the trans-differentiation of BM-MSCs towards a CAF-like phenotype after the contact with the tumor CM. Consequently, we investigated if the acquisition of this activated phenotype could in turn improve the pro-tumorigenic activity of BM-MSCs. A crucial step in the progression of tumor malignancy, is the trans-endothelial migration, the passage of cells from the tumor stroma to the lumen of the blood vessel. Thus, we prepared CM derived from BM-MSCs which were maintained in St Med (CM BM-MSCsSt) or stimulated with CM derived from HOS cells (CM BM-MSCs^{HOS}) for 48 h. We chose HOS cells since they display the more aggressive

phenotype in terms of invasion and migration potential [375,376]. HOS were treated for 48 h with CM BM-MSCs-derived and then, we evaluated the migration, invasion and trans-endothelial migration abilities. The migration assay was performed as already described for BM-MSCs. with the only difference that in the upper part of the transwell, adhering to the porous membrane was placed a layer of Matrigel in a concentration of 50μg/cm^2. Considering the phenotypic differences of the 3 OS lines, assays were performed with different cell numbers and times depending on the line used. In particular, 5 x 10^4 HOS cells and 1x10^5 Saos-2 and MG-63 cells were plated. The trans-endothelial migration was performed by plating 5x10^4 endothelial cells (ECs) on the bottom of each transwell to form a monolayer that mimics the wall of the vessel. The ECs used in the assays were HUVECs, pretreated for 24h with TNF-α 10 ng/mL, to promote the formation of tight junctions between cells. OS cells were conditioned with the CMs of the BM-MSCs 24h before the assay and labeled with carboxyfluorescein succinimidyl ester (CFSE). At the end of the test the transwells were fixed in methanol, observed under a fluorescence microscope, and photographed. We found that both BM-MSCsSt and BM-MSCs^{HOS} potentiate the invasive behavior of OS cells, suggesting an increase of OS malignancy induced by BM-MSCs despite their activation levels (Fig 2D-F).

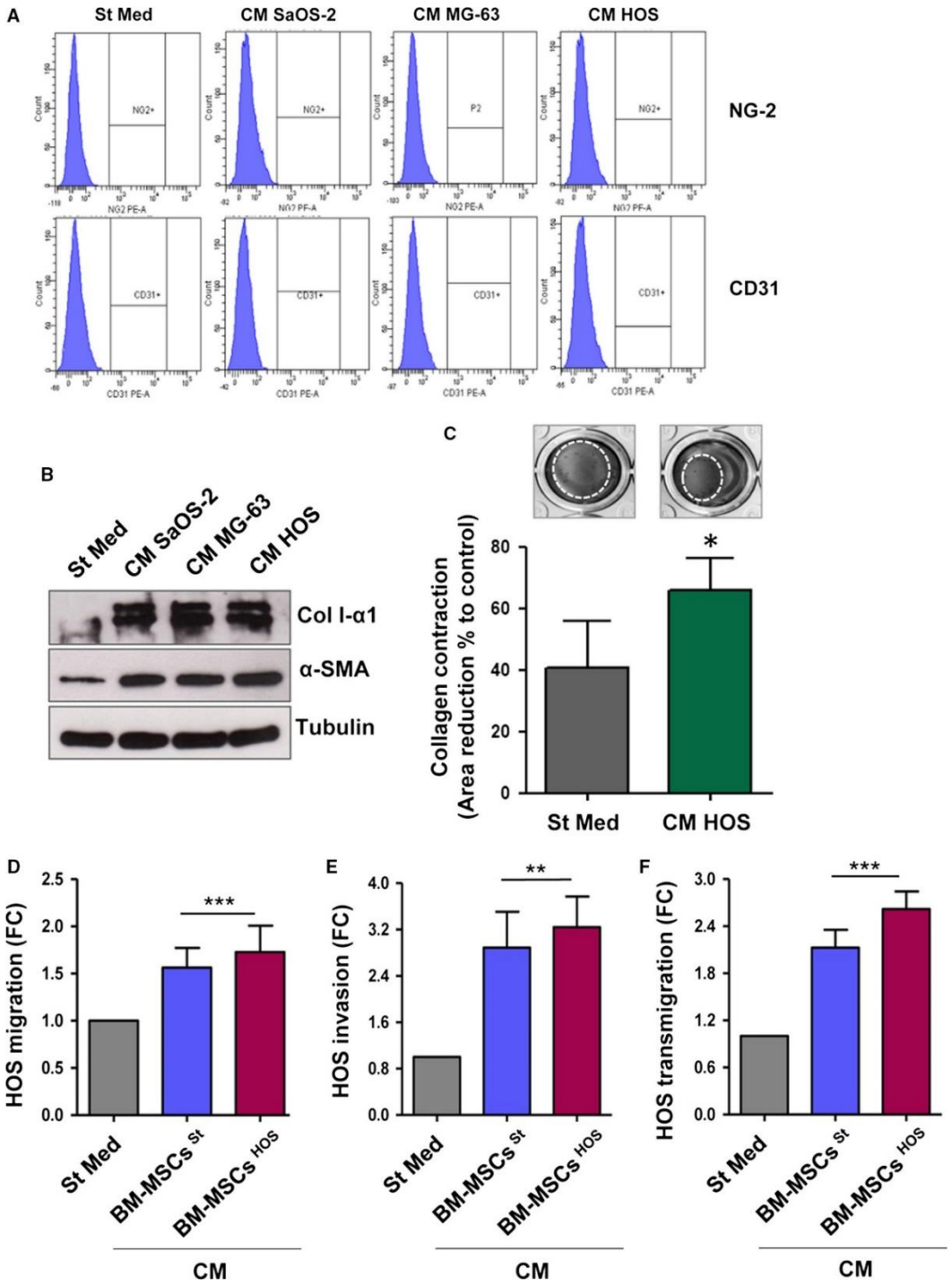

Figure 2. CM derived from OS cells stimulates the BM-MSCs trans-differentiation into CAF-like cells. (A) FACS analysis of NG-2 and CD31 expression in BM-MSCs treated for 48 h with CM OS cells. (B) Immunoblot analysis evaluating α-SMA and Col I-α1 performed on BM-MSCs stimulated for 48 h with CM derived from OS cells. (C) Collagen contraction assay of BM-MSCs treated for 24 h with St Med or HOS CM. Data are expressed as percentages of the relative area of collagen disc following contraction in comparison with an empty well. (D) Migration assay of HOS cells stimulated for 48 h with CM derived from BM-MSCs previously activated or not activated by CM of tumor cells (CM BM-MSCs $^{St/HOS}$). Cells were let to migrate toward complete medium (FBS 10%). (E) Invasion and transmigration (F) assays of HOS cells treated as in (D). Mean ± SD, n = 3 independent experiments. ** $P < 0.005$ vs. St Med; *** $P < 0.001$ vs. St Med.

3.3.3 The crosstalk between BM-MSCs and OS leads OS cells towards amoeboid motility.

In recent years, it has become clear that *stimuli* from tumor microenvironment (TME), such as cell-cell or cell-ECM interactions, growth factors and cytokines produced by stromal cells, influence the abilities of cancer cells to shift from one type of motility to another. The ability of cells to take advantages from different migration strategies based on the microenvironment changes, is defined "migratory plasticity", a typical feature of more aggressive cancer cells [235,246]. As we have already described above (see Introduction), the two main single-cell migration strategies are mesenchymal motility and amoeboid motility. The MAT generally occurs in the terminal stages of the metastatic process, during blood or lymphatic dissemination. In particular, it is useful during the final steps of extravasation and colonization of the secondary site.

Then, we decided to investigate the activity and the expression of MMPs in the OS cells treated with BM-MSCs OS-derived CM, to study deeply the molecular mechanism leading to increased invasion potential of OS cells induced by BM-MSCs. In the following experiments we decided to use only CM derived from tumor-activated BM-MSCs, given that BM-MSCsSt and BM-MSCs^{HOS} showed a similar effect on OS migration capacities, mimicking the *in vivo* conditions. Through zymography assay, we confirmed that all tumors cell lines produce significant amounts of pro-gelatinases MMP-2 and MMP-9 (Fig. 3A). As you can see, HOS cells secrete the highest levels of these MMPs; but there isn't an increase of this gelatinases after the treatment with CM BM-MSCs ^{HOS}. Although MG-63 cells show a similar behavior, SaOS-2 cells exhibit an increase in pro-MMP2 following 48 h of incubation with CM derived from BM-MSCs^{SaOS}. Next, we analyzed the activation levels of the small GTPases RhoA and Rac1. After the contact with CM derived from tumor-activated BM-MSCs, there is a significant decrease of bound Rac1-GTP, with a parallel increase of bound RhoA-GTP in OS cells. Particularly, the CM treatment induces an approximately two-fold increase in the RhoA/Rac1 ratio in all the OS cell lines tested (Fig. 3B, left and right panels). These data suggest a shift in the migration strategy of OS cells from a mesenchymal to an amoeboid-like motility. Moreover, to better characterize the type of movement acquired by OS cells, we performed a confocal analysis. First, we evaluated the distribution of F-actin filaments (staining with FITC-Phalloidin). The analysis shows clearly that MG-63 cells acquire a rounded morphology and undergo a

redistribution of actin fibers as cortical rings following the treatment with CM derived from tumor-activated BM-MSCs (Fig. 3C). Accordingly, then we demonstrated that the active form of myosin light chain (p-MLC), which is the downstream of RhoA signalling, organizes in cortical rings, similar to cells treated with the RhoA activator, Calpeptin. By contrast, control cells (St Med) show an elongated morphology and actin-myosin cytoskeleton organized in parallel bundles along the cytoplasm, typical of mesenchymal phenotype. The shift toward an amoeboid motility style is also supported by live imaging of MG-63 cells in a three-dimensional collagen lattice (Fig. 3D). This assay is performed seeding the cells, labeled with CFSE, in a 3D collagen matrix, and let them to invade overnight. This technique allows the operator to verify the phenotypic movement-style of the cells in 3D matrices. Crucially, when exposed to three-dimensional matrices of type I collagen, untreated MG-63 cells move through a spindle-shaped mesenchymal and proteolytic stage. By contrast, the MG-63 cells conditioned with CM from tumor-activated BM-MSCs show a rounded squeezing movement, independent of matrix degradation, typical of amoeboid motility style.

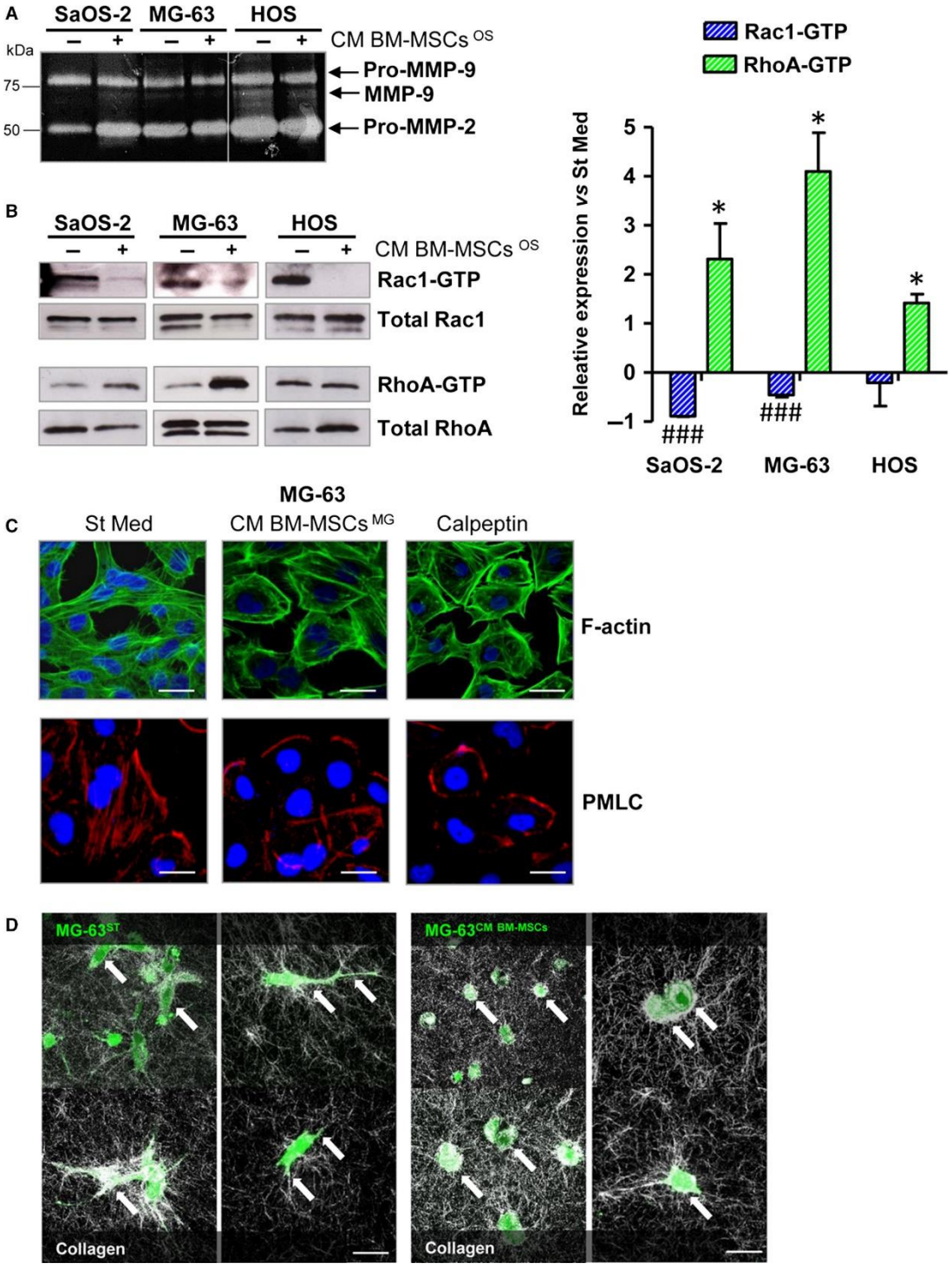
A
SaOS-2
MG-63
HOS
– + – + – +
CM BM-MSCs OS
kDa
75
50
Pro-MMP-9
MMP-9
Pro-MMP-2
B
SaOS-2
MG-63
HOS
– + – + – +
CM BM-MSCs OS
Rac1-GTP
Total Rac1
RhoA-GTP
Total RhoA
Rac1-GTP
RhoA-GTP
Releative expression vs St Med
5
4
3
2
1
0
–1
*
*
*
###
###
SaOS-2
MG-63
HOS
C
MG-63
St Med
CM BM-MSCs MG
Calpeptin
F-actin
PMLC
D
MG-63ST
MG-63CM BM-MSCs
Collagen
Collagen

Figure 3. Crosstalk between BM-MSCs and OS cells promotes the acquisition of an amoeboid-like motility in cancer cells. (A) Gelatin zymography of CM obtained from SaOS-2, MG-63 and HOS cells stimulated or not stimulated for 48 h with CM derived from BM-MSCs activated by each OS cell line (CM BM-MSCs^{OS}). The white line indicates the junction of two different gels. (B) Representative images of pull-down assay of Rac1 and RhoA GTPases (left panel) and related quantification (right panel). The assay was performed on OS cells grown for 48 h in CM from tumor-activated BM-MSCs (CM BM-MSCs OS) or in starvation medium. Rac1-GTP and RhoA-GTP expression was normalized with respect to total Rac1 and RhoA in OS lysates. ### $P < 0.001$, Rac1-GTP CM BM-MSCs vs. Rac1-GTP St Med. * $P < 0.05$, RhoA-GTP CM BM-MSCs vs. RhoA-GTP St Med. (C) Confocal analysis of F-actin (FITC phalloidin) and P-MLC staining in MG-63 cells treated or not treated with CM BM-MSCs^{MG63} for 48 h. Scale bar: 10 μm. (D) Live imaging of MG-63 cell migration in three-dimensional collagen matrix. CFSE-labeled MG-63 cells were incorporated into the collagen matrix and monitored by confocal fluorescence-reflection video microscopy. Tumor cells are visualized in green and the back-scatter signal of the collagen I is shown in white. On the left, arrows indicate the point at which MG-63, treated with ST medium, shows an elongated morphology. In MG-63 cells treated for 48 h with CM from tumor-activated BM-MSCs (right), arrowheads indicate the rounded shape of the cells squeezing across collagen I fibers. Scale bar: 20 μm.

Finally, in order to further demonstrate the shift toward an amoeboid-like motility, we performed both invasion and trans-endothelial migration assays with OS cells stimulated by CM of tumor-activated BM-MSCs and treated with a wide-range MMPs inhibitor, Ilomastat (Ilo). According to the data obtained, OS cells present a lack of sensitivity to the treatment for both assays, indeed there isn't a decrease in their invasion and migration abilities (Figs.4 A, B). Interestingly, we also observed a significant increase in the levels of tissue inhibitor of MMPs, (TIMP)-1 and -2, secretion in BM-MSCs stimulated for 48 h with CM from HOS and MG-63 cells (Fig. 4C). All together, these data suggest that the reciprocal interplay between BM-MSCs and cancer cells promotes tumor cell plasticity characterized by a shift toward an amoeboid-like phenotype.

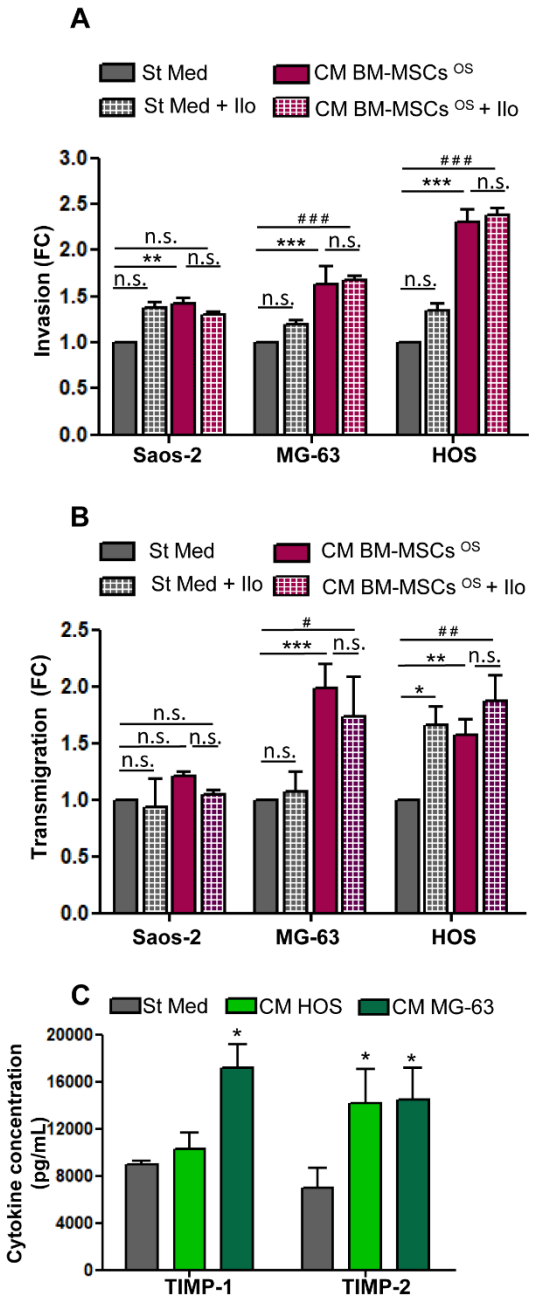

Figure 4. OS cells motility was not affected by MMPs inhibitor Ilomastat. OS cells were cultured for 48 h in St Med or CM derived from tumor-activated BM-MSCs (CM BM-MSCs ^{OS}) supplemented or not with MMPs inhibitor Ilomastat, 50 μM. The invasion (A) or trans-endothelial migration (B) was evaluated by counting migrating cells in four randomly chosen fields. * $P < 0.05$ St Med vs. St Med + Ilo; ** $P < 0.01$ St Med vs. CM BM-MSCs ^{OS}; *** $P < 0.001$ St Med vs. CM BM-MSCs ^{OS}; # $P < 0.05$ St Med vs. CM BM-MSCs ^{OS} + Ilo; ## $P < 0.01$ St Med vs. CM BM-MSCs ^{OS} + Ilo; ### $P < 0.001$ St Med vs. CM BM-MSCs ^{OS} + Ilo. (C) 3.5×10^5 BM-MSCs were starved (St Med) or conditioned with CM from HOS and MG-63 cells for 48 h. Then, BM-MSCs were starved for a further 24 h and media were collected, centrifuged and analyzed by ELISA for quantification of TIMP-1 and -2. Results are expressed as mean ± SD of three biological replicates. * $P < 0.001$ vs. St Med.

3.3.4 *GRO-a, IL-6, IL-8 and MCP-1 produced by BM-MSCs determine the migration plasticity of OS cells*

The crosstalk that occurs between BM-MSCs and OS cancer cells is mediated by soluble factors that are secreted into the TME, such as growth factors and cytokines. In order to identify the soluble factors produced by BM-MSCs responsible for changes induced in the style of motility of OS cells, we performed a cytokine immunoarray of CM derived from unconditioned and tumor-activated BM-MSCs (Fig. 5A). Expression value > 10 000 arbitrary units was set to identify a threshold for cytokines to be considered. The cytokine immunoarray is an assay that allows to analyze the expression of 80 cytokines and growth factors simultaneously in the medium. It is a test based on an ELISA assay that uses several antibodies fixed on a membrane that bind cytokines. A secondary antibody HRP-streptavidin conjugated is then used, following the addition of its own substrate, develops an enzymatic reaction that produces a colored product visible in chemiluminescence in correspondence with the antigen complex. The expression of each protein is evaluated thanks to densitometric analysis, carried out through the ImageJ software. As shown in Fig. 5A, among the 80 cytokines, we found detectable spots of GRO-α, IL-6, IL8, osteoprotegerin (OPG), a decoy receptor of RANKL, MCP-1, TIMP-1 and TIMP-2. The relative bar plot is showed in Fig. 5B.

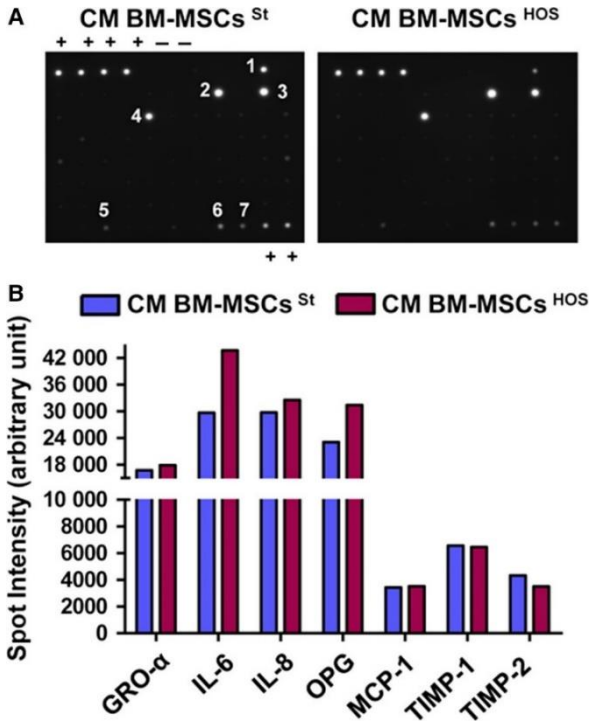

Figure 5. BM-MSCs secrete a specific pattern of cytokines and growth factors. (A) CM from BM-MSCs grown in St Med or HOS CM was collected and analyzed with Human Cytokine Antibody Array according to manufacturer's protocol; (1) GRO; (2) IL-6; (3) IL-8; (4) MCP1; (5) OPG; (6) TIMP-1; (7) TIMP-2. (B) Bar graph reporting the spot density quantified on each membrane with ImageJ. Expression values > 10 000 arbitrary units were set to identify a threshold for cytokines to be considered.

To verify if different OS cell lines share this pattern of cytokines and growth factors, we stimulated BM-MSCs isolated from two different donors with CM from both HOS and MG cells. Levels of GRO-α, IL-6, IL-8 and MCP-1 were measured by ELISA immunoassay (Table 1). As shown, we confirmed that even if some differences in cytokines concentration are present at the basal level, due to intra-individual variability, the amount of these cytokines is similar between the two donors. Furthermore, the increase of cytokines expression following conditioning with CM from both OS cell lines (HOS and MG-63) follows a similar trend, suggesting the crucial role of these cytokines in promoting aggressiveness of OS cell lines.

	BM-MSC 1			**BM-MSC 2**		
	St Med	CM HOS	CM MG-63	St Med	CM HOS	CM MG-63
GRO-a	7 pg mL $^{-1}$ ±0,2	11 pg mL $^{-1}$ ±1	13 pg mL $^{-1}$ ±1	6 pg mL $^{-1}$ ±0,1	8 pg mL $^{-1}$ ±0,3	28 pg mL $^{-1}$ ±9
IL-6	11 pg mL $^{-1}$ ±3	24 pg mL $^{-1}$ ±5	700 pg mL $^{-1}$ ±190	79 pg mL $^{-1}$ ±13	223 pg mL $^{-1}$ ±13	6557 pg mL $^{-1}$ ±223
IL-8	6 pg mL $^{-1}$ ±0,33	50 pg mL $^{-1}$ ±6	177 pg mL $^{-1}$ ±20	10 pg mL $^{-1}$ ±2	42 pg mL $^{-1}$ ±12	382 pg mL $^{-1}$ ±73
MCP-1	89 pg mL $^{-1}$ ±21	598 pg mL $^{-1}$ ±151	647 pg mL $^{-1}$ ±120	783,9 pg mL $^{-1}$ ±151	1104,9 pg mL $^{-1}$ ±126	991,8 pg mL $^{-1}$ ±177

Table 1. BM-MSCs isolated from two different healthy donors (BM-MSC 1 and 2) were grown to confluence, then serum-starved (St Med) or stimulated with CM from HOS and MG-63 cells for 48 h. The media were replaced with St Med for another 24 h, then collected, clarified by centrifugation and analyzed by ELISA

To validate the role of these factors in modulating the migratory abilities of cancer cells, we performed invasion and transmigration assay on HOS cells stimulated with CM BM-MSCs ^{HOS} and then treated or not with neutralizing antibodies against IL-6, IL-8, MCP-1 and SB225002. As showed in Fig 6A, the invasion of cancer cells is strongly dependent on this pattern of cytokines. In particular, the inhibitors of IL-6 and GRO-α drastically impairs HOS cell invasion. On the other hand, HOS transmigration is significantly affected by IL-8 and MCP-1 inhibition. By contrast, blocking GRO-α signalling does not affect the migration of cancer cells across the endothelial monolayer (Fig 6B).

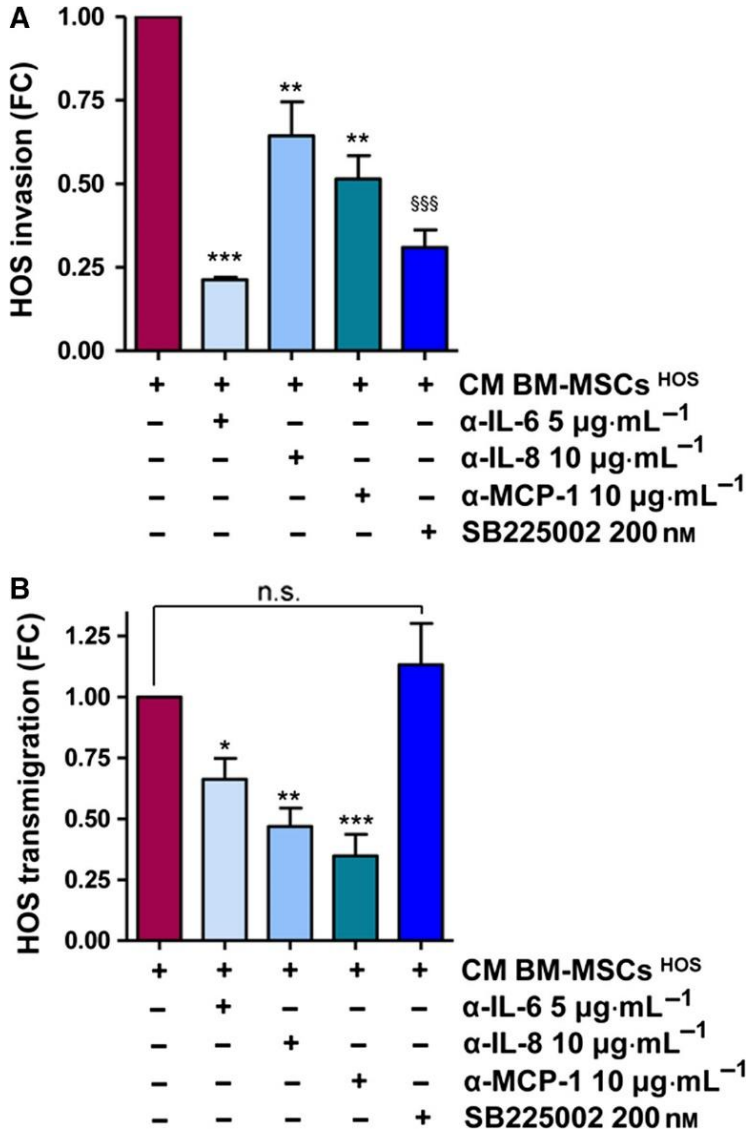

Figure 6. The pro-tumorigenic activities of BM-MSCs depend on GRO-α, IL-6, IL-8 and MCP-1 secretion. (A) Invasion assay of HOS cells treated with CM BM-MSCs ^{HOS} supplemented or not with antibodies against IL-6 (5 µg/mL^{-1}), IL-8 (10 µg/mL^{-1}) and MCP-1 (10 µg/mL^{-1}) and GRO-α receptor inhibitor (SB 225002, 200 nM). ** P < 0.005 CM BM-MSCs^{HOS} vs. CM BM-MSCs^{HOS} + α-IL-8 and CM BM-MSCs^{HOS} vs. CM BM-MSCs^{HOS} + α-MCP-1; *** P < 0.001, CM BM-MSCs ^{HOS} vs. CM BM-MSCs ^{HOS} + α-IL-6; §§§ P < 0.001, CM BM-MSCs HOS vs. CM BM-MSCs ^{HOS} + SB 225002. (B) Trans-endothelial migration assay of HOS cells treated as in (A). * P < 0.05, CM BM-MSCs^{HOS} vs. CM BM-MSCs^{HOS} + α-IL-6; ** P < 0.005, CM BM-MSCs^{HOS} vs. CM BM-MSCs^{HOS} + α-IL-8; *** P < 0.001, CM BM-MSCs^{HOS} vs. CM BM-MSCs^{HOS} + α-MCP-1.

3.4 Discussion

The TME is a complex *milieu* consisting of cells, signalling molecules and ECM that supports tumor growth and progression. Several studies, both *in vitro* and *in vivo*, have demonstrated high tropism of BM-MSCs for different types of primary tumors. Many cytokines and growth factors, have been found involved in recruiting MSCs from their *niche* in the bone marrow towards different types of epithelial carcinoma, such as melanoma, breast, prostatic, hepatic, and ovarian cancer [350–355]. Here, we investigated the effects induced by the cross-talk between BM-MSCs and OS cells on tumor malignancy. First, we found that BM-MSCs are efficiently recruited by three different OS cell lines (SaOS-2, MG-63 and HOS) identifying MCP-1, GRO-α and TGF-β1 as key molecules in promoting this tropism. We excluded the involvement of CXCR4/SDF-1 axis in this migration. In agreement with our results, several reports indicate that BM-MSCs secrete high levels of SDF-1 but express low levels of CXCR4, whereas OS cells release small amounts of SDF-1 but express elevated levels of CXCR4, crucial to promote the metastatic spread of the tumor to the lung [366,377,378].

It is well known that, following cytokine and growth factor stimulation, BM-MSCs trans-differentiate into different stromal components, leading to promotion of tumor aggressiveness. We have demonstrated that BM-MSCs, subsequent to the contact with CM from OS cells, trans-differentiate into α-SMA-expressing fibroblasts, CAFs. Unexpectedly, we observed that activated CAF-like BM-MSCs induce a comparable increase in the migratory/invasive abilities of OS cells with respect to non-activated BM-MSCs. Most probably because we tested only standard conditions (without hypoxia or acidosis), and because OS is a mesenchymal tumor with a high aggressiveness.

Once engrafted into the TME, BM-MSCs are able to encourage tumor growth and progression. Accordingly with data in literature, showing that cytokines secreted by BM-MSCs, not previously in contact with cancer cells, can directly support proliferation and migration of tumor cells [355,379–381], we demonstrated that BM-MSCs promote both invasion and trans-endothelial migration of OS cells, suggesting an increase in the metastatic potential of cancer cells. This mutual interaction between BM-MSCs and OS cells is led by the mesenchymal stroma, activated by tumor cells itself, which secretes higher levels of

IL-6, IL-8, GRO-α and MCP-1 in the TME; OS cells, in turn, due to the changes of the microenvironment, undergo MAT, further enhancing their aggressiveness, increasing invasion and trans-endothelial migration abilities and, consequently, their metastatic potential. We have demonstrated that recruited BM-MSCs promote a shift to an amoeboid phenotype in OS cells. In keeping with our results, *Cortini et al.* [382], have recently demonstrated that IL-6 secreted by the mesenchymal stroma is critical to promote OS stemness and migratory potential. In line with this, a previous work by our group showed that CAFs co-operate with endothelial progenitor cells to engage a clear MAT in prostate cancer cells critical to promote cancer cell adhesion to endothelium and trans-endothelial migration [247]. To date, very little is known about the molecular mechanisms that govern this transition. In the present study, we showed that BM-MSCs promote MAT in OS cells through the secretion of a specific pattern of cytokines: GRO-α, IL-6, IL-8 and MCP-1. We demonstrated that each of these cytokines, particularly IL-6 and GRO-α, modulates the invasive behavior of tumor cells, using specific inhibitors. By contrast, the mechanism of trans-endothelial migration is completely independent of GRO-α/CXCR2 signalling. According to our results, it has been reported that in squamous carcinoma cells, melanoma and stromal fibroblasts, IL-6 pathway activates ROCK and generates a high level of actomyosin contractility [220]. Additionally, it has been shown that the activation of IL-8 signalling pathways leads to RhoA activation and actin stress fibers formation in cancer and endothelial cells [383,384]. Lastly, several studies have showed that MCP-1 secreted by tumoral and stromal cells induces trans-endothelial migration of monocytes, T cells, smooth muscle cells and adult neural stem cells [385–387]. Moreover, in our study, given to the differences in morphology, aggressiveness and proliferation kinetics of three different OS cell lines, due to the dissimilar genetic mutations [376,388], we characterized the response of each cell lines investigated. In particular, following the contact with CM from BM-MSCs, SaOS-2 cells seem to act in a different manner compared with MG-63 and HOS cells with regard to cell migration and MMPs expression. This effect is probably due to their prominent mesenchymal phenotype. On the other hand, SaOS-2 cells showed the higher reduction of the active form of Rac-1, underlining that the mesenchymal stromal compartment can strongly affect the tumor cell phenotype and thus in the OS evolution.

Interestingly, we showed that the pattern of cytokines secreted by both BM-MSCs and OS cells is very similar, confirming the common mesenchymal origin of these two cell types

[372,373]. Most likely, the recruitment of BM-MSCs to the tumor site promotes a local increase of the cytokines which are already produced by tumor cells themselves. Thus, both cell populations concurrently contribute to the generation of a *milieu* enriched in cytokines, which stimulates in an additive manner the migratory and invasive properties of OS cells. In conclusion our data indicate that the recruitment of BM-MSCs into the OS stroma is a crucial event to promote tumor progression. Crucially, both recruitment of BM-MSCs to the OS site and cytokine-induced MAT of tumor cells represent innovative targets to test *in vivo* OS models to design innovative therapeutic approaches aiming to hinder the metastatic dissemination of OS cells.

To date, less is still known about MSCs promoting osteosarcoma mechanisms. Moreover, there is not new evidence describing the role of BM-MSCs in MAT promotion in tumors. Nevertheless, a fascinating debate is still open about the role of BM-MSCs in tumor progression or suppression (our laboratory recently published an interestingly review describing also this topic [389]). For instance, Zhang et al., lately, described the role of miR-206 exosomal BM-MSCs derived as tumor suppressor [390], already known to be involved as inhibitor of malignant progression in osteosarcoma cells, targeting Notch3 signaling [391]. Whereas Qin et al, described microRNA-208a exosomal MSCs-derived as promoter of proliferation, invasiveness and aggressiveness of osteosarcoma cells [392]. These recent papers illustrate clear as the crosstalk between osteosarcoma and MSCs in tumor progression is still largely unclear, needing further investigations.

4. Part 2

4.1 Malignant melanoma

Melanoma is a malignancy that affect the melanocytes, a melanin-producing cells resident in the basal layer of the epidermis. Normally melanocytes are responsible for the basic pigmentation of the skin, and for the protection versus UV lights [393].

Metastatic melanoma is one of the most aggressive and lethal malignancies with a poor prognosis. Indeed, until cancer cells remain localized into the skin compartment, melanoma patients generally have a better outcome, but once they spread to distant organs, mostly to the brain, lungs, liver, and small bowel, life expectancy strongly decreases. Even if in recent years, with the immunotherapy admission, the overall survival seems to be increased [394], new therapies aimed at targeting invasive cells and prevent their metastatic dissemination are urgently needed.

Etiology

Nowadays melanoma is considered as a multi-factorial disease, indeed, in the pathogenesis of melanoma are involved several factors both environmental and genetic. One of the most important environmental risk is UVs radiation. There is a direct correlation between time of exposure under the sun and risk of melanoma [395]. On the other hand, genetic factors are particularly important for the pathogenesis of melanomas, the mutations involved could activate oncogenes or inactivate tumor-suppressor genes.

Data published in the Cancer Genome Atlas (TCGA) Network classified melanomas on the basis of the mutations that are found: with mutations in *BRAF*, *RAS*, *NF1* and the so-called triple negative melanomas [396,397].

BRAF or *RAS* mutations are the most common in primary melanomas, generally not observed concomitantly, while, in 13-25% of the case, have been co-reported with mutations in *NRAS* gene. All these genes are involved in MAPK pathways, its constitutive activation, present in the 98% of melanomas, promote cellular proliferation, survival and angiogenesis [398,399]. The most recent data of Pan-Cancer Analysis of Whole Genomes highlighted that in 107 melanomas analyzed have been found 52 mutations of *BRAF*, 20 in *TP53* and 74 in *TERT*, moreover it was discovered frequently mutated genes *CDKN2A* (also called ARF or p16-INK4) and *CDKN2B*, both involved in cell cycle regulation [400]. While some of these genes mutated (*BRAF*, *NRAS* and *TERT*) are present in benign and

malignant lesions, alterations in *CDKN2A*, *TP53* and *PTEN* are observed only in invasive melanomas [401].

Although transformation of melanocytes to melanoma cells is still largely unclear, several molecular pathways seems to be involved in progression of normal melanocyte to metastatic malignant cells, such us a polymorphism on melanocortin 1 receptor gene (MC1R) [402–404].

Furthermore, alteration of cell cycle proteins has a key role in transformation and progression in melanocytic tumors. It has been demonstrated that the loss of p16 could be involved in transformation from benign nevi to melanoma and to metastatic melanoma as well as increased expression of cyclin D1 and pRb is associated with progression to melanoma cells [405]. Higher expression of protease-activated receptor- 1 (PAR-1), that mediates high levels of Cx-43, has been observed in melanoma cell lines and tissue specimens. This molecule is involved in tumor cell diapedesis and attachment to endothelial cells [406]. It is also shown that downregulation of E-cadherin and upregulation of N-cadherin could have a role in proliferation, invasion, and migration in melanoma cells [407]. Moreover, the *Sviatoha et al.* demonstrated that there is a higher expression of CD44 antigen in melanomas with known metastases than in those without metastases, but this difference was not statistically significant [408]. Finally, the interaction of the transcription factor E2F-1 with EGFR can act as driving force in melanoma progression [409].

Epidemiology

Malignant melanoma accounts for 1% of skin tumors and causes of 60% mortality due to skin cancers. Over the past four decades, the incidence of melanoma has been increase worldwide and is currently the highest incidence in Australia, with 40/100.000 of new cases per year [410]. The incidence of melanoma is not equal in men and women, with higher incident in women, but is uncommon in children. Taking age into account, adolescent and young adult women are more susceptible to melanoma than men. This could be due to the different way of the sun exposure among females. By contrast after the 40 years old, rates reverse, and melanoma incidence among men is greater than that of women. If considering overall, men are more susceptible to melanoma [411].

The incidence of melanoma is uneven also among ethinicity. For instance, in the United States, melanoma is 15 times more common in whites than blacks. Moreover, in groups with low economic status, the mortality rate is higher [410]. The most important risk factor

for malignant melanoma is the presence of etiologic melanocytic macules with a melanoma family history, which increases the risk of 2-8 times. The incidence of melanoma worldwide is related to geographic site, indeed the United States Academy of Dermatology has reported that melanoma is prevalent in Australia and New Zealand, but it is also common in Asia, Africa and Latin America. In the United States, Europe and Australia, 25, 20 and 45% of reported cancers, respectively, in one year are skin cancers. [410,412]. A representative study showed that the most common sites are the trunk (43.5%), extremities (33.9%), acral sites (11.9%), and head and neck (10.7%) [413,414]. Head, neck, and extremity melanomas are associated with chronic sun exposure, whereas truncal lesions are associated with intermittent UV radiations [415,416]. Nowadays, there the mortality rate of this disease continues to rise and it is influenced by age, sex, ethnicity and geography [411]. Median survival rates after metastasis occurs have been reported as from 6 to 9 months, with records of a 5-year survival rate less than 5% to 10% [415,417,418]. For these reasons new therapies are needed.

Current therapy

The first-line treatment for malignant melanoma is surgical resection, but in about 20% of patients who undergo surgical resection involved in a metastatic relapse following their primary treatment of melanoma and their prognosis is poor, with a median survival under 12 months, if untreated. Starting from 2011, dacarbazine was used as the international standard cytotoxic chemotherapy for metastatic melanoma, offering at best a 15% objective response rate. However, in the last decade, scientific progresses have led to an extraordinary shift in management of more aggressive melanoma. Two new agents were approved in 2011 and 2012 with survival benefit. They derived from two different classes of molecules: inhibitors of the MAPK pathway and antibodies against immune checkpoint [419].

First of all, vemurafenib (and then dabrafenib), an oral biological serine/threonine kinase inhibitor targeting BRAF, was approved for use in patients with metastatic melanoma with a BRAFV600 gene mutation. Randomized trials of vemurafenib [420,421], and the more recently of dabrafenib [422], showed a good response rate, around 50%. Unfortunately, it has been described the development of resistance, with a median progression-free survival (PFSs) little major of six months. Additionally, these treatments cause several side effects,

among them has been reported: photosensitivity (occurring within days of starting the treatment), rash, myalgia, fatigue, arthralgia and incidence of other skin lesions. [423].

As regard the immunotherapeutic approaches, ipilimumab is a humanized monoclonal antibody blocking CTLA4, which it was licensed in Europe in the 2011 for the treatment of advanced melanoma patients who have already received systemic therapy. It was demonstrated, by an international multi-center randomized trial, a gained in survival rate of 10.1 months after the treated group compared with 6.4 months of the control group [424]. In a second randomized study, with patients affect by untreated metastatic melanoma, standard treatment with dacarbazine or combined treatment with dacarbazine and ipilimumab was evaluated; the survival rate was significantly higher in the combined treatment group (11.2 months versus 9.1 months, HR= 0.72, P = 0.0009) [425]. On the other hand, 1 on 10 patients treated with ipilimumab develops immune-related side effects including: colitis, skin reactions and endocrinopathies [426].

Nowadays the numbers of immune checkpoint molecules developed are increasing, and ipilimumab as single agents and in combination with BRAF/MEK inhibitors or nivolumab are the standard therapies in melanoma which developed resistance to other therapies or become metastatic [427]. Moreover, there are other promising T-cell immune checkpoints targets like TIM-3, LAG3, KIR, VISTA as well as oncolytic viruses for which new treatments are being developed [427]. Determining the optimal combinations will be one of the main challenges for the future therapies.

4.2 Honokiol (HNK)

Honokiol (HNK) is a biphenolic compound found in the extracts of *Magnolia officinalis*, *Magnolia obovate*, and *Magnolia grandiflora* (Fig. 8). For centuries it has been used in traditional Chinese medicines for the treatment of a wide range of the disorders [428–430].

Figure 8. Magnolia officinalis, Magnolia obovate and Magnolia grandiflora, respectively.

HNK exerts several biological activities such as anti-microbial [431,432], anti-fungal [433], anti-inflammatory [434] , anxiolytic [435,436], anti-depressant [437,438], antiarrhythmic [439], anti-oxidative [440], neuroprotective [434,441], anti-angiogenesis [442,443], anti-nociceptive [444], anti-thrombocytic [445], anti-spasmodic [446], gamma-aminobutyric acid (GABA) modulator [447] and anti-human immunodeficiency virus (HIV) [448]. Moreover, both *in vitro* and *in vivo* studies have demonstrated the efficacy of HNK as antitumoral treatment in many cancers such as hepatocarcinoma lung, breast, colon, prostate and skin cancer [449]. But HNK anti-cancer activity is still to be defined clinically.

The effects of HNK are exerted through modulation of the expression of several genes involved in different hallmarks of cancer including:

Cell cycle

HNK modulates several proteins involved in the cell cycle [450,451]. Indeed, in human gastric carcinoma and human neuroglioma cells HNK decreases the expression of cyclin-B1, CDC2, and CDC25C [452,453]. *Huang K.J. et al.*, have been reported that, in human oral squamous cell carcinoma (OSCC) cells, HNK reduces proliferation by downregulation of cyclin dependent kinase (CDK)-2 and CDK-4 and overexpressing of p21 and p27[454]. Moreover, HNK arrests cell cycle in prostate cancer cells by downregulating the expression of c-Myc [455].

Apoptosis

HNK increases the expression of the pro-apoptotic proteins Bax, Bid and Bak and decreases the expression of the anti-apoptotic proteins Bcl-2 and Bcl-XL, *in vitro* as well as *in vivo*. Furthermore, HNK induces the release of cytochrome c into the cytosol activating caspase cascades [456,457].

EGFR signaling

HKN acts on EGFR signaling decreasing its expression by inhibiting its phosphorylation [458–460]. Indeed, overexpression of EGFR, found in several kind of tumors, trigger an altered metabolism enhancing cell survival and proliferation [461–463]. HNK decreases EGFR expression both *in vitro* and *in xenograft* mouse models of head and neck squamous cell carcinoma (HNSCC). Furthermore, molecular docking analysis demonstrated that HNK binds and inhibits EGFR with better binding affinity than the inhibitor used in clinical therapy: gefitinib [459].

STAT3, mTOR and NF-κB pathway

STAT3 is involved in various physiological and unphysiological processes such as metabolism, differentiation, immunity as well as cancer [464]. Studies have demonstrated that HNK downregulates STAT3 expression both *in vitro* and *in vivo* [465,466].

mTOR controls numerous cellular processes such as cell growth, proliferation, and metabolism. In cancer, mTOR pathway is constitutively activated by the upregulation of PI3K/Akt pathway [72]. HNK inhibits the activation of mTOR downregulating the ERK pathway and suppressing the mTOR signaling mediators 4E-BP1 and p70 S6 kinase through overexpressing of PTEN. It has been shown that in breast cancer cells the combination of Rapamycin, an inhibitor of mTOR, with HNK increased the apoptosis [458,467]. Additionally, HNK through the downregulation of the PI3K/mTOR pathway reduces the immuno-resistance of several cancer *in vitro* such as breast, glioblastoma, and prostate cancer [468].

NF- κB is involved in early and late developmental stages of cancer, in which is constitutively expressed, but it regulates also in several biological processes such as differentiation, immunity and metabolism [469]. It was demonstrated that HNK inhibits NF-κB activation via Akt signaling pathway suppression. Moreover, HNK, modulating NF-κB pathway, inhibits invasion and osteoclastogenesis and increases cell apoptosis [470].

Autophagy

Autophagy is a mechanism which allows the cell to orderly disassemble and recycle different cellular component. Autophagy is a promising target for cancer therapy because counteracts different malignancies by supporting cell death [471,472]. It has been demonstrated that HNK activates autophagy in cancer models by several preclinical studies. For example, in human osteosarcoma cells, HNK stimulates autophagic cell death through ROS/ERK1/2 and PI3K/Akt/mTOR signaling pathways [473,474], in KRAS mutant lung cancer cells HNK induces autophagy by regulating the AMPK-mTOR signaling pathway [475] and in neuroblastoma cells by activation of the PI3K/Akt/mTOR and ERK1/2 pathways [476,477].

4.2.1 A Honokiol analogue: Claisened Hexafluoro

Due to the increasing popularity of HNK in modern medical research, several new synthetic analogues have been synthesized and some of them have been developed for delivery through oral, liposomal, intravenous and transdermal preparations [478–481]

Claisened hexafluoro is obtained by adding bis-trifluoro-methyl radicals to Honokiol (Fig. 9).

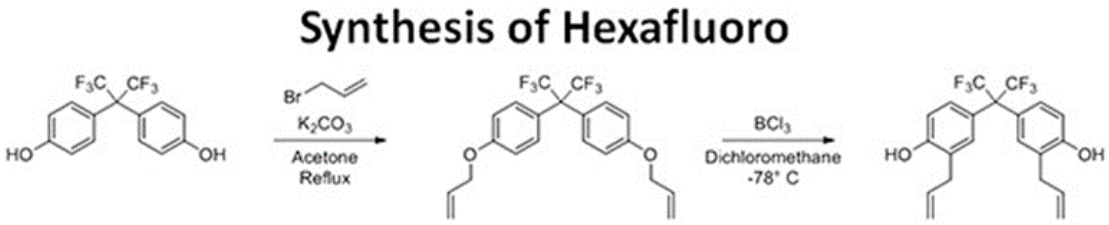

Figure 9. Synthesis of honokiol analogs: Claisened Hexafluoro. (Figure from Bonner et.al 2016)

Although the mechanisms of action of this compound are still to be clarified, it has been shown that Claisened hexafluoro regulates the expression of SIRT3 mitigating the organ fibrosis. Indeed, Claisened hexafluoro impairs the downstream TGF-β signaling, decreasing the phosphorylation of Smad 2/3 proteins and increasing the levels of SIRT3 expression, therefore suppressing the transcription of fibrotic genes [482]. Since SIRT3 is a sirtuin protein plays a crucial role in the preservation of the integrity of the mitochondria modulating the oxidative stress and the homeostasis of fibroblasts [483]. Moreover, *Bonner M.Y et al*., demonstrated that both Honokiol's analogues, Honokiol DCA and Claisened Hexafluoro, decrease the proliferation of vemurafenib resistant melanoma *in vivo* and promote the respiration and ROS generation [484].

4.3 Aim of the project

Cell motility is a physio-pathological process occurring during embryo-morphogenesis, wound repair, angiogenesis, and immune responses, as well as during different steps of the cancer metastatic process of cancer cells [154]. Cells can adopt several migration strategies that can be divided into two main groups: single cell and collective motility. Among the first group, amoeboid and mesenchymal motilities have been described, both strictly implicated in the metastatic process but endowed with different cell morphology, adhesive [157,158,485] and contractile abilities [159,160], Rho-family GTPase signaling activity [161,233], and cytoskeletal organization [155,163,164]. In particular, amoeboid motility is described as the fastest migratory phenotype, often associated with a stem-like phenotype [248]. Cells employing amoeboid motility are characterized by rounded morphology and are able to move rapidly through the fibers of the ECM without the need for proteolytic enzymes production [224,485]. Moreover, amoeboid cells display a lack of polarization and a strong actomyosin contractility [155,213] promoted by the contraction of the actin filaments organized to form cortical rings [218]. A key player of this process is the small GTPase RhoA and its downstream effectors ROCK and MLC [212,486].

Metastatic melanoma is one of the most aggressive and lethal malignancies with a poor prognosis. Indeed, until cancer cells remain localized into the skin compartment, melanoma patients generally have a better outcome, but once they spread to distant organs, mostly to the brain, lungs, liver, and small bowel, life expectancy strongly decreases. Even if in recent years with the immunotherapy admission the overall survival seems to be increased [394], new therapies aimed at targeting invasive cells and prevent their metastatic dissemination are urgently needed.

Targeting ameboid motility in melanoma could be a promising strategy to prevent the metastatic dissemination. Indeed, melanoma cells are able to shift between mesenchymal and amoeboid motility, thus displaying a great plasticity in migration [226]. Amoeboid motility is more efficient and less energy-consuming compared to the mesenchymal strategy thus potentiating the ability to migrate in the complex and dynamic ECM

environment, even under stressful conditions, such as hypoxia [487]. For these reasons, dampening the amoeboid motility of melanoma cells may reduce the possibility of cancer cells to find a strategy to metastasize to different organs, thereby strongly increasing the hope of recovery of melanoma patients.

Claisened Hexafluoro is a chemical analog of HKL, a biphenolic compound derived from *Magnolia officinalis.* For centuries HKL has been used in traditional Chinese medicine for the treatment of a wide range of disorders, thanks to its biological activities, such as anti-inflammatory [434], antiarrhythmic [439], anti-oxidative [440], neuroprotective [434,441], anti-angiogenesis [442,443], and others [431–433,435,437,438]. Moreover, several studies have demonstrated the antitumoral efficacy of HNK in numerous cancer types, such as hepatocarcinoma, lung, breast, colon, prostate, and melanoma cancers both *in vitro* and *in vivo* [449,488] and also its ability to prevent the metastatic dissemination of breast cancer and melanoma [489,490].

Less is known about the antitumoral properties of Claisened Hexafluoro and, to date, no data are available about its mechanism of action. However, it has been recently demonstrated that Claisened Hexafluoro can regulate the expression of SIRT3, mitigating the organ fibrosis [482]. Furthermore, it decreases the proliferation of *in vivo* Vemurafenib-resistant melanoma by promoting an increase in ROS generation [484].

Starting from these evidences, we wondered whether Claisened Hexafluoro could be adopted also in the treatment of metastatic melanoma. Here we tested Claisened Hexafluoro on melanoma cells derived from lung metastasis, as an inhibitor of amoeboid motility and of *in vivo* tumor dissemination. Our results may pave the way for possible future application of this compound to fight melanoma invasion, thanks to its extraordinary effectiveness in blocking amoeboid migration.

4.4 Results

4.4.1 Claisened Hexafluoro inhibits amoeboid motility and invasion ability

To test Claisened Hexafluoro as a potential inhibitor of amoeboid motility, we utilized the human metastatic melanoma A375M6 cell line. Really, highly invasive metastatic melanoma cells are characterized by an increased amoeboid motility style [200,219,220,491]. First, we performed a crystal violet assay to determine the maximal non-toxic concentration of Claisened Hexafluoro after 24h and 48h on A375M6 (Fig.1A). On the basis of the obtained results, we decided to perform all the experiments with 10μM Claisened Hexafluoro. First of all, we tested the effect of Claisened Hexafluoro treatment on two of the main amoeboid markers: the activity of the small GTPase RhoA and the expression of EphA2 (an upstream RhoA activator) [226]. As shown in Fig 1B and 1C, Claisened Hexafluoro treatment induces a decrease of Rho-GTP level (Fig. 1B) as well as EphA2 expression (Fig. 1C). To verify whether this reduced activation in RhoA was also correlated with a decrease in cell motility, we performed invasion assays with both Boyden chamber coated with Matrigel and 3D invasion. A375M6 treated for 24h with Claisened Hexafluoro in starvation medium, were let to migrate for 5h towards complete medium (FBS 10%) (Fig.1D). As expected, the cells show a strong decrease in their invasion ability after the treatment. Next, we tested Claisened Hexafluoro on the invasion abilities of the Hs294T cells, characterized by a mesenchymal phenotype [248]. Results confirm that Claisened Hexafluoro specifically block amoeboid motility since it is not affective on mesenchymal moving cells.

In addition, the 3D invasion assay (Fig. 1F), performed on spheroids grown on agar in the presence of Matrigel, with or without Claisened Hexafluoro, confirmed a strong decrease in the invasion ability of A375M6 following the treatment.

To corroborate the obtained results, we next visualized the motility of A375M6 cells in 3D collagen I matrix, monitored by time lapse confocal video microscopy. Cells, treated with or without Claisened Hexafluoro for 24h, were seeded in a matrix of collagen and let to invade overnight. The videos and images obtained clearly show that, compared to untreated cells, Claisened Hexafluoro-treated cells almost completely lose their ability to

move with amoeboid motility and to squeeze between the collagen fibers (Fig.1G, photograms).

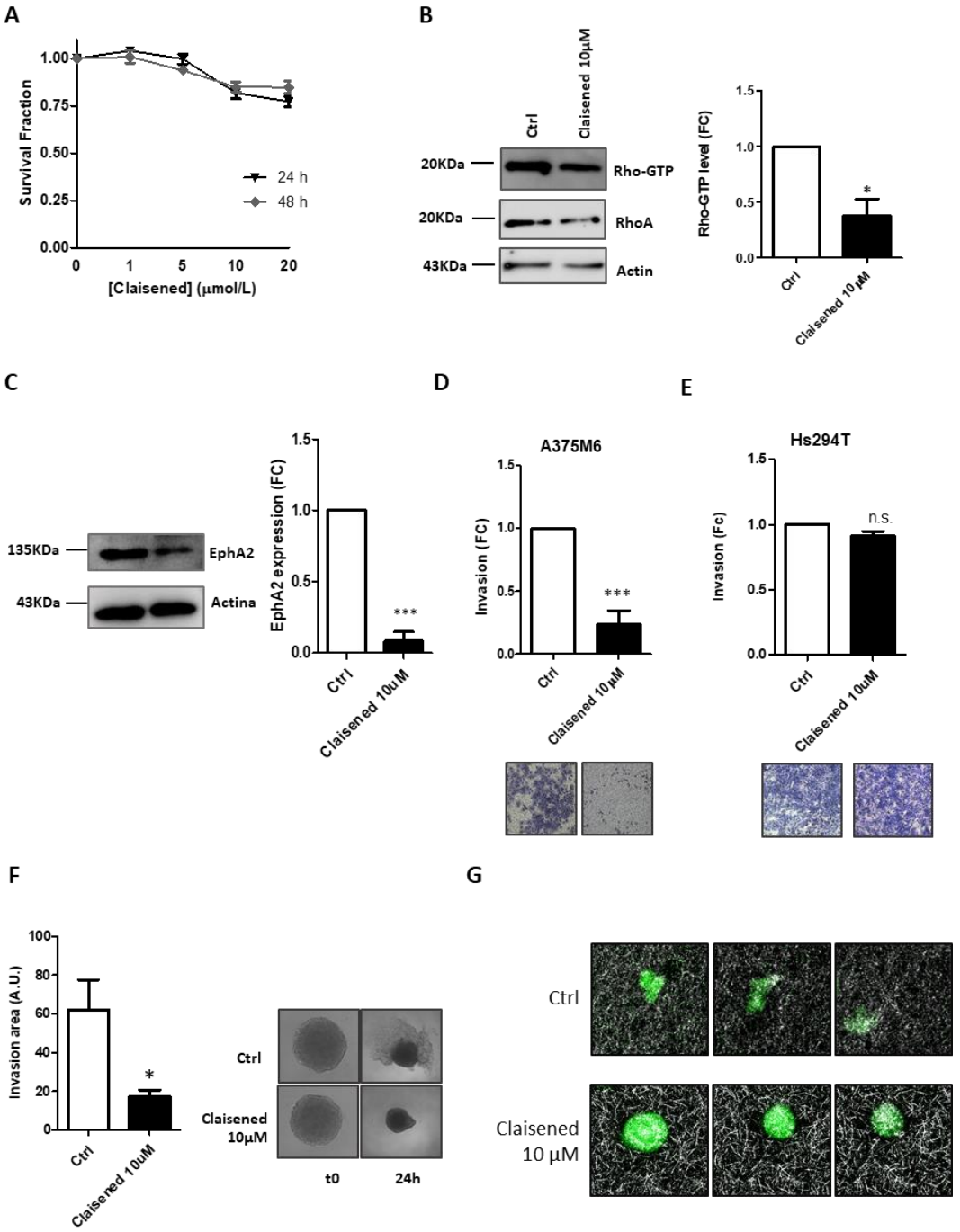

Figure 1. Treatment with Claisened Hexafluoro decreases amoeboid motility of metastatic A375M6 melanoma cells. The A375M6 cells were serum-starved for 24h and then treated for 24h or 48h with different concentration of Claisened Hexafluoro; Cristal violet assays was performed to determine the maximum no-toxic concentration (A). The cells were serum-starved for 24h and then treated with 10μM Claisened Hexafluoro. Pull Down assay was then performed to test RhoA activation. An anti-total RhoA and anti actin immunoblots were performed for normalization (B). (C) Western blot analysis was performed to test EphA2 protein levels. (D-E) Boyden Chamber invasion: A375M6 or Hs294T cells were treated as in B) then $5x10^4$ or $6x10^4$ cells (respectively) were transferred to a Boyden chamber coated with Matrigel (50 $\mu g/cm^2$) and allowed to invade for 5h or 24h toward complete medium (FBS 10%). Cell invasion was evaluated after Diff-Quick staining by counting cells in three randomly chosen fields. The results are representative of three experiments with similar results. 3D invasion assay was performed by seeding cells in 96-well plate and, following the spheroids formation (4 days), Matrigel (50 $\mu g/cm^2$) were added in each well and the cells were treated or not with Claisened Hexafluoro (10μM) for 24h (F). The pictures were then taken, and invasion area was calculated by subtracting the inner spheroid area from the total area by Image J software. (G) The cells treated or not with Claisened Hexafluoro for 24h before the assay, were seeded in a matrix collagen and a time lapse video was performed. Here are represented some photograms of the videos. Data were shown in mean ± SEM, t-test, for fig. 1 A and B; 1-way-ANOVA, for fig.1 C; * $p< 0.05$, **$p<0.01$, *** $P< 0,001$.

4.4.2 Claisened Hexafluoro decreases adhesion ability and trans-endothelium migration of A375M6 cells.

One of the first steps of metastatic dissemination is the adhesion of cells to the ECM,a crucial step for tumor cell migration [154]. To test Claisened Hexafluoro as a potential inhibitor of metastatic dissemination, we performed adhesion assays using two main ECM components: collagen and fibronectin, as supports. Cells were pre-treated for 24h with Claisened Hexafluoro, then were let to adhere for 10 minutes on plates previously coated with collagen or fibronectin. Results show that Claisened Hexafluoro decreases the adhesion ability of A375M6 cells to both ECM components (Fig. 2 A, B).

The ability of tumor cells to enter the vessels and survive into the vasculature is a fundamental prerequisite for ensuring their metastatic spread. Therefore, to investigate if Claisened Hexafluoro is able to inhibit this central metastatic step in melanoma cell dissemination, we performed an adhesion assay to the endothelium and trans-endothelial migration assay.

The adhesion assay was performed by seeding A375M6 cells onto the HUVEC's monolayer and let to adhere for 30 minutes. For the trans-endothelium migration assays cells were seeded and let to migrate overnight through the monolayer. After the treatment with Claisened Hexafluoro, we observe a decrease in the adhesion ability to the endothelium (Fig. 2C) as well as in trans-migration capacity (Fig.2 D), suggesting an

impairment of melanoma cells to enter the blood vessels and, in this way, to spread to distant organs.

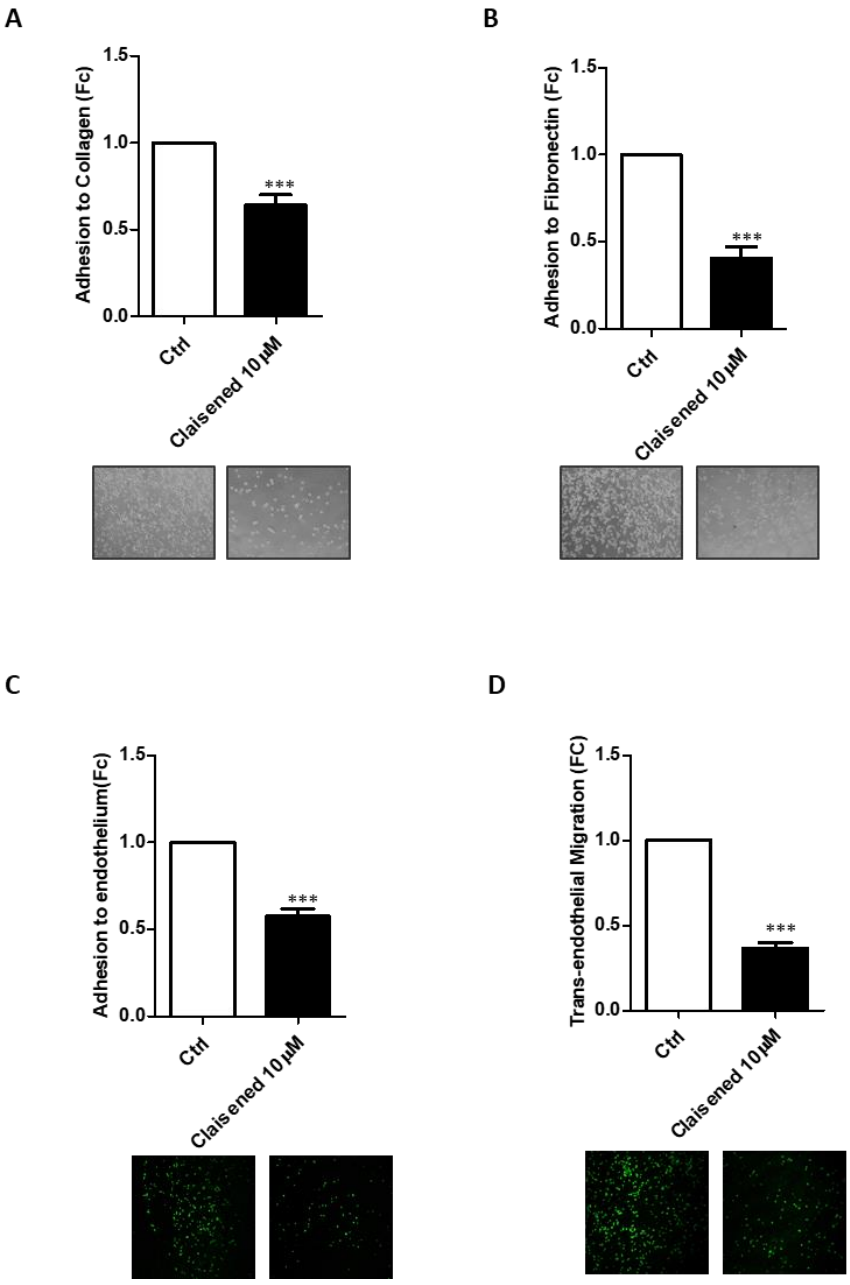

Figure 2. Claisened Hexafluoro inhibits adhesion ability of A375M6 to ECM and endothelium and trans-endothelium migration of melanoma cell. Adhesion assays to collagen (A) and fibronectin (B). Cells were let to adhere to collagen or to fibronectin coated plates for 10 minutes. Adherent cells were photographed and, then the number of attached cells was evaluated. (C) Adhesion assay to the endothelium: $3x10^5$CSFE labeled A375M6 cells, treated or not with Claisened Hexafluoro for 24h were seeded and let to adhere for 30 minutes onto a monolayer of HUVEC cells. The adherent cells were photographed using an inverted fluorescent microscope and then quantified by counting the CSFE-positive cells. (D) Trans-endothelial migration assay: Cells treated as in A) were let to migrate overnight towards complete medium. Migrated cells were photographed using an inverted fluorescent microscope and quantifiedData were shown in mean ± SEM, t-test; *** P< 0,001

4.4.3 Claisened Hexafluoro inhibits the stemness features of A375M6 cells

The amoeboid phenotype is frequently correlated with stemness features and it is often acquired by the most aggressive sub-populations within the tumor [248]. To investigate whether Claisened Hexafluoro is a potential inhibitor of the stem-like phenotype, we analyzed the expression of the main melanoma stemness markers by FACS analysis and RT-PCR.

First, we treated the A375M6 cells with or without Claisened Hexafluoro for 48h and we evaluated the expression levels of CD133 through FACS analysis. Results point out a decrease of about 40% in CD133 levels in treated cells compared to control ones (Fig. 3 A).

Moreover, we analyzed by RT-PCR the expression levels of a set of genes involved in stemness features and able to induce pluripotency [492,493]: OCT3/4, KLF4 and NANOg (Fig. 3B). The results obtained showed a decrease in the expression of all the selected markers in A375M6 cells after the treatment with Claisened Hexafluoro.

Finally, we performed a melanospheres formation assay to confirm the reduction of the stem-like phenotype following Claisened Hexafluoro treatment. This assay is based on the ability of stem cells to survive in non-adherent conditions and to self-renew in a serum-free medium [494]. The results obtained clearly show that the treatment with the compound decreases the ability of A375M6 cells to form melanospheres (Fig. 3C). Taken together, these results suggest that Claisened Hexafluoro, besides its ability to decrease amoeboid motility, acts as a potential inhibitor of melanoma stem-like phenotype.

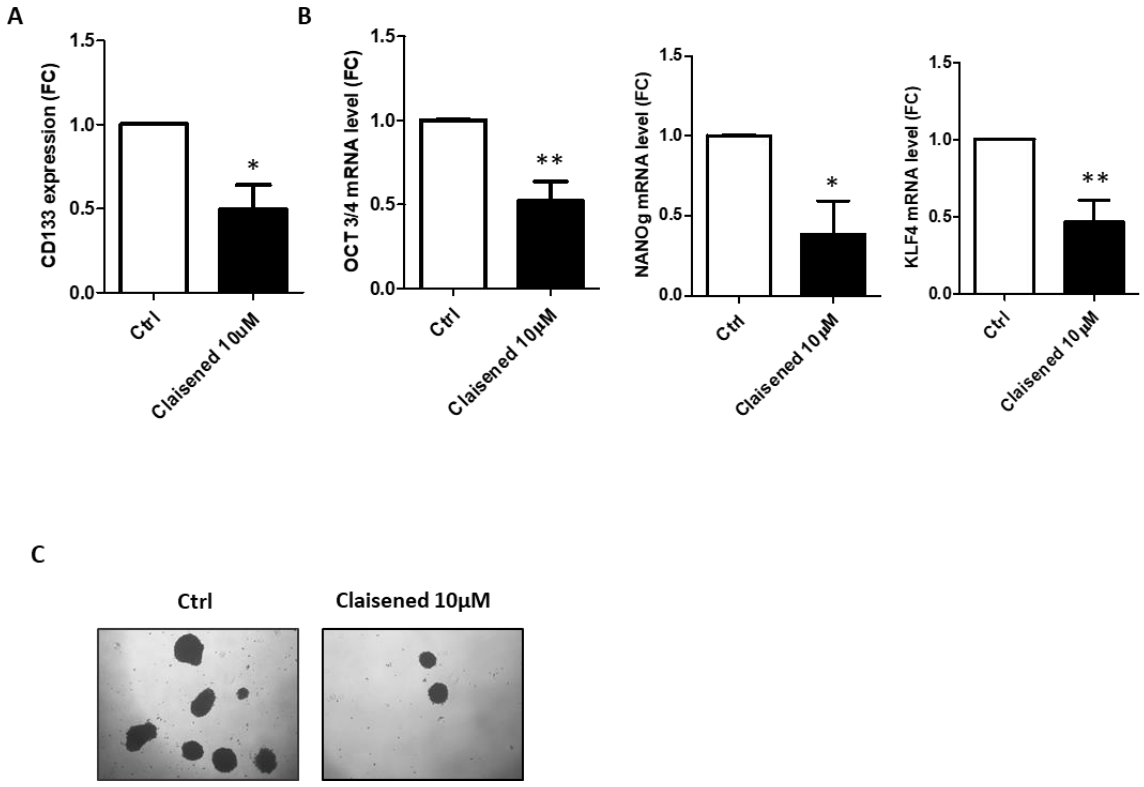

Figure 3. Claisened Hexafluoro decreases the stem-like phenotype of A375M6. (A) Percentage of CD133-positive cells: Cells were treated with Claisened Hexafluoro for 48h and then CD133 expression level was evaluated by FACS analysis. (B) OCT3/4, NANOg and KLF4 expression levels were analyzed by q-RT-PCR. (C) A375M6 cells were treated or not with Claisened Hexafluoro 10µM for 24h and then 1000 cells were seeded in a no-adherent plate (100cm^2). After 15 days the photos were taken. *Data were shown in mean ± SEM, t-test; * p< 0.05, **p<0.01, *** P< 0,001.*

4.4.4 Claisened Hexafluoro inhibits the mitochondrial activity and ATP production.

Several evidences support the existence of a strong correlation between increased motility and altered mitochondrial metabolism in cancer cells [123]. In order to evaluate whether changes in motility induced by Claisened Hexafluoro treatment are correlated with an altered mitochondrial activity, we performed Seahorse XFe96 Mito Stress analysis. A375M6 cells were pre-treated for 24h with or without 10µM Claisened Hexafluoro before performing the metabolic assay.

Interestingly, the treatment with the compound induces a strong decrease in the cellular oxygen consumption rate (OCR) both in basal conditions and after the treatment with different mitochondrial drugs (namely Oligomycin, FCCP and Rotenone/antimycin A) (Fig. 4 A, B,). In particular, the significant reduction in the ATP-linked OCR measured in treated cells indicated that the compound strongly impairs mitochondrial functionality (Fig. 4D). Moreover, treated cells also display a slight increase in OCR following FCCP injection indicating a diminished spare respiratory capacity, defined as the difference between maximal and basal respiration (Fig. 4A). In keeping with an impairment in mitochondrial functionality, we can expect that treated cells enhance glycolytic activity in trying to overcome the lack of ATP availability. Indeed, we measured higher extracellular lactate release (Fig. 4E) and decreased OCR/ECAR ratio (Fig. 4C) in A375M6 cells after 24h of treatment with the compound.

Altogether, these data suggest that the treatment with Claisened Hexafluoro impairs the mitochondrial functionality.

Mitochondrial activity disfunction frequently correlates with increased mitochondrial-ROS (mt-ROS) production [495]. In order to further confirm the compound-induced alteration in mitochondrial functionality, we assayed the mt-ROS content in treated and untreated cells. As expected, MitoSOX staining analysis pointed out a strong increase of the oxidative stress inside the mitochondria following the treatment with the compound (Fig. 4F). Furthermore, we measured the mitochondrial membrane potential by staining A375M6 cells, treated with or without Claisened Hexafluoro, with tetramethylrhodamine ethyl ester (TMRE). In line with our previous results, A375M6 cells showed a decrease in the mitochondrial membrane potential after the treatment with the compound (Fig. 4G), further suggesting a decrease of mitochondrial activity induced by Claisened Hexafluoro treatment. On the other hand, through MitoTracker Green staining we showed an increase in mitochondrial mass measured by FACS analysis (Fig. 4H) and the presence of extensive mitochondrial fusions by confocal microscopy (Fig.4I). All together these data suggest that treated cells increase the mitochondrial mass as a compensatory mechanism to overcome the mitochondrial dysfunction induced by the treatment.

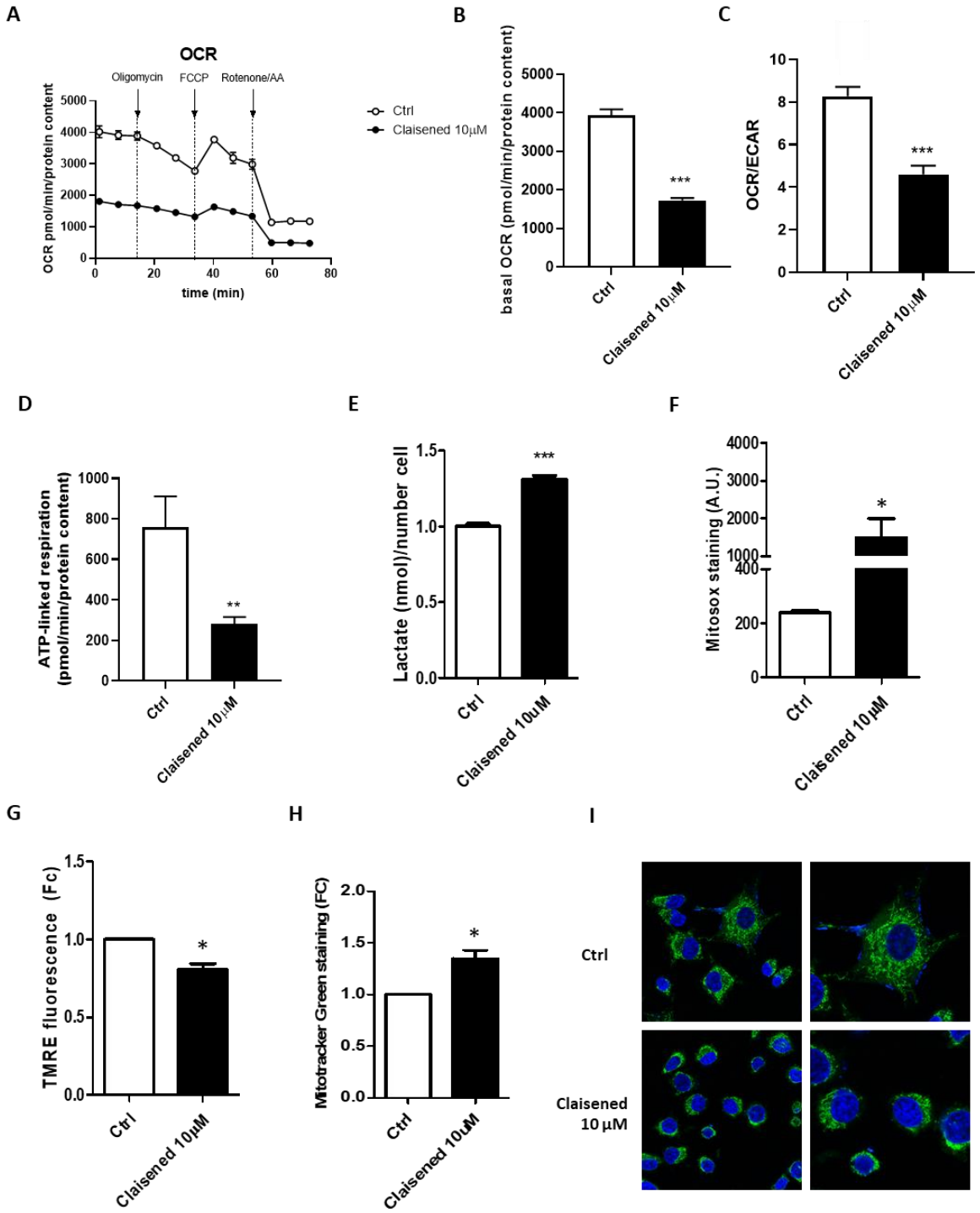
A
OCR
Oligomycin
FCCP
Rotenone/AA
OCR pmol/min/protein content
time (min)
Ctrl
Claisened 10μM
B
basal OCR (pmol/min/protein content)
***
Ctrl
Claisened 10μM
C
OCR/ECAR
***
Ctrl
Claisened 10μM
D
ATP-linked respiration (pmol/min/protein content)
**
Ctrl
Claisened 10μM
E
Lactate (nmol)/number cell
***
Ctrl
Claisened 10uM
F
Mitosox staining (A.U.)
*
Ctrl
Claisened 10μM
G
TMRE fluorescence (Fc)
*
Ctrl
Claisened 10μM
H
Mitotracker Green staining (FC)
*
Ctrl
Claisened 10uM
I
Ctrl
Claisened 10 μM

Figure 4. Claisened Hexafluoro decreases the mitochondrial activity of A375M6 cells and increases mitochondrial ROS production. Oxygen consumption rate (OCR) measured in real time with Seahorse XFe96 Mito Stress Test analysis in A375M6 cells treated or not with Claisened Hexafluoro (A). The respiratory capacity was calculated based on the OCR after the administration of the ATP synthase inhibitor oligomycin, the proton uncoupler carbonilcyanide p-triflouromethoxyphenylhydrazone (FCCP), and the respiratory complex I inhibitor rotenone, together with the respiratory complex III inhibitor antimycin A. (B) Basal OCR and (C) the ratio OCR/ECAR are shown. (D) ATP-linked respiration is reported. (E) Lactate production in medium was measured. (F) Mitochondrial ROS level, (G) mitochondrial membrane potential (TMRE) and Mitochondrial mass (MitoTracker Green) (H) were analysed by FACS analysis after treatment with Claisened Hexafluoro. Mitochondrial morphology of A375M6 cells, treated as above, were analysed by confocal analysis after labelling with MitoTracker Green and Hoechst 33342 (I). *Data were shown in mean ± SEM; 1-way-ANOVA, for fig.5 A, B, C, D; t-test, for fig. 4 E and F; * p< 0.05, **p<0.01, *** P< 0,001.*

4.4.5 Claisened Hexafluoro affects AMPK signalling

Alterations in mitochondrial energetics have been related to the activation of the AMPK signalling as a result of the impaired energy balance and the consequent increase in the AMP/ATP ratio [496]. AMPK is the main sensor of cellular energy status and a key player of different cellular functions [150].

In order to evaluate whether Claisened Hexafluoro-induced mitochondrial dysfunction has an impact also on the energy status of treated cells, we measured the AMP/ATP ratio. Interestingly, following Claisened Hexafluoro treatment it is possible to observe an increase of the AMP/ATP ratio (Fig. 5A) indicating an energy stress.

Accordingly, in Claisened Hexafluoro treated melanoma cells, we found increased level of AMPK phosphorylation (on Thr-172) and hence its activation (Fig. 5B). Interestingly, AMPK pathway is implicated in several cellular processes, including cell motility, adhesion and invasion [497]. In order to evaluate whether AMPK activation may mediate the reported decrease in cellular motility, we assayed cell invasion in the presence of Compound C [498], a selective AMPK inhibitor. Interestingly, the impairment of cell invasion following Claisened Hexafluoro treatment is almost completely reversed in the presence of Compound C, confirming the involvement of AMPK activation in Claisened-induced inhibition of cell migration (Fig. 5C).

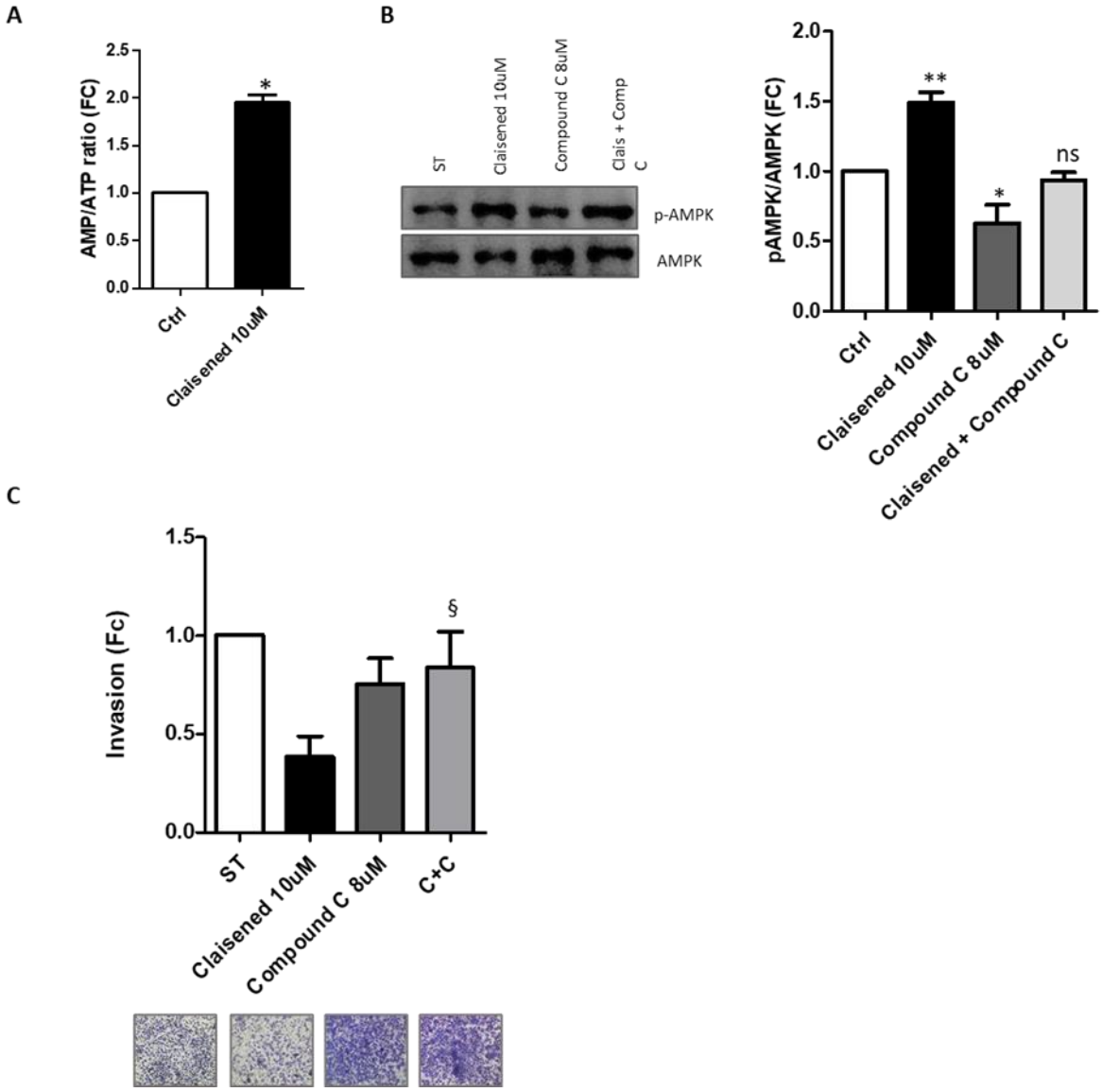

Figure 5. AMPK activity is involved in the inhibition of ameboid motility after treatment with Claisened Hexafluoro. The graph represents the AMP/ATP ratio in A375M6 treated or not with 10µM Claisened Hexafluoro (A). Phosphorylation levels of AMPK normalized on total levels of AMPK in A375M6 treated or not with10µM Claisened Hexafluoro and/or 8µM Compound C (B). Invasion assay of A375M6 cells treated as in B (C). *Data were shown in mean ± SEM, t-test; * p< 0.05, **p<0.01, *** P< 0,001 vs ctrl. §p< 0.05 C+C vs Claisened 10µ*M.

4.4.6 Claisened Hexafluoro decreases the in vivo lung metastasis formation.

Finally, to prove whether Claisened Hexafluoro could decrease A375M6 metastatic dissemination *in vivo*, we performed an experimental metastasis assay in *NU-Foxn1^{nu}*

mice. A375M6 cells were injected into the tail vein of the mice and Claisened Hexafluoro was administrated intraperitoneally five a week. Results shown in Fig. 6 highlight that Claisened Hexafluoro treatment strongly inhibits lung colonization of circulating melanoma cells, as demonstrated by the decrease in the number of metastatic nodules in treated mice. Moreover, it is possible to observed a better conserved morphology of the lung parenchyma in Claisened Hexafluoro treated mice. These data confirm a crucial role of Claisened Hexafluoro-mediated inhibition of amoeboid motility in the *in vivo* metastatic process of melanoma cells.

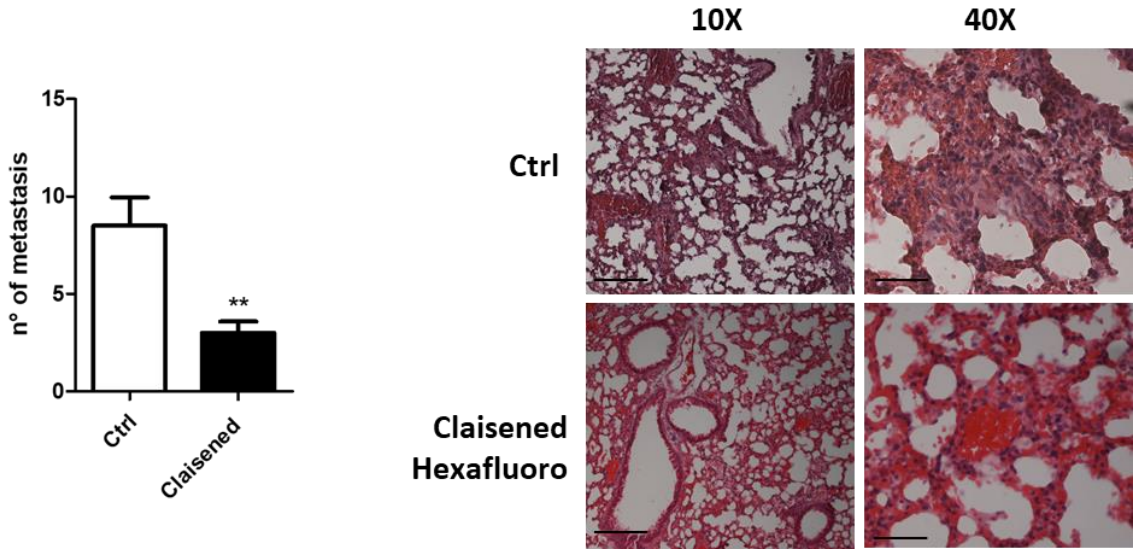

Figure 6 Claisened Hexafluoro decreases lung colonization in NU-Foxn1^{nu} mice. Lung colonization assay: mice were injected into the lateral tail vein with 1 x 10^6 A375M6 cells. Claisened Hexafluoro 3 mg/mouse/day in 30% intralipid was administered intraperitoneally five times a week. Mice were sacrificed after *8 weeks* and the lungs were inspected for metastatic nodules. *The graph reports the number of metastatic nodules per group Student t-test, * $p < 0.05$ treated vs untreated.*

4.5 Discussion

Cancer cell dissemination is one of the major deleterious phenomenon during cancer progression, frequently representing the leading cause of the fatal outcome of this pathology. The metastatic disease is particularly aggressive especially because, besides increased invasive abilities, disseminating cells are also endowed with metabolic alterations allowing them to adapt to changes occurring in the tumor *milieu*, and with enhanced resistance to both *anoikis* and existing therapies [499]. Altogether, these characteristics allow disseminating cells to overcome all the metastatic steps and facilitate the formation of new lesions.

Metastatic melanoma accounts for the majority of skin cancer deaths (over 80%) and, for this reason, halting melanoma dissemination through developing new therapeutic approaches represents one of the most promising challenges in the clinic. In this context, besides the successful therapies aimed at inhibiting oncogenes involved in melanoma and the efficacious immunotherapy (described in detail in the introduction part), there is a real need for therapies that specifically target the metastatic process.

Actually, different types of cell motility have been described in melanoma, such as the rounded/amoeboid-type motility, the elongated/mesenchymal-type motility, and the collective motility [232,233,500], supporting the idea that melanoma cells are highly plastic and can switch between different migration styles, mainly depending on changes in the tumor microenvironment [165,230,232,233]. However, several studies have recognized the amoeboid motility as a detrimental feature of metastatic melanoma. *Lorentzen et al.*, showed that a selected melanoma A375 population characterized by increased metastatic potential contain a higher proportion of cells (90%) which move through squeezing amoeboid motility with respect to the less metastatic parental cell line [219]. Moreover, rounded cells predominate in the invasive front of melanoma, confirming the relevance of amoeboid motility in the invasive process [220].

It is well known that high levels of Rho-ROCK signaling are strongly required for rounded-amoeboid, blebs-based movement with respect to the elongated, protrusive one [232,233,501,502]. In keeping with these observations, several Rho GTPase proteins have been found overexpressed or mutated in tumors [503]. Furthermore, recently, *Misek et al.* showed that activation of RhoA family GTPases is present in ~50-60% of melanoma cell lines with

Vemurafenib resistance acquired *in vitro*, reinforcing the idea that this signaling has a key role in the achievement of aggressive features by melanoma cells [504]. In this context, some efforts have been made in order to arrest melanoma invasion by blocking Rho activity. Even if the sole pharmacological inhibition of ROCK is efficacious in decreasing cell invasion [505], due to the great plasticity of melanoma cells, only the combination of different drugs aimed at inhibiting both elongated, mesenchymal-type and rounded, amoeboid motility [232,233,506] is really efficacious in blocking the metastatic process in melanoma.

In this study, we demonstrated that Claisened Hexafluoro, a fluorinated synthetic Honokiol analogue, is efficient in blocking the amoeboid movement of metastatic melanoma cells. In particular, we observed that, differently from other described inhibitors of the amoeboid motility, Claisened Hexafluoro does not induce a shift towards the mesenchymal style, suggesting a possible use of this compound to block the metastatic process of tumour cells. This approach is particularly promising for the treatment of melanoma, endowed with a great plasticity in cell motility. Furthermore, Claisened Hexafluoro exerts its action specifically on cells which moves through amoeboid motility since it is completely inefficient in inhibiting the migration abilities of melanoma cells with mesenchymal features (Figs. 1D-E). Altogether, the aforementioned features suggest that Claisened Hexafluoro displays a real therapeutic potential for melanoma treatment.

Moreover, our results show that Claisened Hexafluoro is able to inhibit several steps of the metastatic process, especially the trans-endothelial migration, a feature necessary to extra/intravasate during the disseminating process. Coherently, this phenomenon is mainly based on the ability of cancer cells to pass-through the endothelial barriers by an amoeboid motility style. The inhibition of melanoma cell ability to trans-migrate is strictly correlated with the observed decrease in the number of metastatic nodules in the *in vivo* experimental metastases model (Fig. 6). Moreover, we showed that Claisened Hexafluoro inhibits the stemness phenotype of melanoma cells as well as the ability to form melanospheres (Fig. 3). These data are in keeping with previous results showing that the achievement of amoeboid motility is characterised by increased stemness and clonogenic features in melanoma cells [248]. In looking for the molecular mechanism through which Claisened Hexafluoro displays these promising effects, we found that it has a strong impact on the metabolic features of melanoma cells. Indeed, the treatment with this compound severely

affects mitochondrial functionality as demonstrated by decreased OCR levels, mitochondrial depolarization and decreased mitochondria-related ATP production (Fig 4). Thanks to its detrimental effects on mitochondrial functionality, Claisened Hexafluoro, could be of great utility in the treatment of tumors which are dependent on mitochondrial respiration in a similar manner to what has been observed for Honokiol [507]. Interestingly, melanoma treated with MAPK-signaling inhibitors shift their metabolism from glycolysis to OXPHOS [508,509], thus the concomitant co-treatment with Claisened Hexafluoro could be very beneficial in targeted therapies. In keeping, *Bonner et al.*, reported that Claisened Hexafluoro is effective in decreasing proliferation of Vemurafenib resistant melanoma cells [484].

We also observed that the reduction of respiratory chain function following Claisened Hexafluoro treatment is strictly connected with an increase in both the AMP/ATP ratio and the activation of the AMPK signaling (Fig. 5A-B). Our data show that the inhibition of cell invasion induced by Claisened Hexafluoro is strictly dependent on AMPK phosphorylation/activation, as it is almost completely reverted by treating cells with Compound C, an inhibitor of AMPK [498]. Indeed, AMPK signaling, acting as the "sensor" of the energy status of the cell, play crucial roles also in the regulation of cell migration as demonstrated by the correlation between AMPK and Rho A signaling. Indeed, *Gayard M et al.*, showed that AMPK is able to phosphorylate RhoA on Ser188 and to subsequently restrain the RhoA/ROCK signaling [510]. In keeping with these data, *Guo et al.*, demonstrated that in melanoma cells, AMPK-mediated inhibition of RhoA decreases cell invasion and migration [511]. In this light, we hypothesize that the AMPK/RhoA/ROCK axis could be an indirect target of Claisened Hexafluoro action: the mitochondrial dysfunction caused by the treatment, sustaining the AMPK signaling, finally leads to a decrease in RhoA activation and to an impairment of amoeboid motility (Fig 5).

Collectively, data herein presented suggest that Claisened Hexafluoro could be a powerful tool to counteract the amoeboid motility and the metastatic dissemination of melanoma cells.

5. Materials and Methods

5.1 Materials

5.1.1 Isolation and culture cell

Human OS cell lines (SaOS-2, MG-63 and HOS) and HUVECs cells were purchased from Sigma Aldrich (ECACC). A375M6 metastatic melanoma cells were kindly donated by prof. Lido Calorini, isolated in its laboratory from lung metastasis of SCID *bg/bg* mice as previously described [512]. Hs294T mesenchymal melanoma cells was purchased from ATCC. Tumor cells were routinely maintained in Dulbecco's modified Eagle's medium (DMEM) high glucose with 2 mM L-glutamine (Euroclone, Milan, Italy) supplemented with fetal bovine serum (FBS; 10% v/v, Euroclone) and penicillin/streptomycin (P/S, 1% v/v, Sigma-Aldrich, St. Louis, MO), in cell culture flasks until 70–80% cell confluence. HUVECs were cultured in complete endothelial cell growth medium (EBM-2 Basal Medium, Lonza, Basel, Switzerland) plus the SingleQuots Kit, supplemented with 2 mM L-glutamine, P/S (1% v/v) and FBS (10% v/v). A375M6 and Hs294T starvation medium was supplied with 1% of FBS, 1% P/S and 2mM L-glutamine. Human BM-MSCs used in this study were isolated from healthy donors and characterized by Dr Bambi's Unit (AOU Meyer Hospital, Florence, Italy) as previously reported [364]. BM-MSCs were cultured in DMEM low glucose (Euroclone) containing FBS (10% v/v), 2 mM L-glutamine and P/S (1% v/v).

5.1.2 Preparation of conditioned media (CM)

OS CM were obtained from $1x10^6$ tumor cells maintained in low glucose media deprived of serum (St Med) for 48 h at 37 °C in 5% CO2 humidified atmosphere. CM derived from untreated ($BM\text{-}MSCs^{St)}$ and conditioned MSCs ($BM\text{-}MSCs^{OS}$) were obtained from BM-MSCs grown to sub-confluence and serum starved in low glucose media or stimulated with CM from OS cells for 48 h. Media were then removed and replaced with St Med (low glucose) for an additional 24 h. CM derived from the different experimental conditions were harvested, clarified by centrifugation and frozen at 80 °C until use.

5.1.3 Antibodies and material

The following antibodies were used for western blot analysis: CollagenI-α1 (NB600-408, rabbit; Novus Biologicals, Littleton, CO, USA), a-SMA (A2547, mouse), Rac1 (07-1464, rabbit) and tubulin (T5168, mouse) from Sigma-Aldrich (St. Louis, MO, USA) RhoA (sc-418, mouse, and βActin (sc-47778) were from Santa Cruz Biotechnology, AMPK (#2532), p-AMPK (Thr172) (#2535) were from Cell Signaling, EphA2 (Fisher Scientific). Secondary antibodies were from Santa Cruz Biotechnology. For the immunofluorescence experiments, FITCphalloidin (F432, Molecular Probes, Eugene, OR, USA), anti-p-MLC (Ser 19) antibodies (3671, Cell Signaling, Danvers, MA, USA) and secondary antibodies conjugated with AlexaFluor 488 (A-11034, Life Technologies Invitrogen, Carlsbad, CA, USA) were used. Hoechst 33342 (62249) was from Thermofisher scientific. For the migration experiments, blocking antibodies were used against: CXCR4 (555971, BD Bioscience, Franklin Lakes, NJ, USA), MCP-1 (555055, BD Biosciences), IL-6 (mabg-hil6-3, InvivoGen, San Diego, CA, USA) and IL-8 (MAB208-100, R&D System, Minneapolis, MN, USA). SB225002 [(N-(2-hydroxy-4-nitrophenyl)-N0 -(2-bromophenyl) urea, 559405] and Ilomastat (GM 6001, 364205) were from Merck Millipore (Billerica, MS, USA). TGF-β1R blocker (TbR blk, p17) was developed by Digna Biotech (Pamplona, Spain) as previously described (Barcellos-de-Souza et al., 2016). MatrigelTM Basement Membrane Matrix (356234) was from BD Biosciences. Rho Activator (calpeptin, CN01) was from Cytoskeleton, Inc. (Denver, CO, USA); GST-Rhotekin (14-662) and recombinant human TNF-α (300-01A) were from Peprotech (Peprotech Inc, Rocky Hill, NJ, USA) and CFSE (C34554) was from Life Technologies. Collagen I rat tail was BD biosciences (354236). Claisened Hexafluoro was provided by Jack L. Arbiser from Emory University.

5.2 Methods

5.2.1 In vitro migration assays

Migration assays were performed in Boyden Chamber with 8μm pore size filters (CC3422, CostarTM, Corning, NY, USA). In BM-MSC chemotaxis assays, $2.5x10^4$ cells were serum-starved for 24 h and allowed to migrate overnight toward CM from SaOS2, MG-63 and HOS cells. Untreated cells (St Med) were used as control. Migrating cells were fixed,

stained and counted in four randomly chosen fields in bright field. In chemotaxis experiments with inhibitors, BM-MSCs were starved overnight in the presence or absence of 20 μg/mL^{-1} anti- CXCR4 blocking antibodies, 200 nM SB225002 and 100 μg/mL^{-1} TbR blk. Anti-MCP-1 neutralizing antibodies 5 μg/mL^{-1} were added to CM 1 h before performing the assays. Migration assays of HOS cells were performed by treating 3.5x10^5 tumor cells with CM BM-MSCsSt or CM BM-MSCs^{OS} for 24 h. St Med was used as control. Then, 5x10^4 HOS cells were allowed to migrate for 6 h toward complete medium (FBS 10%). Invasion assays were achieved by covering the upper compartment of the Boyden chamber with 50 μg/cm^2 of reconstituted Matrigel. OS cells were treated with CM from starved or tumor-activated BM-MSCs for 36 h. Then 5x10^4 HOS and 1x10^5 SaOS-2 or MG-63 were allowed to migrate toward complete medium (10% FBS) for 5 h, overnight or 24 h, respectively. Trans-endothelial migration was performed with OS cells treated as above and stained with CFSE. Tumor cells (3x10^4 HOS and 8x10^4 MG-63 and SaOS-2) were seeded onto 5x10^4 HUVECs activated with 10 ng/mL^{-1} TNF-α and allowed to migrate toward 500 μL of complete medium (HOS for 5 h, MG-63 and SaOS-2 for 16 h). In invasion and trans-endothelial migration assays with inhibitors, conditioned HOS cells were treated or not treated with neutralizing antibodies against IL-6 (5 μg/mL^{-1}), IL-8 (10 μg/mL^{-1}), MCP-1 (10 μg/mL^{-1}) and SB225002 (200 nM). To evaluate MMP dependence, OS cells treated or not treated with BM-MSCs, CM were incubated overnight with 50μM Ilomastat. The number of migrating cells was determined by counting in four randomly chosen fields in an inverted optical or fluorescent microscope for invasion and trans-endothelial migration, respectively. Recruitment assays of HUVECs were performed allowing migration or invasion of 5x10^4 cells for 6 h toward CM HOSSt and CM HOS$^{BM-MSCs}$. St Med was used as negative control.

A375M6 or HS294T cells were serum starved for 24h and then were treated or not with 10μM Claisened Hexafluoro for other 24h combined with or without 8μM Compound C. Then 5x10^5 or 6x10^{5}cells, respectively, were seeded onto Matrigel-precoated Boyden chamber (performed as above) in starvation medium (FBS 1%). In the lower chamber complete medium FBS 10% was used as chemoattractant. Following 5h (or 24h for Hs294T) of incubation, the inserts were removed and the noninvading cells on the upper surface were removed with a cotton swab. The filters were then stained using the Diff-

Quik kit (BD Biosciences) and photographs of randomly chosen fields are taken. The quantification was performed by Image J software.

For trans-endothelial migration assays, HUVECs were grown to confluence on the separating filter of a Boyden chamber (8-mm pore size, 6.5 mm diameter) and were activated with 10 ng/mL^{-1} TNFα for 90 minutes. Thereafter, culture media were changed with fresh media and cells incubated for an additional 2.5 hours. A375M6 cells treated or not with 10µM Claisened Hexafluoro for 24h and stained with CFSE (360 ng/mL^{-1}) were seeded onto HUVECs monolayer and allowed to migrate toward complete medium overnight. Then, the noninvading cells were removed on the upper surface with a cotton swab and the cells fixed with methanol 70% (Sigma Aldrich). The number of migrated cells to the lower face of the filter was evaluated by counting the fluorescent cells using an inverted fluorescent microscope and quantified with Image J software.

5.2.2 3D invasion assay

2x10^4 A375M6 cells were seeded in 96-multiwell plates coated with 1,5% Agar. Then, after 4 days, spheroids were obtained and photographed (t0). Subsequently, Matrigel (50 µg/cm2) was added to each well and the cells were treated or not with 10µM Claisened Hexafluoro. The photos were taken 24h (t1) after the treatment. The invasive capacity was calculated by subtracting the inner area, which represents the initial spheroid, from the total area. The area was calculated with ImageJ software.

5.2.3 Western blotting

Cells were lysed on ice in radioimmunoprecipitation assay (RIPA) buffer (50 mM TrisHCl pH 7.5, 150 mM NaCl, 100 mM NaF, 2 mM EGTA, 1% triton X-100, 10 µL/mL protease and phosphatase inhibitor; Sigma-Aldrich), 20 to 50 µg of total proteins were loaded on SDS-PAGE gels and transferred to PVDF membranes (BioRad, Hercules, CA). Membranes were incubated overnight at 4°C with the primary antibody. After washing in PBS-Tween 20 (0.1%) membranes were incubated with the appropriate horseradish peroxidase-conjugated secondary antibodies (Santa Cruz Biotechnology) for 1 hour. Proteins were detected using Clarity Western ECL (BioRad) and images were acquired by using Amersham Imager 600 luminometer (Amersham, Buckinghamshire, UK). Quantification of bands was carried out by using the Amersham quantification software.

5.2.4 RhoA and Rac1 activity assays

Cells were directly lysed in RIPA buffer, the lysates were clarified by centrifugation, and RhoA-GTP or Rac1-GTP levels were quantified. Briefly, lysates were incubated with 10 μg of Rhotekin–glutathione S-transferase (GST) or p21 activated kinase (PAK)-GST fusion protein both absorbed on glutathione-Sepharose beads for 1 h at 4°C. GST pulled-down immunoreactive RhoA or Rac 1 were then quantified by Western blot analysis. Lysates were normalized for RhoA or Rac1 content by immunoblot.

5.2.5 Collagen contraction assay

BM-MSCs $1.5x10^5$ maintained for 24 h in St Med or HOS CM were harvested and resuspended in a DMEM solution containing 1 mg/mL^{-1} Collagen A (L7220, Merck Millipore) as previously reported [364]. The area of each gel (number of pixels) was determined using IMAGEJ. 2.7. Gelatin zymography CM derived from untreated or conditioned MSCs was collected, centrifuged and concentrated 10-fold with Amicon Ultra 4 mL centrifugal filter (UFC800324, Merck Millipore). Gelatin zymography was performed as previously described [248].

5.2.2 Confocal analysis

MG-63 treated with CM from tumor-activated BM-MSCs CM was fixed in p-formaldehyde (4% v/v in PBS) for 20 min, permeabilized in Triton X-100 (0.5% v/v in PBS) for 5 min, then washed twice with bovine serum albumin (BSA; 1% v/v) and FBS (5% v/v in PBS) solution and incubated overnight at 4 °C with primary antibodies against p-MLC (1 : 100). After two washes with PBS, cells were incubated with anti-rabbit AlexaFluor 488 antibodies (1: 1000) and FITC-phalloidin for 1 h at room temperature in the dark. As positive control, we used 1 U/mL^{-1} Calpeptin, a RhoA activator. The coverslips were mounted in Gel MountTM Aqueous Mounting Medium (Sigma-Aldrich). A Nikon Eclipse TE2000-U (Nikon, Tokyo, Japan) confocal microscope was used for data acquisition.

A375M6 cells were treated with or without 10μM Claisened Hexafluoro and then labeled with 30nM MitoTracker Green (M7514, Thermofisher scientific) used accordingly to

manufacturers' instructions and 1μg/mL Hoechst 33342. Then, the cells were analyzed by confocal imaging (Leica TCS SP8).

5.2.3 Flow Cytometric Analysis

Staining of BM-MSCs cultivated in St Med or treated with CM from OS cells for 48 h was performed as previously described [364].

A375M6 cells were serum starved for 24h were treated with 10μM Claisened Hexafluoro for 48h. Then, the cells were detached with Accutase (Sigma) and stained with anti-CD133-APC (566596, BD Biosciences) antibody for 30 minutes and analyzed through flow cytometry analysis.

For mitochondrial superoxide detection, cells were treated in starvation medium (FBS 1%) with or without 10μM Claisened Hexafluoro for 24h. Cells were then incubated for 10 minutes at 37°C with 5 μM MitoSox (M36008, Thermofisher scientific) in PBS. Cells were detached with Accutase, centrifuged, washed with PBS, and resuspended in 300 μL PBS. A flow cytometer analysis was then performed (MitoSox excitation/emission: 510/580 nm).

For mitochondrial analysis, 30nM MitoTracker Green and TMRE were used accordingly to manufacturers' instructions (Thermofisher scientific, T669). Cell were analyzed by flow cytometry using FACScan flow cytometer (BD Biosciences) or by confocal imaging (Leica TCS SP5).

5.2.4 ELISA and cytokine antibody array

Cytokine concentration in CM from MG-63 cells and from BM-MSCs was determined by ELISA single kits for IL-1 alpha (EH2IL1A), IL-6 (EH2IL6), IL-8 (EH2IL8), IL-17 (EH2IL17), GRO-a (EHCXCL1), MCP-1 (KHC1011), PDGF-BB (EHCSRP2), TGF-b1 (EHTGFBI) and TNF-a (EH3TNFA), according to the manufacturer's instructions (Invitrogen). The qualitative analysis of cytokines and growth factors produced by BM-MSCs was performed in CM obtained from 7.5 9 105 cells grown in St Med or stimulated with CM from HOS cells for 48 h. Cells were then starved for a further 24 h and CM was collected, clarified by centrifugation and analyzed with Human Cytokine Antibody Array C5 (AAH-CYT-5, RayBiotech, Aachen, Germany) according to the manufacturer's

protocol. Membranes were developed with streptavidin-HRP chemiluminescence reaction and then exposed to X-ray film. Pixel densities of detectable spots were calculated using IMAGEJ software. The intensity of each spot was normalized to the intensities obtained using positive antibody array controls and subtracted from the related background. Expression values higher than 10 000 arbitrary units were set to identify a cut-off for cytokines to be considered. The same type of analysis was performed in CM obtained from HOS cells stimulated or not stimulated with CM from tumor-activated BM-MSCs to determine the relative amounts of pro-angiogenic factors.

5.2.5 RT-qPCR

Total RNA was purified from cells using the RNeasy mini Kit (Qiagen, Hilden, Germany) according to the manufacturer's instructions. Total RNA amount was quantified at NanoDrop Microvolume Spectrophotometers and Fluorometer. The reverse transcription reaction was performed with QuantiTech reverse transcription Kit (Qiagen) using 1 µg of total RNA. mRNA expression was performed using QuantiFast SYBR Green (Qiagen). The primers for NANOG: 5′-ACCTTGGCTGCCGTCT CTGG-3′ (forward), 5′-AGCAAAGCCTCCCAATCCCAA ACA-3′ (reverse); KLF4: 5′-GCAGCCACCTGGCGAGTC TG-3′ (forward), 5′-CCGCCAGCGGTTATTCGGGG-3′ (reverse) and OCT3/4: 5′-TTTTGGTACCCCAGGCTATG-3′ (forward), 5′-GCAGGCACCTCAGTTTGAAT-3′ (reverse). β_2 microglobulin: 5′-AGTATGCCTGCCGTGTGAAC-3′ (forward), 5′-GCGGCATCTTCACAAACCTCCA-3′ (reverse) was used as normalizer. All the amplifications were run on 7500 Fast Real-Time PCR System (BioRad). Data were reported as relative quantity with respect to the calibrator sample using the −ΔΔ 2 Ct method.

5.2.6 Cell migration in three-dimensional collagen matrices

Reconstruction by time-lapse video microscopy and confocal microscopy was performed on MG-63 or A375M6 cells. Subconfluent MG-63 cells treated or not treated with CM from tumor-activated BM-MSCs or A375M6 cells treated or not with Claisened Hexafluoro 10µM previously for 24 h, were labelled by CFSE (360 ng/mL^{-1}) and then were detached by EDTA (2 mM), washed, incorporated into three dimensional collagen lattice (1.67 mg/mL^{-1} ; native dermal bovine type I collagen; RD Systems for MG-63, or collagen

I, rat tail, BD biosciences for A375M6) and monitored by time-lapse video microscopy (Brocker, 2004; Friedl, 2004). For three-dimensional time-lapse confocal microscopy (Leica-SP5 system), cells were scanned for 12 h at 3- min time intervals for simultaneous fluorescence and back scatter signal (reflection), and reconstructed. Three-dimensional motility of cells is shown by time lapse of xyzt analysis (three-dimensional analysis over time).

5.2.7 Cell viability assay

A375M6 cells ($2x10^4$) were seeded in 24-multiwell plates and serum starved for 24 h before treatment with or without increasing concentration of Claisened Hexafluoro for 24 and 48 h. Cell viability were evaluated by the addition of a crystal violet solution (0,5% in 20% methanol). After 5 min of staining, the fixed cells were washed with phosphate-buffered saline (PBS) and solubilized with 200 µl/well of 0.1 M sodium citrate, pH 4.2. The absorbance at 595 nm was evaluated using a microplate reader.

5.2.8 Adhesion assay

A375M6 cells were serum starved for 24h and then treated or not with 10µM Claisened Hexafluoro for 24h. $1x10^5$ melanoma cells were seeded on 24-multiwell plates coated with 300 µg/mL collagen (354236, rat tail I collagen; RD Bioscience) as already described by [513] or 2,5µg/cm^2 fibronectin (Sigma Aldrich - F2006) for 10 minutes. Adherent cells were fixed with methanol and photos of the wells were taken. Cells were counted using the ImageJ software. Adhesion to endothelium assay was performed as previously described [514]. Briefly, A375M6 cells treated as above and stained with CFSE (360 ng/mL^{-1}) were seeded onto a transwell precoated with $5x10^4$ HUVECs activated with 10 ng/mL^{-1} TNF-a for 90' and allowed to adhere for 30 minutes.

5.2.9 Melanospheres formation

For melanospheres formation assay, A375M6 cells, treated or not with 10µM of Claisened Hexafluoro for 24h, were detached using Accutase (Sigma) and plated at 1000 cells/plate on low attachment 100 mm plate in serum-free DMEM/F12 1:1 (Invitrogen, Carlsbad, CA, USA) supplemented with N2 (Invitrogen), 0.6% glucose (Sigma), 20 µg/ml insulin (Eli

Lilly), 10 ng/ml b-FGF and 10 ng/ml EGF. Cells were grown under these conditions for 15 days to obtain melanospheres.

5.2.10 Seahorse XFe96 Metabolic Assays

Cells were seeded in XFe96 cell culture plates with $3x10^5$ cells per well and subjected to the XF mito stress test. The cells were treated or not with 10μM Claisened Hexafluoro for 24h. Medium was replaced with XF base medium supplemented with 25 mM glucose, 2 mM glutamine and 1 mM sodium pyruvate. Cells were incubated for 1 h at 37 °C in a non-CO_2 incubator before the analysis. Mito Stress test analysis reveals basal respiration, maximal respiration and the ability of the cells to exploit mitochondrial oxidative metabolism. This analysis is performed by real-time measurement of extracellular acidification (ECAR) and of oxygen consumed (OCR) after a sequence of compounds that interfere with the electron transport chain: oligomycin (1 μM), carbonyl cyanide-4 (trifluoromethoxy) phenylhydrazone (FCCP) (1 μM) and Rotenone/Antimycin A (0.5 μM). Protein quantification was used to normalize the results.

5.2.11 Lactate quantification assay

A375M6 cells were treated for 24h with or without 10μM of Claisened Hexafluoro and Lactate Colorimetric/Fluorimetric Assay Kit (Biovision) was performed according to the manufacturer's instructions. All data were normalized on cell protein content.

5.2.12 ADP/ATP quantification assay

A375M6 cells were treated for 24h with or without 10μM of Claisened Hexafluoro and the ADP/ATP Ratio Colorimetric/Fluorometric Assay Kit (Biovision) was performed according to the manufacturer's instructions. All data were normalized on cell protein content

5.2.13 Lung colonization assay

The tail vein injection method was developed and approved by the Institutional Animal Care and Use Committee (IACUC) of Emory University, and all in vivo experiments were performed in accordance with the approved IACUC protocol guidelines and regulations. Male NU-Foxn1^{nu} mice (8 weeks old, 5 animals per group) were injected with $1x10^6$

A375M6 into the tail veins. The mice were treated for 8 weeks with or without Claisened Hexafluoro: 3mg/animal/day, 5 times a week in 30 % Intralipid. Claisened Hexafluoro was dissolved in 100% ethanol at 100 mg/mL, diluted 1:10 in 30 % intralipid, and 300 µL was injected via IP. Claisened Hexafluoro was prepared fresh. Lungs were inspected for metastatic nodules by histological analysis after hematoxylin-eosin staining. The number of metastatic nodules is expressed as mean and standard errors of the mean (SEM).

5.2.14 Statistical analysis

Statistical analysis for part 1 were performed by one-way ANOVA followed by a Bonferroni comparison test and Student's t-test (two-tailed), used to determine statistical significance with a *p-value* threshold set at < 0.05. Statistical analysis of the data was performed by unpaired Student t test for pairwise comparison of groups if not specified. All data were expressed as the mean ± SEM. A *p value* < 0.05 was considered statistically significant. Statistical analysis was carried out on three biological replicates.

6. References

1. WHO | World Cancer Report 2014. *WHO*. Published online 2015.
2. Hanahan D, Weinberg RA. The hallmarks of cancer. *Cell*. 2000;100(1):57-70. doi:10.1016/S0092-8674(00)81683-9
3. Hanahan D, Weinberg RA. Hallmarks of cancer: The next generation. *Cell*. 2011;144(5):646-674. doi:10.1016/j.cell.2011.02.013
4. Cairns RA, Harris IS, Mak TW. Regulation of cancer cell metabolism. *Nat Rev Cancer*. 2011;11(2):85-95. doi:10.1038/nrc2981
5. Warburg O. Über den Stoffwechsel der Carcinomzelle. *Naturwissenschaften*. 1924;12(50):1131-1137. doi:10.1007/BF01504608
6. WARBURG O. On respiratory impairment in cancer cells. *Science (80-)*. 1956;124(3215):269-270. Accessed September 28, 2020. https://pubmed.ncbi.nlm.nih.gov/13351639/
7. Weinhouse S. The Warburg hypothesis fifty years later. *Zeitschrift für Krebsforsch und Klin Onkol*. 1976;87(2):115-126. doi:10.1007/BF00284370
8. DeBerardinis RJ, Mancuso A, Daikhin E, et al. Beyond aerobic glycolysis: Transformed cells can engage in glutamine metabolism that exceeds the requirement for protein and nucleotide synthesis. *Proc Natl Acad Sci U S A*. 2007;104(49):19345-19350. doi:10.1073/pnas.0709747104
9. Vander Heiden MG, Cantley LC, Thompson CB. Understanding the Warburg Effect: The Metabolic Requirements of Cell Proliferation NIH Public Access. *Science (80-)*. 2009;324(5930):1029-1033. doi:10.1126/science.1160809
10. Sonveaux P, Végran F, Schroeder T, et al. Targeting lactate-fueled respiration selectively kills hypoxic tumor cells in mice. *J Clin Invest*. 2008;118(12):3930-3942. doi:10.1172/JCI36843
11. K S Dimmer, B Friedrich, F Lang, J W Deitmer and SB. The low-affinity monocarboxylate transporter MCT4 is adapted to the export of lactate in highly glycolytic cellsTitle. *Biochem J*. Published online 2000. https://www.ncbi.nlm.nih.gov/pmc/articles/PMC1221245/
12. McCullagh KJA, Poole RC, Halestrap AP, O'Brien M, Bonen A. Role of the lactate transporter (MCT1) in skeletal muscles. *Am J Physiol - Endocrinol Metab*. 1996;271(1 34-1). doi:10.1152/ajpendo.1996.271.1.e143
13. Pavlides S, Whitaker-Menezes D, Castello-Cros R, et al. The reverse Warburg effect: Aerobic glycolysis in cancer associated fibroblasts and the tumor stroma. *Cell Cycle*. 2009;8(23):3984-4001. doi:10.4161/cc.8.23.10238

14. Fiaschi T, Marini A, Giannoni E, et al. Reciprocal metabolic reprogramming through lactate shuttle coordinately influences tumor-stroma interplay. *Cancer Res*. 2012;72(19):5130-5140. doi:10.1158/0008-5472.CAN-12-1949
15. Cirri P, Chiarugi P. Cancer associated fibroblasts: the dark side of the coin. *Am J Cancer Res*. 2011;1(4):482-497. Accessed October 12, 2020. http://www.ncbi.nlm.nih.gov/pubmed/21984967
16. Martinez-Outschoorn UE, Trimmer C, Lin Z, et al. Autophagy in cancer associated fibroblasts promotes tumor cell survival: Role of hypoxia, HIF1 induction and NFκB activation in the tumor stromal microenvironment. *Cell Cycle*. 2010;9(17):3515-3533. doi:10.4161/cc.9.17.12928
17. Lunt SY, Vander Heiden MG. Aerobic glycolysis: Meeting the metabolic requirements of cell proliferation. *Annu Rev Cell Dev Biol*. 2011;27:441-464. doi:10.1146/annurev-cellbio-092910-154237
18. Doherty JR, Cleveland JL. Targeting lactate metabolism for cancer therapeutics. *J Clin Invest*. 2013;123(9):3685-3692. doi:10.1172/JCI69741
19. Vazquez A, Kamphorst JJ, Markert EK, Schug ZT, Tardito S, Gottlieb E. Cancer metabolism at a glance. *J Cell Sci*. 2016;129(18):3367-3373. doi:10.1242/jcs.181016
20. Yang M, Vousden KH. Serine and one-carbon metabolism in cancer. *Nat Rev Cancer*. 2016;16(10):650-662. doi:10.1038/nrc.2016.81
21. Jain M, Nilsson R, Sharma S, et al. Metabolite profiling identifies a key role for glycine in rapid cancer cell proliferation. *Science (80-)*. 2012;336(6084):1040-1044. doi:10.1126/science.1218595
22. Davidson SM, Papagiannakopoulos T, Olenchock BA, et al. Environment impacts the metabolic dependencies of ras-driven non-small cell lung cancer. *Cell Metab*. 2016;23(3):517-528. doi:10.1016/j.cmet.2016.01.007
23. Tardito S, Oudin A, Ahmed SU, et al. Glutamine synthetase activity fuels nucleotide biosynthesis and supports growth of glutamine-restricted glioblastoma. *Nat Cell Biol*. 2015;17(12):1556-1568. doi:10.1038/ncb3272
24. Bannai S, Ishii T. A novel function of glutamine in cell culture: Utilization of glutamine for the uptake of cystine in human fibroblasts. *J Cell Physiol*. 1988;137(2):360-366. doi:10.1002/jcp.1041370221
25. Mullen AR, Wheaton WW, Jin ES, et al. Reductive carboxylation supports growth in tumour cells with defective mitochondria. *Nature*. 2012;481(7381):385-388. doi:10.1038/nature10642
26. Dolfi SC, Chan LL-Y, Qiu J, et al. The metabolic demands of cancer cells are coupled to

their size and protein synthesis rates. *Cancer Metab*. 2013;1(1):20. doi:10.1186/2049-3002-1-20

27. Possemato R, Marks KM, Shaul YD, et al. Functional genomics reveal that the serine synthesis pathway is essential in breast cancer. *Nature*. 2011;476(7360):346-350. doi:10.1038/nature10350
28. Locasale JW, Grassian AR, Melman T, et al. Phosphoglycerate dehydrogenase diverts glycolytic flux and contributes to oncogenesis. *Nat Genet*. 2011;43(9):869-874. doi:10.1038/ng.890
29. Maddocks ODK, Berkers CR, Mason SM, et al. Serine starvation induces stress and p53-dependent metabolic remodelling in cancer cells. *Nature*. 2013;493(7433):542-546. doi:10.1038/nature11743
30. Tedeschi PM, Johnson-Farley N, Lin H, et al. Quantification of folate metabolism using transient metabolic flux analysis. *Cancer Metab*. 2015;3(1). doi:10.1186/s40170-015-0132-6
31. Labuschagne CF, van den Broek NJF, Mackay GM, Vousden KH, Maddocks ODK. Serine, but not glycine, supports one-carbon metabolism and proliferation of cancer cells. *Cell Rep*. 2014;7(4):1248-1258. doi:10.1016/j.celrep.2014.04.045
32. Oppenheim EW, Adelman C, Liu X, Stover PJ. Heavy Chain Ferritin Enhances Serine Hydroxymethyltransferase Expression and de Novo Thymidine Biosynthesis. *J Biol Chem*. 2001;276(23):19855-19861. doi:10.1074/jbc.M100039200
33. Lewis CA, Parker SJ, Fiske BP, et al. Tracing Compartmentalized NADPH Metabolism in the Cytosol and Mitochondria of Mammalian Cells. *Mol Cell*. 2014;55(2):253-263. doi:10.1016/j.molcel.2014.05.008
34. Kim D, Fiske BP, Birsoy K, et al. SHMT2 drives glioma cell survival in ischaemia but imposes a dependence on glycine clearance. *Nature*. 2015;520(7547):363-367. doi:10.1038/nature14363
35. Ye J, Fan J, Venneti S, et al. Serine catabolism regulates mitochondrial redox control during hypoxia. *Cancer Discov*. 2014;4(12):1406-1417. doi:10.1158/2159-8290.CD-14-0250
36. Vousden KH, Prives C. Blinded by the Light: The Growing Complexity of p53. *Cell*. 2009;137(3):413-431. doi:10.1016/j.cell.2009.04.037
37. Levine AJ, Oren M. The first 30 years of p53: Growing ever more complex. *Nat Rev Cancer*. 2009;9(10):749-758. doi:10.1038/nrc2723
38. Olivier M, Hussain SP, Caron de Fromentel C, Hainaut P, Harris CC. TP53 mutation spectra and load: a tool for generating hypotheses on the etiology of cancer. *IARC Sci Publ*. 2004;(157):247-270. Accessed November 28, 2020.

https://europepmc.org/article/med/15055300

39. Schwartzenberg-Bar-Yoseph F, Armoni M, Karnieli E. The Tumor Suppressor p53 Down-Regulates Glucose Transporters GLUT1 and GLUT4 Gene Expression. *Cancer Res*. 2004;64(7):2627-2633. doi:10.1158/0008-5472.CAN-03-0846
40. Kondoh H, Lleonart ME, Gil J, et al. Glycolytic enzymes can modulate cellular life span. *Cancer Res*. 2005;65(1):177-185.
41. Bensaad K, Tsuruta A, Selak MA, et al. TIGAR, a p53-Inducible Regulator of Glycolysis and Apoptosis. *Cell*. 2006;126(1):107-120. doi:10.1016/j.cell.2006.05.036
42. Zhang C, Liu J, Liang Y, et al. Tumour-associated mutant p53 drives the Warburg effect. *Nat Commun*. 2013;4. doi:10.1038/ncomms3935
43. Kawauchi K, Araki K, Tobiume K, Tanaka N. p53 regulates glucose metabolism through an IKK-NF-κB pathway and inhibits cell transformation. *Nat Cell Biol*. 2008;10(5):611-618. doi:10.1038/ncb1724
44. Kawauchi K, Araki K, Tobiume K, Tanaka N. Loss of p53 enhances catalytic activity of IKKβ through O-linked β-N-acetyl glucosamine modification. *Proc Natl Acad Sci U S A*. 2009;106(9):3431-3436. doi:10.1073/pnas.0813210106
45. Matoba S, Kang JG, Patino WD, et al. p53 regulates mitochondrial respiration. *Science (80-)*. 2006;312(5780):1650-1653. doi:10.1126/science.1126863
46. Stambolic V, MacPherson D, Sas D, et al. Regulation of PTEN transcription by p53. *Mol Cell*. 2001;8(2):317-325. doi:10.1016/S1097-2765(01)00323-9
47. Wang L, Xiong H, Wu F, et al. Hexokinase 2-Mediated Warburg Effect Is Required for PTEN- and p53-Deficiency-Driven Prostate Cancer Growth. *Cell Rep*. 2014;8(5):1461-1474. doi:10.1016/j.celrep.2014.07.053
48. Feng Z, Levine AJ. The regulation of energy metabolism and the IGF-1/mTOR pathways by the p53 protein. *Trends Cell Biol*. 2010;20(7):427-434. doi:10.1016/j.tcb.2010.03.004
49. Boidot R, Veģran F, Meulle A, et al. Regulation of monocarboxylate transporter MCT1 expression by p53 mediates inward and outward lactate fluxes in tumors. *Cancer Res*. 2012;72(4):939-948. doi:10.1158/0008-5472.CAN-11-2474
50. Dang C V. MYC on the path to cancer. *Cell*. 2012;149(1):22-35. doi:10.1016/j.cell.2012.03.003
51. Kress TR, Sabò A, Amati B. MYC: Connecting selective transcriptional control to global RNA production. *Nat Rev Cancer*. 2015;15(10):593-607. doi:10.1038/nrc3984
52. Felsher DW, Bishop JM. Reversible tumorigenesis by MYC in hematopoietic lineages. *Mol Cell*. 1999;4(2):199-207. doi:10.1016/S1097-2765(00)80367-6
53. Shachaf CM, Kopelman AM, Arvanitis C, et al. MYC inactivation uncovers pluripotent

differentiation and tumour dormancy in hepatocellular cancer. *Nature*. 2004;431(7012):1112-1117. doi:10.1038/nature03043

54. Soucek L, Whitfield J, Martins CP, et al. Modelling Myc inhibition as a cancer therapy. *Nature*. 2008;455(7213):679-683. doi:10.1038/nature07260
55. Annibali D, Whitfield JR, Favuzzi E, et al. Myc inhibition is effective against glioma and reveals a role for Myc in proficient mitosis. *Nat Commun*. 2014;5. doi:10.1038/ncomms5632
56. Murphy TA, Dang C V., Young JD. Isotopically nonstationary 13C flux analysis of Myc-induced metabolic reprogramming in B-cells. *Metab Eng*. 2013;15(1):206-217. doi:10.1016/j.ymben.2012.07.008
57. Le A, Lane AN, Hamaker M, et al. Glucose-independent glutamine metabolism via TCA cycling for proliferation and survival in b cells. *Cell Metab*. 2012;15(1):110-121. doi:10.1016/j.cmet.2011.12.009
58. Yuneva MO, Fan TWM, Allen TD, et al. The metabolic profile of tumors depends on both the responsible genetic lesion and tissue type. *Cell Metab*. 2012;15(2):157-170. doi:10.1016/j.cmet.2011.12.015
59. Dang C V., Kim JW, Gao P, Yustein J. The interplay between MYC and HIF in cancer. *Nat Rev Cancer*. 2008;8(1):51-56. doi:10.1038/nrc2274
60. Gao P, Tchernyshyov I, Chang TC, et al. C-Myc suppression of miR-23a/b enhances mitochondrial glutaminase expression and glutamine metabolism. *Nature*. 2009;458(7239):762-765. doi:10.1038/nature07823
61. Israelsen WJ, Vander Heiden MG. Pyruvate kinase: Function, regulation and role in cancer. *Semin Cell Dev Biol*. 2015;43:43-51. doi:10.1016/j.semcdb.2015.08.004
62. David CJ, Chen M, Assanah M, Canoll P, Manley JL. HnRNP proteins controlled by c-Myc deregulate pyruvate kinase mRNA splicing in cancer. *Nature*. 2010;463(7279):364-368. doi:10.1038/nature08697
63. Luan W, Wang Y, Chen X, et al. PKM2 promotes glucose metabolism and cell growth in gliomas through a mechanism involving a let-7a/c-Myc/hnRNPA1 feedback loop. *Oncotarget*. 2015;6(15):13006-13018. doi:10.18632/oncotarget.3514
64. Shim H, Chun YS, Lewis BC, Dang C V. A unique glucose-dependent apoptotic pathway induced by c-Myc. *Proc Natl Acad Sci U S A*. 1998;95(4):1511-1516. doi:10.1073/pnas.95.4.1511
65. Wise DR, Deberardinis RJ, Mancuso A, et al. Myc regulates a transcriptional program that stimulates mitochondrial glutaminolysis and leads to glutamine addiction. *Proc Natl Acad Sci U S A*. 2008;105(48):18782-18787. doi:10.1073/pnas.0810199105

66. Lewis BC, Prescott JE, Campbell SE, Shim H, Orlowski RZ, Dang C V. Tumor induction by the c-Myc target genes rcl and lactate dehydrogenase A. *Cancer Res*. 2000;60(21):6178-6183.

67. Fan Y, Dickman KG, Zong WX. Akt and c-Myc differentially activate cellular metabolic programs and prime cells to bioenergetic inhibition. *J Biol Chem*. 2010;285(10):7324-7333. doi:10.1074/jbc.M109.035584

68. Maya-Mendoza A, Ostrakova J, Kosar M, et al. Myc and Ras oncogenes engage different energy metabolism programs and evoke distinct patterns of oxidative and DNA replication stress. *Mol Oncol*. 2015;9(3):601-616. doi:10.1016/j.molonc.2014.11.001

69. Doherty JR, Yang C, Scott KEN, et al. Blocking lactate export by inhibiting the myc target MCT1 disables glycolysis and glutathione synthesis. *Cancer Res*. 2014;74(3):908-920. doi:10.1158/0008-5472.CAN-13-2034

70. San-Millán I, Brooks GA. Reexamining cancer metabolism: Lactate production for carcinogenesis could be the purpose and explanation of the Warburg Effect. *Carcinogenesis*. 2017;38(2):119-133. doi:10.1093/carcin/bgw127

71. Khatri S, Yepiskoposyan H, Gallo CA, Tandon P, Plas DR. FOXO3a regulates glycolysis via transcriptional control of tumor suppressor TSC1. *J Biol Chem*. 2010;285(21):15960-15965. doi:10.1074/jbc.M110.121871

72. Guertin DA, Sabatini DM. Defining the Role of mTOR in Cancer. *Cancer Cell*. 2007;12(1):9-22. doi:10.1016/j.ccr.2007.05.008

73. Semenza GL. HIF-1: upstream and downstream of cancer metabolism. *Curr Opin Genet Dev*. 2010;20(1):51-56. doi:10.1016/j.gde.2009.10.009

74. Guzy RD, Schumacker PT. Oxygen sensing by mitochondria at complex III: The paradox of increased reactive oxygen species during hypoxia. In: *Experimental Physiology*. Vol 91. Blackwell Publishing Ltd; 2006:807-819. doi:10.1113/expphysiol.2006.033506

75. Porporato PE, Dhup S, Dadhich RK, Copetti T, Sonveaux P. Anticancer targets in the glycolytic metabolism of tumors: A comprehensive review. *Front Pharmacol*. 2011;AUG. doi:10.3389/fphar.2011.00049

76. Kapitsinou PP, Haase VH. The VHL tumor suppressor and HIF: Insights from genetic studies in mice. *Cell Death Differ*. 2008;15(4):650-659. doi:10.1038/sj.cdd.4402313

77. Selak MA, Armour SM, MacKenzie ED, et al. Succinate links TCA cycle dysfunction to oncogenesis by inhibiting HIF-α prolyl hydroxylase. *Cancer Cell*. 2005;7(1):77-85. doi:10.1016/j.ccr.2004.11.022

78. King A, Selak MA, Gottlieb E. Succinate dehydrogenase and fumarate hydratase: Linking mitochondrial dysfunction and cancer. *Oncogene*. 2006;25(34):4675-4682.

doi:10.1038/sj.onc.1209594

79. de Saedeleer CJ, Copetti T, Porporato PE, Verrax J, Feron O, Sonveaux P. Lactate Activates HIF-1 in Oxidative but Not in Warburg-Phenotype Human Tumor Cells. *PLoS One*. 2012;7(10). doi:10.1371/journal.pone.0046571
80. Chiaradonna F, Gaglio D, Vanoni M, Alberghina L. Expression of transforming K-Ras oncogene affects mitochondrial function and morphology in mouse fibroblasts. *Biochim Biophys Acta - Bioenerg*. 2006;1757(9-10):1338-1356. doi:10.1016/j.bbabio.2006.08.001
81. Baracca A, Chiaradonna F, Sgarbi G, Solaini G, Alberghina L, Lenaz G. Mitochondrial Complex I decrease is responsible for bioenergetic dysfunction in K-ras transformed cells. *Biochim Biophys Acta - Bioenerg*. 2010;1797(2):314-323. doi:10.1016/j.bbabio.2009.11.006
82. Yang D, Wang MT, Tang Y, et al. Impairment of mitochondrial respiration in mouse fibroblasts by oncogenic H-RASQ61L. *Cancer Biol Ther*. 2010;9(2). doi:10.4161/cbt.9.2.10379
83. Asati V, Mahapatra DK, Bharti SK. PI3K/Akt/mTOR and Ras/Raf/MEK/ERK signaling pathways inhibitors as anticancer agents: Structural and pharmacological perspectives. *Eur J Med Chem*. 2016;109:314-341. doi:10.1016/j.ejmech.2016.01.012
84. Yun J, Rago C, Cheong I, et al. Glucose deprivation contributes to the development of KRAS pathway mutations in tumor cells. *Science (80-)*. 2009;325(5947):1555-1559. doi:10.1126/science.1174229
85. Son J, Lyssiotis CA, Ying H, et al. Glutamine supports pancreatic cancer growth through a KRAS-regulated metabolic pathway. *Nature*. 2013;496(7443):101-105. doi:10.1038/nature12040
86. McCleland ML, Adler AS, Deming L, et al. Lactate dehydrogenase B is required for the growth of KRAS-dependent lung adenocarcinomas. *Clin Cancer Res*. 2013;19(4):773-784. doi:10.1158/1078-0432.CCR-12-2638
87. Baenke F, Chaneton B, Smith M, et al. Resistance to BRAF inhibitors induces glutamine dependency in melanoma cells. *Mol Oncol*. 2016;10(1):73-84. doi:10.1016/j.molonc.2015.08.003
88. Ying H, Kimmelman AC, Lyssiotis CA, et al. Oncogenic kras maintains pancreatic tumors through regulation of anabolic glucose metabolism. *Cell*. 2012;149(3):656-670. doi:10.1016/j.cell.2012.01.058
89. Haq R, Shoag J, Andreu-Perez P, et al. Oncogenic BRAF regulates oxidative metabolism via PGC1α and MITF. *Cancer Cell*. 2013;23(3):302-315. doi:10.1016/j.ccr.2013.02.003
90. Han D, Williams E, Cadenas E. Mitochondrial respiratory chain-dependent generation of superoxide anion and its release into the intermembrane space. *Biochem J*.

2001;353(2):411-416. doi:10.1042/0264-6021:3530411

91. Murphy MP. How mitochondria produce reactive oxygen species. *Biochem J*. 2009;417(1):1-13. doi:10.1042/BJ20081386

92. Brand MD. The sites and topology of mitochondrial superoxide production. *Exp Gerontol*. 2010;45(7-8):466-472. doi:10.1016/j.exger.2010.01.003

93. Glasauer A, Chandel NS. Targeting antioxidants for cancer therapy. *Biochem Pharmacol*. 2014;92(1):90-101. doi:10.1016/j.bcp.2014.07.017

94. Hecht F, Pessoa CF, Gentile LB, Rosenthal D, Carvalho DP, Fortunato RS. The role of oxidative stress on breast cancer development and therapy. *Tumor Biol*. 2016;37(4):4281-4291. doi:10.1007/s13277-016-4873-9

95. Valko M, Rhodes CJ, Moncol J, Izakovic M, Mazur M. Free radicals, metals and antioxidants in oxidative stress-induced cancer. *Chem Biol Interact*. 2006;160(1):1-40. doi:10.1016/j.cbi.2005.12.009

96. Kumari S, Badana AK, Murali Mohan G, Shailender G, Malla RR. Reactive Oxygen Species: A Key Constituent in Cancer Survival. *Biomark Insights*. 2018;13. doi:10.1177/1177271918755391

97. Koppenol WH, Bounds PL, Dang C V. Otto Warburg's contributions to current concepts of cancer metabolism. *Nat Rev Cancer*. 2011;11(5):325-337. doi:10.1038/nrc3038

98. Fan J, Kamphorst JJ, Mathew R, et al. Glutamine-driven oxidative phosphorylation is a major ATP source in transformed mammalian cells in both normoxia and hypoxia. *Mol Syst Biol*. 2013;9. doi:10.1038/msb.2013.65

99. Hensley CT, Faubert B, Yuan Q, et al. Metabolic Heterogeneity in Human Lung Tumors. *Cell*. 2016;164(4):681-694. doi:10.1016/j.cell.2015.12.034

100. Kim JW, Tchernyshyov I, Semenza GL, Dang C V. HIF-1-mediated expression of pyruvate dehydrogenase kinase: A metabolic switch required for cellular adaptation to hypoxia. *Cell Metab*. 2006;3(3):177-185. doi:10.1016/j.cmet.2006.02.002

101. Papandreou I, Cairns RA, Fontana L, Lim AL, Denko NC. HIF-1 mediates adaptation to hypoxia by actively downregulating mitochondrial oxygen consumption. *Cell Metab*. 2006;3(3):187-197. doi:10.1016/j.cmet.2006.01.012

102. Martinez-Outschoorn UE, Balliet RM, Rivadeneira DB, et al. Oxidative stress in cancer associated fibroblasts drives tumor-stroma co-evolution: A new paradigm for understanding tumor metabolism, the field effect and genomic instability in cancer cells. *Cell Cycle*. 2010;9(16):3256-3276. doi:10.4161/cc.9.16.12553

103. Chandel NS, Tuveson DA. The Promise and Perils of Antioxidants for Cancer Patients. *N Engl J Med*. 2014;371(2):177-178. doi:10.1056/nejmcibr1405701

104. Piskounova E, Agathocleous M, Murphy MM, et al. Oxidative stress inhibits distant metastasis by human melanoma cells. *Nature*. 2015;527(7577):186-191. doi:10.1038/nature15726

105. Samaranayake GJ, Troccoli CI, Huynh M, et al. Thioredoxin-1 protects against androgen receptor-induced redox vulnerability in castration-resistant prostate cancer. *Nat Commun*. 2017;8(1). doi:10.1038/s41467-017-01269-x

106. Attardi LD, Donehower LA. Probing p53 biological functions through the use of genetically engineered mouse models. *Mutat Res - Fundam Mol Mech Mutagen*. 2005;576(1-2):4-21. doi:10.1016/j.mrfmmm.2004.08.022

107. Jain RK. Normalization of tumor vasculature: An emerging concept in antiangiogenic therapy. *Science (80-)*. 2005;307(5706):58-62. doi:10.1126/science.1104819

108. Abdal Dayem A, Choi HY, Kim JH, Cho SG. Role of oxidative stress in stem, cancer, and cancer stem cells. *Cancers (Basel)*. 2010;2(2):859-884. doi:10.3390/cancers2020859

109. Porporato PE, Payen VL, Baselet B, Sonveaux P. Metabolic changes associated with tumor metastasis, part 2: Mitochondria, lipid and amino acid metabolism. *Cell Mol Life Sci*. 2016;73(7):1349-1363. doi:10.1007/s00018-015-2100-2

110. McCubrey JA, LaHair MM, Franklin RA. Reactive oxygen species-induced activation of the MAP kinase signaling pathways. *Antioxidants Redox Signal*. 2006;8(9-10):1775-1789. doi:10.1089/ars.2006.8.1775

111. Salmeen A, Andersen JN, Myers MP, et al. Redox regulation of protein tyrosine phosphatase 1B involves a sulphenyl-amide intermediate. *Nature*. 2003;423(6941):769-773. doi:10.1038/nature01680

112. Kwon J, Lee SR, Yang KS, et al. Reversible oxidation and inactivation of the tumor suppressor PTEN in cells stimulated with peptide growth factors. *Proc Natl Acad Sci U S A*. 2004;101(47):16419-16424. doi:10.1073/pnas.0407396101

113. Seth D, Rudolph J. Redox regulation of MAP kinase phosphatase 3. *Biochemistry*. 2006;45(28):8476-8487. doi:10.1021/bi060157p

114. Chen Z, Trotman LC, Shaffer D, et al. Crucial role of p53-dependent cellular senescence in suppression of Pten-deficient tumorigenesis. *Nature*. 2005;436(7051):725-730. doi:10.1038/nature03918

115. Ray PD, Huang BW, Tsuji Y. Reactive oxygen species (ROS) homeostasis and redox regulation in cellular signaling. *Cell Signal*. 2012;24(5):981-990. doi:10.1016/j.cellsig.2012.01.008

116. Douma S, Van Laar T, Zevenhoven J, Meuwissen R, Van Garderen E, Peeper DS. Suppression of anoikis and induction of metastasis by the neurotrophic receptor TrkB.

Nature. 2004;430(7003):1034-1040. doi:10.1038/nature02765

117. Vooijs M, Gort E, Groot A, der Wall E, van Diest P. Hypoxic Regulation of Metastasis via Hypoxia-Inducible Factors. *Curr Mol Med*. 2008;8(1):60-67. doi:10.2174/156652408783565568

118. Nakamura K, Martin KC, Jackson JK, Beppu K, Woo CW, Thiele CJ. Brain-derived neurotrophic factor activation of TrkB induces vascular endothelial growth factor expression via hypoxia-inducible factor-1α in neuroblastoma cells. *Cancer Res*. 2006;66(8):4249-4255. doi:10.1158/0008-5472.CAN-05-2789

119. P Longati , D Albero PMC. Hepatocyte growth factor is a pleiotropic factor protecting epithelial cells from apoptosis. *Cell Death Differ*. Published online 1996. https://pubmed.ncbi.nlm.nih.gov/17180051/

120. Giannoni E, Buricchi F, Raugei G, Ramponi G, Chiarugi P. Intracellular Reactive Oxygen Species Activate Src Tyrosine Kinase during Cell Adhesion and Anchorage-Dependent Cell Growth. *Mol Cell Biol*. 2005;25(15):6391-6403. doi:10.1128/mcb.25.15.6391-6403.2005

121. Giannoni E, Buricchi F, Grimaldi G, et al. Redox regulation of anoikis: Reactive oxygen species as essential mediators of cell survival. *Cell Death Differ*. 2008;15(5):867-878. doi:10.1038/cdd.2008.3

122. Giannoni E, Chiarugi P. Redox circuitries driving Src regulation. *Antioxidants Redox Signal*. 2014;20(13):2011-2025. doi:10.1089/ars.2013.5525

123. Porporato PE, Payen VL, Pérez-Escuredo J, et al. A mitochondrial switch promotes tumor metastasis. *Cell Rep*. 2014;8(3):754-766. doi:10.1016/j.celrep.2014.06.043

124. Chandel NS, McClintock DS, Feliciano CE, et al. Reactive oxygen species generated at mitochondrial Complex III stabilize hypoxia-inducible factor-1α during hypoxia: A mechanism of O2 sensing. *J Biol Chem*. 2000;275(33):25130-25138. doi:10.1074/jbc.M001914200

125. Xia C, Meng Q, Liu LZ, Rojanasakul Y, Wang XR, Jiang BH. Reactive oxygen species regulate angiogenesis and tumor growth through vascular endothelial growth factor. *Cancer Res*. 2007;67(22):10823-10830. doi:10.1158/0008-5472.CAN-07-0783

126. Esteller M. CpG island hypermethylation and tumor suppressor genes: A booming present, a brighter future. *Oncogene*. 2002;21(35 REV. ISS. 3):5427-5440. doi:10.1038/sj.onc.1205600

127. Herman JG, Baylin SB. Gene Silencing in Cancer in Association with Promoter Hypermethylation. *N Engl J Med*. 2003;349(21):2042-2054. doi:10.1056/NEJMra023075

128. Lim SO, Gu JM, Kim MS, et al. Epigenetic Changes Induced by Reactive Oxygen Species in Hepatocellular Carcinoma: Methylation of the E-cadherin Promoter. *Gastroenterology*.

2008;135(6). doi:10.1053/j.gastro.2008.07.027

129. DAVIES SP, HAWLEY SA, WOODS A, CARLING D, HAYSTEAD TAJ, HARDIE DG. Purification of the AMP-activated protein kinase on ATP-γ-Sepharose and analysis of its subunit structure. *Eur J Biochem*. 1994;223(2):351-357. doi:10.1111/j.1432-1033.1994.tb19001.x

130. Dasgupta B, Chhipa RR. Evolving Lessons on the Complex Role of AMPK in Normal Physiology and Cancer. *Trends Pharmacol Sci*. 2016;37(3):192-206. doi:10.1016/j.tips.2015.11.007

131. Ross FA, Jensen TE, Hardie DG. Differential regulation by AMP and ADP of AMPK complexes containing different γ subunit isoforms. *Biochem J*. 2016;473(2):189-199. doi:10.1042/BJ20150910

132. Hardie DG, Ross FA, Hawley SA. AMPK: A nutrient and energy sensor that maintains energy homeostasis. *Nat Rev Mol Cell Biol*. 2012;13(4):251-262. doi:10.1038/nrm3311

133. Voss M, Paterson J, Kelsall IR, et al. Ppm1E is an in cellulo AMP-activated protein kinase phosphatase. *Cell Signal*. 2011;23(1):114-124. doi:10.1016/j.cellsig.2010.08.010

134. Hawley SA, Boudeau J, Reid JL, et al. Complexes between the LKB1 tumor suppressor, STRAD alpha/beta and MO25 alpha/beta are upstream kinases in the AMP-activated protein kinase cascade. *J Biol*. 2003;2(4):28. doi:10.1186/1475-4924-2-28

135. Woods A, Johnstone SR, Dickerson K, et al. LKB1 Is the Upstream Kinase in the AMP-Activated Protein Kinase Cascade. *Curr Biol*. 2003;13(22):2004-2008. doi:10.1016/j.cub.2003.10.031

136. Shaw RJ, Kosmatka M, Bardeesy N, et al. The tumor suppressor LKB1 kinase directly activates AMP-activated kinase and regulates apoptosis in response to energy stress. *Proc Natl Acad Sci U S A*. 2004;101(10):3329-3335. doi:10.1073/pnas.0308061100

137. Woods A, Dickerson K, Heath R, et al. Ca2+/calmodulin-dependent protein kinase kinase-β acts upstream of AMP-activated protein kinase in mammalian cells. *Cell Metab*. 2005;2(1):21-33. doi:10.1016/j.cmet.2005.06.005

138. Hawley SA, Pan DA, Mustard KJ, et al. Calmodulin-dependent protein kinase kinase-β is an alternative upstream kinase for AMP-activated protein kinase. *Cell Metab*. 2005;2(1):9-19. doi:10.1016/j.cmet.2005.05.009

139. Hurley RL, Anderson KA, Franzone JM, Kemp BE, Means AR, Witters LA. The Ca2+/calmodulin-dependent protein kinase kinases are AMP-activated protein kinase kinases. *J Biol Chem*. 2005;280(32):29060-29066. doi:10.1074/jbc.M503824200

140. Davies SP, Helps NR, Cohen PTW, Hardie DG. 5′-AMP inhibits dephosphorylation, as well as promoting phosphorylation, of the AMP-activated protein kinase. Studies using

bacterially expressed human protein phosphatase-2Cα and native bovine protein phosphatase-2Ac. *FEBS Lett*. 1995;377(3):421-425. doi:10.1016/0014-5793(95)01368-7

141. Hardie DG, Scott JW, Pan DA, Hudson ER. Management of cellular energy by the AMP-activated protein kinase system. *FEBS Lett*. 2003;546(1):113-120. doi:10.1016/S0014-5793(03)00560-X
142. Kemp BE, Stapleton D, Campbell DJ, et al. AMP-activated protein kinase, super metabolic regulator. In: *Biochemical Society Transactions*. Vol 31. Portland Press Ltd; 2003:162-168. doi:10.1042/bst0310162
143. Kahn BB, Alquier T, Carling D, Hardie DG. AMP-activated protein kinase: Ancient energy gauge provides clues to modern understanding of metabolism. *Cell Metab*. 2005;1(1):15-25. doi:10.1016/j.cmet.2004.12.003
144. Oakhill JS, Chen ZP, Scott JW, et al. β-Subunit myristoylation is the gatekeeper for initiating metabolic stress sensing by AMP-activated protein kinase (AMPK). *Proc Natl Acad Sci U S A*. 2010;107(45):19237-19241. doi:10.1073/pnas.1009705107
145. Momcilovic M, Hong SP, Carlson M. Mammalian TAK1 activates Snf1 protein kinase in yeast and phosphorylates AMP-activated protein kinase in vitro. *J Biol Chem*. 2006;281(35):25336-25343. doi:10.1074/jbc.M604399200
146. Jeon SM. Regulation and function of AMPK in physiology and diseases. *Exp Mol Med*. 2016;48(7):e245. doi:10.1038/emm.2016.81
147. Alessi DR, Sakamoto K, Bayascas JR. LKB1-dependent signaling pathways. *Annu Rev Biochem*. 2006;75:137-163. doi:10.1146/annurev.biochem.75.103004.142702
148. Bolster DR, Crozier SJ, Kimball SR, Jefferson LS. AMP-activated protein kinase suppresses protein synthesis in rat skeletal muscle through down-regulated mammalian target of rapamycin (mTOR) signaling. *J Biol Chem*. 2002;277(27):23977-23980. doi:10.1074/jbc.C200171200
149. Hardie DG, Carling D. The AMP-activated protein kinase. Fuel gauge of the mammalian cell? *Eur J Biochem*. 1997;246(2):259-273. doi:10.1111/j.1432-1033.1997.00259.x
150. Hardie DG. Sensing of energy and nutrients by AMP-activated protein kinase. In: *American Journal of Clinical Nutrition*. Vol 93. Am J Clin Nutr; 2011. doi:10.3945/ajcn.110.001925
151. Shackelford DB, Shaw RJ. The LKB1-AMPK pathway: Metabolism and growth control in tumour suppression. *Nat Rev Cancer*. 2009;9(8):563-575. doi:10.1038/nrc2676
152. Green AS, Chapuis N, Lacombe C, Mayeux P, Bouscary D, Tamburini J. LKB1/AMPK/mTOR signaling pathway in hematological malignancies: From metabolism to cancer cell biology. *Cell Cycle*. 2011;10(13):2115-2120. doi:10.4161/cc.10.13.16244
153. Hadad SM, Fleming S, Thompson AM. Targeting AMPK: A new therapeutic opportunity in

breast cancer. *Crit Rev Oncol Hematol*. 2008;67(1):1-7. doi:10.1016/j.critrevonc.2008.01.007

154. Friedl P, Wolf K. Tumour-cell invasion and migration: Diversity and escape mechanisms. *Nat Rev Cancer*. 2003;3(5):362-374. doi:10.1038/nrc1075
155. Friedl P, Wolf K. Plasticity of cell migration: A multiscale tuning model. *J Cell Biol*. 2010;188(1):11-19. doi:10.1083/jcb.200909003
156. Friedl P, Entschladen F, Conrad C, Niggemann B, Zänker KS. CD4+ T lymphocytes migrating in three-dimensional collagen lattices lack focal adhesions and utilize β1 integrin-independent strategies for polarization, interaction with collagen fibers and locomotion. *Eur J Immunol*. 1998;28(8):2331-2343. doi:10.1002/(SICI)1521-4141(199808)28:08<2331::AID-IMMU2331>3.0.CO;2-C
157. Renkawitz J, Schumann K, Weber M, et al. Adaptive force transmission in amoeboid cell migration. *Nat Cell Biol*. 2009;11(12):1438-1443. doi:10.1038/ncb1992
158. Sroka J, Madeja Z, Michalik M, Przestalski S, Korohoda W. Folic acid, ascorbic acid and sodium selenite restore the motility of Dictyostelium discoideum inhibited by triethyllead. *Toxicology*. 2002;180(3):275-292. doi:10.1016/S0300-483X(02)00419-5
159. Leader WM, Stopak D, Harris AK. *INCREASED CONTRACTILE STRENGTH AND TIGHTENED ADHESIONS TO THE SUBSTRATUM RESULT FROM REVERSE TRANSFORMATION OF CHO CELLS BY DIBUTYRYL CYCLIC ADENOSINE MONOPHOSPHATE*. Vol 64.; 1983.
160. Polte TR, Eichler GS, Wang N, Ingber DE. Extracellular matrix controls myosin light chain phosphorylation and cell contractility through modulation of cell shape and cytoskeletal prestress. *Am J Physiol - Cell Physiol*. 2004;286(3 55-3). doi:10.1152/ajpcell.00280.2003
161. Kolyada AY, Riley KN, Herman IM. Rho GTPase signaling modulates cell shape and contractile phenotype in an isoactin-specific manner. *Am J Physiol - Cell Physiol*. 2003;285(5 54-5). doi:10.1152/ajpcell.00177.2003
162. Sanz-Moreno V, Gadea G, Ahn J, et al. Rac Activation and Inactivation Control Plasticity of Tumor Cell Movement. *Cell*. 2008;135(3):510-523. doi:10.1016/j.cell.2008.09.043
163. Pelham RJ, Wang YL. Cell locomotion and focal adhesions are regulated by substrate flexibility. *Proc Natl Acad Sci U S A*. 1997;94(25):13661-13665. doi:10.1073/pnas.94.25.13661
164. Young WC, Herman IM. Extracellular matrix modulation of endothelial cell shape and motility following injury in vitro. *J Cell Sci*. 1985;VOL. 73:19-32. Accessed November 26, 2020. https://pubmed.ncbi.nlm.nih.gov/3894383/
165. Hegerfeldt Y, Tusch M, Bröcker EB, Friedl P. Collective cell movement in primary

melanoma explants: Plasticity of cell-cell interaction, β1-integrin function, and migration strategies. *Cancer Res*. 2002;62(7):2125-2130.

166. Hashizume R, Koizumi H, Ihara A, Ohta T, Uchikoshi T. Expression of β-catenin in normal breast tissue and breast carcinoma: A comparative study with epithelial cadherin and α-catenin. *Histopathology*. 1996;29(2):139-146. doi:10.1046/j.1365-2559.1996.d01-499.x
167. Madhavan M, Srinivas P, Abraham E, et al. Cadherins as predictive markers of nodal metastasis in breast cancer. *Mod Pathol*. 2001;14(5):423-427. doi:10.1038/modpathol.3880329
168. Friedl P, Noble PB, Walton PA, et al. Migration of Coordinated Cell Clusters in Mesenchymal and Epithelial Cancer Explants in Vitro. *Cancer Res*. 1995;55(20).
169. Lauffenburger DA, Horwitz AF. Cell migration: A physically integrated molecular process. *Cell*. 1996;84(3):359-369. doi:10.1016/S0092-8674(00)81280-5
170. Dai J, Sheetz MP. Membrane tether formation from blebbing cells. *Biophys J*. 1999;77(6):3363-3370. doi:10.1016/S0006-3495(99)77168-7
171. Estecha A, Sánchez-Martín L, Puig-Kröger A, et al. Moesin orchestrates cortical polarity of melanoma tumour cells to initiate 3D invasion. *J Cell Sci*. 2009;122(19):3492-3501. doi:10.1242/jcs.053157
172. Poincloux R, Collin O, Lizárraga F, et al. Contractility of the cell rear drives invasion of breast tumor cells in 3D Matrigel. *Proc Natl Acad Sci U S A*. 2011;108(5):1943-1948. doi:10.1073/pnas.1010396108
173. Friedl P, Maaser K, Klein CE, Niggemann B, Krohne G, Zänker KS. Migration of highly aggressive MV3 melanoma cells in 3-dimensional collagen lattices results in local matrix reorganization and shedding of α2 and β1 integrins and CD44. *Cancer Res*. 1997;57(10):2061-2070. Accessed November 29, 2020. https://pubmed.ncbi.nlm.nih.gov/9158006/
174. Burridge K, Chrzanowska-Wodnicka M. Focal adhesions, contractility, and signaling. *Annu Rev Cell Dev Biol*. 1996;12:463-519. doi:10.1146/annurev.cellbio.12.1.463
175. L P Cramer. Organization and polarity of actin filament networks in cells: implications for the mechanism of myosin-based cell motility. *Biochem Soc Symp*. Published online 1999.
176. Cukierman E, Pankov R, Stevens DR, Yamada KM. Taking cell-matrix adhesions to the third dimension. *Science (80-)*. 2001;294(5547):1708-1712. doi:10.1126/science.1064829
177. Leavesley DI, Ferguson GD, Wayner EA, Cheresh DA. Requirement of the integrin β3 subunit for carcinoma cell spreading or migration on vitronectin and fibrinogen. *J Cell Biol*. 1992;117(5):1101-1107. doi:10.1083/jcb.117.5.1101
178. Maaser K, Wolf K, Klein CE, et al. Functional hierarchy of simultaneously expressed

adhesion receptors: Integrin α2β1 but not CD44 mediates MV3 melanoma cell migration and matrix reorganization within three-dimensional hyaluronan-containing collagen matrices. *Mol Biol Cell*. 1999;10(10):3067-3079. doi:10.1091/mbc.10.10.3067

179. Rabinovitz I, Mercurio AM. The integrin α6β4 functions in carcinoma cell migration on laminin-1 by mediating the formation and stabilization of actin-containing motility structures. *J Cell Biol*. 1997;139(7):1873-1884. doi:10.1083/jcb.139.7.1873
180. Randolph Byers H, Fujiwara K. Stress fibers in cells in Situ: Immunofluorescence visualization with antiactin, antimyosin, and anti-alphaactinin. *J Cell Biol*. 1982;93(3):804-811. doi:10.1083/jcb.93.3.804
181. Katoh K, Kano Y, Amano M, Onishi H, Kaibuchi K, Fujiwara K. Rho-kinase-mediated contraction of isolated stress fibers. *J Cell Biol*. 2001;152(3):569-583. doi:10.1083/jcb.153.3.569
182. Kaibuchi K, Kuroda S, Amano M. Regulation of the cytoskeleton and cell adhesion by the Rho family GTPases in mammalian cells. *Annu Rev Biochem*. 1999;68:459-486. doi:10.1146/annurev.biochem.68.1.459
183. Totsukawa G, Yamakita Y, Yamashiro S, Hartshorne DJ, Sasaki Y, Matsumura F. Distinct roles of ROCK (Rho-kinase) and MLCK in spatial regulation of MLC phosphorylation for assembly of stress fibers and focal adhesions in 3T3 fibroblasts. *J Cell Biol*. 2000;150(4):797-806. doi:10.1083/jcb.150.4.797
184. Kamm KE, Stull JT. Dedicated Myosin Light Chain Kinases with Diverse Cellular Functions. *J Biol Chem*. 2001;276(7):4527-4530. doi:10.1074/jbc.R000028200
185. Somlyo A V., Phelps C, Dipierro C, et al. Rho kinase and matrix metalloproteinase inhibitors cooperate to inhibit angiogenesis and growth of human prostate cancer xenotransplants. *FASEB J*. 2003;17(2):223-234. doi:10.1096/fj.02-0655com
186. Verkhovsky AB, Svitkina TM, Borisy GG. Myosin II filament assemblies in the active lamella of fibroblasts: Their morphogenesis and role in the formation of actin filament bundles. *J Cell Biol*. 1995;131(4):989-1002. doi:10.1083/jcb.131.4.989
187. Palecek SP, Loftust JC, Ginsberg MH, Lauffenburger DA, Horwitz AF. Integrin-ligand binding properties govern cell migration speed through cell-substratum adhesiveness. *Nature*. 1997;385(6616):537-540. doi:10.1038/385537a0
188. Potter DA, Tirnauer JS, Janssen R, et al. Calpain regulates actin remodeling during cell spreading. *J Cell Biol*. 1998;141(3):647-662. doi:10.1083/jcb.141.3.647
189. Ballestrem C, Hinz B, Imhof BA, Wehrle-Haller B. Marching at the front and dragging behind: Differential αVβ3-integrin turnover regulates focal adhesion behavior. *J Cell Biol*. 2001;155(7):1319-1332. doi:10.1083/jcb.200107107

190. Filardo EJ, Brooks PC, Deming SL, Damsky C, Cheresh DA. Requirement of the NPXY motif in the integrin β3 subunit cytoplasmic tail for melanoma cell migration in vitro and in vivo. *J Cell Biol*. 1995;130(2):441-450. doi:10.1083/jcb.130.2.441

191. Flanagan LA, Chou J, Falet H, Neujahr R, Hartwig JH, Stossel TP. Filamin A, the Arp2/3 complex, and the morphology and function of cortical actin filaments in human melanoma cells. *J Cell Biol*. 2001;155(4):511-517. doi:10.1083/jcb.200105148

192. Hynes RO. Integrins: Bidirectional, allosteric signaling machines. *Cell*. 2002;110(6):673-687. doi:10.1016/S0092-8674(02)00971-6

193. Hofmann UB, Westphal JR, Van Muijen GNP, Ruiter DJ. Matrix metalloproteinases in human melanoma. *J Invest Dermatol*. 2000;115(3):337-344. doi:10.1046/j.1523-1747.2000.00068.x

194. Sameni M, Moin K, Sloane BF. Imaging proteolysis by living human breast cancer cells. *Neoplasia*. 2000;2(6):496-504. doi:10.1038/sj.neo.7900116

195. Rosenthal EL, Hotary K, Bradford C, Weiss SJ. Role of membrane type 1-matrix metalloproteinase and gelatinase A in head and neck squamous cell carcinoma invasion in vitro. *Otolaryngol - Head Neck Surg*. 1999;121(4):337-343. doi:10.1016/S0194-5998(99)70217-2

196. Deryugina EI, Bourdon MA, Reisfeld RA, Strongin A. Remodeling of Collagen Matrix by Human Tumor Cells Requires Activation and Cell Surface Association of Matrix Metalloproteinase-2. *Cancer Res*. 1998;58(16).

197. Maekawa KI, Sato H, Furukawa M, Yoshizaki T. Inhibition of cervical lymph node metastasis by marimastat (BB-2516) in an orthotopic oral squamous cell carcinoma implantation model. *Clin Exp Metastasis*. 2002;19(6):513-518. doi:10.1023/A:1020329411957

198. Rudolph-Owen LA, Chan R, Muller WJ, Matrisian LM. The Matrix Metalloproteinase Matrilysin Influences Early-Stage Mammary Tumorigenesis. *Cancer Res*. 1998;58(23).

199. Sahai E, Olson MF, Marshall CJ. Cross-talk between Ras and Rho signalling pathways in transformation favours proliferation and increased motility. *EMBO J*. 2001;20(4):755-766. doi:10.1093/emboj/20.4.755

200. Clark EA, Golub TR, Lander ES, Hynes RO. Genomic analysis of metastasis reveals an essential role for RhoC. *Nature*. 2000;406(6795):532-535. doi:10.1038/35020106

201. Itoh K, Yoshioka K, Akedo H, Uehata M, Ishizaki T, Narumiya S. An essential part for Rho-associated kinase in the transcellular invasion of tumor cells. *Nat Med*. 1999;5(2):221-225. doi:10.1038/5587

202. Kaneko K, Satoh K, Masamune A, Satoh A, Shimosegawa T. Myosin light chain kinase

inhibitors can block invasion and adhesion of human pancreatic cancer cell lines. *Pancreas*. 2002;24(1):34-41. doi:10.1097/00006676-200201000-00005

203. Their JP. Epithelial-mesenchymal transitions in tumor progression. *Nat Rev Cancer*. 2002;2(6):442-454. doi:10.1038/nrc822
204. Alper Ö, Bergmann-Leitner ES, Bennett TA, Hacker NF, Stromberg K, Stetler-Stevenson WG. Epidermal growth factor receptor signalling and the invasive phenotype of ovarian carcinoma cells. *J Natl Cancer Inst*. 2001;93(18):1375-1384. doi:10.1093/jnci/93.18.1375
205. Giannelli G, Falk-Marzillier J, Schiraldi O, Stetler-Stevenson WG, Quaranta V. Induction of cell migration by matrix metalloprotease-2 cleavage of laminin-5. *Science (80-)*. 1997;277(5323):225-228. doi:10.1126/science.277.5323.225
206. Seftor REB, Seftor EA, Koshikawa N, et al. Cooperative interactions of laminin 5 γ2 chain, matrix metalloproteinase-2, and membrane type-1-matrix/metalloproteinase are required for mimicry of embryonic vasculogenesis by aggressive melanoma. *Cancer Res*. 2001;61(17):6322-6327.
207. Brooks PC, Klemke RL, Schön S, Lewis JM, Schwartz MA, Cheresh DA. Insulin-like growth factor receptor cooperates with integrin αvβ5 to promote tumor cell dissemination in vivo. *J Clin Invest*. 1997;99(6):1390-1398. doi:10.1172/JCI119298
208. Friedl P, Bröcker EB. The biology of cell locomotion within three-dimensional extracellular matrix. *Cell Mol Life Sci*. 2000;57(1):41-64. doi:10.1007/s000180050498
209. M Abercrombie, G A Dunn JPH. The shape and movement of fibroblasts in culture. *Soc Gen Physiol Ser*. 1977;32:57-70. https://pubmed.ncbi.nlm.nih.gov/333596/
210. Regen CM, Horwitz AF. Dynamics of β1 integrin-mediated adhesive contacts in motile fibroblasts. *J Cell Biol*. 1992;119(5):1347-1359. doi:10.1083/jcb.119.5.1347
211. Smilenov LB, Mikhailov A, Pelham RJ, Marcantonio EE, Gundersen GG. Focal adhesion motility revealed in stationary fibroblasts. *Science (80-)*. 1999;286(5442):1172-1174. doi:10.1126/science.286.5442.1172
212. Yamazaki D, Kurisu S, Takenawa T. Regulation of cancer cell motility through actin reorganization. *Cancer Sci*. 2005;96(7):379-386. doi:10.1111/j.1349-7006.2005.00062.x
213. Lämmermann T, Sixt M. Mechanical modes of "amoeboid" cell migration. *Curr Opin Cell Biol*. 2009;21(5):636-644. doi:10.1016/j.ceb.2009.05.003
214. Rebhun LI. Induced amoeboid movement in eggs of the surf-clam Spisula solidissima. *Exp Cell Res*. 1963;29(3):593-602. doi:10.1016/S0014-4827(63)80019-1
215. Trinkaus JP. Surface activity and locomotion of Fundulus deep cells during blastula and gastrula stages. *Dev Biol*. 1973;30(1):68-103. doi:10.1016/0012-1606(73)90049-3
216. Trinkaus JP, Lentz TL. Surface specializations of Fundulus cells and their relation to cell

movements during gastrulation. *J Cell Biol*. 1967;32(1):139-153. doi:10.1083/jcb.32.1.139

217. Yumura S, Mori H, Fukui Y. Localization of actin and myosin for the study of ameboid movement in Dictyostelium using improved immunofluorescence. *J Cell Biol*. 1984;99(3):894-899. doi:10.1083/jcb.99.3.894
218. Friedl P, Hegerfeldt Y, Tusch M. Collective cell migration in morphogenesis and cancer. *Int J Dev Biol*. 2004;48(5-6):441-449. doi:10.1387/ijdb.041821pf
219. Lorentzen HF. Targeted therapy for malignant melanoma. *Curr Opin Pharmacol*. 2019;46:116-121. doi:10.1016/j.coph.2019.05.010
220. Sanz-Moreno V, Gaggioli C, Yeo M, et al. ROCK and JAK1 Signaling Cooperate to Control Actomyosin Contractility in Tumor Cells and Stroma. *Cancer Cell*. 2011;20(2):229-245. doi:10.1016/j.ccr.2011.06.018
221. Werr J, Xie X, Hedqvist P, Ruoslahti E, Lindbom L. β1 integrins are critically involved in neutrophil locomotion in extravascular tissue in vivo. *J Exp Med*. 1998;187(12):2091-2096. doi:10.1084/jem.187.12.2091
222. Brakebusch C, Fillatreau S, Potocnik AJ, et al. β1 integrin is not essential for hematopoiesis but is necessary for the T cell-dependent IgM antibody response. *Immunity*. 2002;16(3):465-477. doi:10.1016/S1074-7613(02)00281-9
223. Friedl P, Zänker KS, Bröcker EB. Cell migration strategies in 3-D extracellular matrix: Differences in morphology, cell matrix interactions, and integrin function. *Microsc Res Tech*. 1998;43(5):369-378. doi:10.1002/(SICI)1097-0029(19981201)43:5<369::AID-JEMT3>3.0.CO;2-6
224. Friedl P, Borgmann S, Bröcker EB. Amoeboid leukocyte crawling through extracellular matrix: lessons from the Dictyostelium paradigm of cell movement. *J Leukoc Biol*. 2001;70(4):491-509. doi:10.1189/jlb.70.4.491
225. Nimnual AS, Taylor LJ, Bar-Sagi D. Redox-dependent downregulation of Rho by Rac. *Nat Cell Biol*. 2003;5(3):236-241. doi:10.1038/ncb938
226. Parri M, Taddei ML, Bianchini F, Calorini L, Chiarugi P. EphA2 reexpression prompts invasion of melanoma cells shifting from mesenchymal to amoeboid-like motility style. *Cancer Res*. 2009;69(5):2072-2081. doi:10.1158/0008-5472.CAN-08-1845
227. Paluch E, Piel M, Prost J, Bornens M, Sykes C. Cortical actomyosin breakage triggers shape oscillations in cells and cell fragments. *Biophys J*. 2005;89(1):724-733. doi:10.1529/biophysj.105.060590
228. Cunningham CC. Actin polymerization and intracellular solvent flow in cell surface blebbing. *J Cell Biol*. 1995;129(6):1589-1599. doi:10.1083/jcb.129.6.1589
229. Paluch E, Sykes C, Prost J, Bornens M. Dynamic modes of the cortical actomyosin gel

during cell locomotion and division. *Trends Cell Biol*. 2006;16(1):5-10. doi:10.1016/j.tcb.2005.11.003

230. Charras GT, Hu CK, Coughlin M, Mitchison TJ. Reassembly of contractile actin cortex in cell blebs. *J Cell Biol*. 2006;175(3):477-490. doi:10.1083/jcb.200602085
231. Keller HU, Bebie H. Protrusive activity quantitatively determines the rate and direction of cell locomotion. *Cell Motil Cytoskeleton*. 1996;33(4):241-251. doi:10.1002/(SICI)1097-0169(1996)33:4<241::AID-CM1>3.0.CO;2-C
232. Sahai E, Marshall CJ. Differing modes for tumour cell invasion have distinct requirements for Rho/ROCK signalling and extracellular proteolysis. *Nat Cell Biol*. 2003;5(8):711-719. doi:10.1038/ncb1019
233. Sanz-Moreno V, Gadea G, Ahn J, et al. Rac Activation and Inactivation Control Plasticity of Tumor Cell Movement. *Cell*. 2008;135(3):510-523. doi:10.1016/j.cell.2008.09.043
234. Rintoul RC, Sethi T. The role of extracellular matrix in small-cell lung cancer. *Lancet Oncol*. 2001;2(7):437-442. doi:10.1016/S1470-2045(00)00421-6
235. Friedl P. Prespecification and plasticity: Shifting mechanisms of cell migration. *Curr Opin Cell Biol*. 2004;16(1):14-23. doi:10.1016/j.ceb.2003.11.001
236. Their JP. Epithelial-mesenchymal transitions in tumor progression. *Nat Rev Cancer*. 2002;2(6):442-454. doi:10.1038/nrc822
237. Nieto MA, Cano A. The epithelial-mesenchymal transition under control: Global programs to regulate epithelial plasticity. *Semin Cancer Biol*. 2012;22(5-6):361-368. doi:10.1016/j.semcancer.2012.05.003
238. Yilmaz M, Christofori G. EMT, the cytoskeleton, and cancer cell invasion. *Cancer Metastasis Rev*. 2009;28(1-2):15-33. doi:10.1007/s10555-008-9169-0
239. Savagner P, Vallés AM, Jouanneau J, Yamada KM, Thiery JP. Alternative splicing in fibroblast growth factor receptor 2 is associated with induced epithelial-mesenchymal transition in rat bladder carcinoma cells. *Mol Biol Cell*. 1994;5(8):851-862. doi:10.1091/mbc.5.8.851
240. Paoli P, Giannoni E, Chiarugi P. Anoikis molecular pathways and its role in cancer progression. *Biochim Biophys Acta - Mol Cell Res*. 2013;1833(12):3481-3498. doi:10.1016/j.bbamcr.2013.06.026
241. Nieto MA. The snail superfamily of zinc-finger transcription factors. *Nat Rev Mol Cell Biol*. 2002;3(3):155-166. doi:10.1038/nrm757
242. Wang Q, Tan YX, Ren Y Bin, et al. Zinc finger protein ZBTB20 expression is increased in hepatocellular carcinoma and associated with poor prognosis. *BMC Cancer*. 2011;11. doi:10.1186/1471-2407-11-271

243. Uchikado Y, Okumura H, Ishigami S, et al. Increased Slug and decreased E-cadherin expression is related to poor prognosis in patients with gastric cancer. *Gastric Cancer*. 2011;14(1):41-49. doi:10.1007/s10120-011-0004-x

244. Yilmaz M, Christofori G, Lehembre F. Distinct mechanisms of tumor invasion and metastasis. *Trends Mol Med*. 2007;13(12):535-541. doi:10.1016/j.molmed.2007.10.004

245. Pani G, Giannoni E, Galeotti T, Chiarugi P. Redox-based escape mechanism from death: The cancer lesson. *Antioxidants Redox Signal*. 2009;11(11):2791-2806. doi:10.1089/ars.2009.2739

246. Wolf K, Mazo I, Leung H, et al. Compensation mechanism in tumor cell migration: Mesenchymal-amoeboid transition after blocking of pericellular proteolysis. *J Cell Biol*. 2003;160(2):267-277. doi:10.1083/jcb.200209006

247. Giannoni E, Taddei ML, Parri M, et al. EphA2-mediated mesenchymal-amoeboid transition induced by endothelial progenitor cells enhances metastatic spread due to cancer-associated fibroblasts. *J Mol Med*. 2013;91(1):103-115. doi:10.1007/s00109-012-0941-9

248. Taddei ML, Giannoni E, Morandi A, et al. *Mesenchymal to Amoeboid Transition Is Associated with Stem-like Features of Melanoma Cells*. Vol 12.; 2014. doi:10.1186/1478-811X-12-24

249. Steeg PS. Tumor metastasis: Mechanistic insights and clinical challenges. *Nat Med*. 2006;12(8):895-904. doi:10.1038/nm1469

250. Wang X, Adjei AA. Lung cancer and metastasis: new opportunities and challenges. *Cancer Metastasis Rev*. 2015;34(2):169-171. doi:10.1007/s10555-015-9562-4

251. Sporn MB. The war on cancer. *Lancet*. 1996;347(9012):1377-1381. doi:10.1016/S0140-6736(96)91015-6

252. Guarino M. Epithelial-mesenchymal transition and tumour invasion. *Int J Biochem Cell Biol*. 2007;39(12):2153-2160. doi:10.1016/j.biocel.2007.07.011

253. Peinado H, Lavotshkin S, Lyden D. The secreted factors responsible for pre-metastatic niche formation: Old sayings and new thoughts. *Semin Cancer Biol*. 2011;21(2):139-146. doi:10.1016/j.semcancer.2011.01.002

254. Lujambio A, Lowe SW. The microcosmos of cancer. *Nature*. 2012;482(7385):347-355. doi:10.1038/nature10888

255. Taddei ML, Giannoni E, Comito G, Chiarugi P. Microenvironment and tumor cell plasticity: An easy way out. *Cancer Lett*. 2013;341(1):80-96. doi:10.1016/j.canlet.2013.01.042

256. Holmgren L, O'reilly MS, Folkman J. Dormancy of micrometastases: Balanced proliferation and apoptosis in the presence of angiogenesis suppression. *Nat Med*.

1995;1(2):149-153. doi:10.1038/nm0295-149

257. Parangi S, O'Reilly M, Christofori G, et al. Antiangiogenic therapy of transgenic mice impairs de novo tumor growth. *Proc Natl Acad Sci U S A*. 1996;93(5):2002-2007. doi:10.1073/pnas.93.5.2002

258. Folberg R, Rummelt V, Parys-Van Ginderdeuren R, et al. The Prognostic Value of Tumor Blood Vessel Morphology in Primary Uveal Melanoma. *Ophthalmology*. 1993;100(9):1389-1398. doi:10.1016/S0161-6420(93)31470-3

259. Qiao L, Liang N, Zhang J, et al. Advanced research on vasculogenic mimicry in cancer. *J Cell Mol Med*. 2015;19(2):315-326. doi:10.1111/jcmm.12496

260. Dudley AC. Tumor endothelial cells. *Cold Spring Harb Perspect Med*. 2012;2(3). doi:10.1101/cshperspect.a006536

261. Jain RK. Determinants of Tumor Blood Flow: A Review. *Cancer Res*. 1988;48(10).

262. Sullivan R, Graham CH. Hypoxia-driven selection of the metastatic phenotype. *Cancer Metastasis Rev*. 2007;26(2):319-331. doi:10.1007/s10555-007-9062-2

263. Ebos JML, Lee CR, Cruz-Munoz W, Bjarnason GA, Christensen JG, Kerbel RS. Accelerated Metastasis after Short-Term Treatment with a Potent Inhibitor of Tumor Angiogenesis. *Cancer Cell*. 2009;15(3):232-239. doi:10.1016/j.ccr.2009.01.021

264. Ebos JML, Lee CR, Kerbel RS. Tumor and host-mediated pathways of resistance and disease progression in response to antiangiogenic therapy. *Clin Cancer Res*. 2009;15(16):5020-5025. doi:10.1158/1078-0432.CCR-09-0095

265. Yilmaz M, Christofori G, Lehembre F. Distinct mechanisms of tumor invasion and metastasis. *Trends Mol Med*. 2007;13(12):535-541. doi:10.1016/j.molmed.2007.10.004

266. Chung LWK, Baseman A, Assikis V, Zhau HE. Molecular insights into prostate cancer progression: The missing link of tumor microenvironment. *J Urol*. 2005;173(1):10-20. doi:10.1097/01.ju.0000141582.15218.10

267. Zervantonakis IK, Hughes-Alford SK, Charest JL, Condeelis JS, Gertler FB, Kamm RD. Three-dimensional microfluidic model for tumor cell intravasation and endothelial barrier function. *Proc Natl Acad Sci U S A*. 2012;109(34):13515-13520. doi:10.1073/pnas.1210182109

268. Ramis-Conde I, Chaplain MAJ, Anderson ARA, Drasdo D. Multi-scale modelling of cancer cell intravasation: The role of cadherins in metastasis. *Phys Biol*. 2009;6(1). doi:10.1088/1478-3975/6/1/016008

269. Wirtz D. Particle-tracking microrheology of living cells: Principles and applications. *Annu Rev Biophys*. 2009;38(1):301-326. doi:10.1146/annurev.biophys.050708.133724

270. Yeung T, Georges PC, Flanagan LA, et al. Effects of substrate stiffness on cell morphology,

cytoskeletal structure, and adhesion. *Cell Motil Cytoskeleton*. 2005;60(1):24-34. doi:10.1002/cm.20041

271. Baker EL, Lu J, Yu D, Bonnecaze RT, Zaman MH. Cancer cell stiffness: Integrated roles of three-dimensional matrix stiffness and transforming potential. *Biophys J*. 2010;99(7):2048-2057. doi:10.1016/j.bpj.2010.07.051
272. Alizadeh AM, Shiri S, Farsinejad S. Metastasis review: from bench to bedside. *Tumor Biol*. 2014;35(9):8483-8523. doi:10.1007/s13277-014-2421-z
273. Gilmore AP. Anoikis. *Cell Death Differ*. 2005;12:1473-1477. doi:10.1038/sj.cdd.4401723
274. Grossmann J. Molecular mechanisms of "detachment-induced apoptosis - Anoikis." *Apoptosis*. 2002;7(3):247-260. doi:10.1023/A:1015312119693
275. Reddig PJ, Juliano RL. Clinging to life: Cell to matrix adhesion and cell survival. *Cancer Metastasis Rev*. 2005;24(3):425-439. doi:10.1007/s10555-005-5134-3
276. Shimizu S, Narita M, Tsujimoto Y. Bcl-2 family proteins regulate the release of apoptogenic cytochrome c by the mitochondrial channel VDAC. *Nature*. 1999;399(6735):483-487. doi:10.1038/20959
277. Thornberry NA. Caspases: Key mediators of apoptosis. *Chem Biol*. 1998;5(5). doi:10.1016/S1074-5521(98)90615-9
278. Tokunaga E, Oki E, Egashira A, et al. Deregulation of the Akt Pathway in Human Cancer. *Curr Cancer Drug Targets*. 2008;8(1):27-36. doi:10.2174/156800908783497140
279. Boudreau NJ, Jones PL. Extracellular matrix and integrin signalling: The shape of things to come. *Biochem J*. 1999;339(3):481-488. doi:10.1042/0264-6021:3390481
280. Taylor RC, Cullen SP, Martin SJ. Apoptosis: Controlled demolition at the cellular level. *Nat Rev Mol Cell Biol*. 2008;9(3):231-241. doi:10.1038/nrm2312
281. Wajant H. The Fas signaling pathway: More than a paradigm. *Science (80-)*. 2002;296(5573):1635-1636. doi:10.1126/science.1071553
282. Valentijn AJ, Gilmore AP. Translocation of full-length bid to mitochondria during anoikis. *J Biol Chem*. 2004;279(31):32848-32857. doi:10.1074/jbc.M313375200
283. Bergin E, Levine JS, Koh JS, Lieberthal W. Mouse proximal tubular cell-cell adhesion inhibits apoptosis by a cadherin-dependent mechanism. *Am J Physiol - Ren Physiol*. 2000;278(5 47-5). doi:10.1152/ajprenal.2000.278.5.f758
284. Kantak SS, Kramer RH. E-cadherin regulates anchorage-independent growth and survival in oral squamous cell carcinoma cells. *J Biol Chem*. 1998;273(27):16953-16961. doi:10.1074/jbc.273.27.16953
285. Orford K, Orford CC, Byers SW. Exogenous expression of β-catenin regulates contact inhibition, anchorage-independent growth, anoikis, and radiation-induced cell cycle arrest. *J*

Cell Biol. 1999;146(4):855-867. doi:10.1083/jcb.146.4.855

286. David McConkey WKAY and PASMADDKHDRBTJM. Regulation of Akt/PKB Activity, Cellular Growth, and Apoptosis in Prostate Carcinoma Cells by MMAC/PTEN. *Cancer Res*. Published online 1999. https://cancerres.aacrjournals.org/content/59/11/2551.long

287. Vitolo MI, Weiss MB, Szmacinski M, et al. Deletion of PTEN promotes tumorigenic signaling, resistance to anoikis, and altered response to chemotherapeutic agents in human mammary epithelial cells. *Cancer Res*. 2009;69(21):8275-8283. doi:10.1158/0008-5472.CAN-09-1067

288. Chen C, Pore N, Behrooz A, Ismail-Beigi F, Maity A. Regulation of glut1 mRNA by hypoxia-inducible factor-1: Interaction between H-ras and hypoxia. *J Biol Chem*. 2001;276(12):9519-9525. doi:10.1074/jbc.M010144200

289. Osada-Oka M, Hashiba Y, Akiba S, Imaoka S, Sato T. Glucose is necessary for stabilization of hypoxia-inducible factor-1α under hypoxia: Contribution of the pentose phosphate pathway to this stabilization. *FEBS Lett*. 2010;584(14):3073-3079. doi:10.1016/j.febslet.2010.05.046

290. Royer C, Lachuer J, Crouzoulon G, et al. Effects of gestational hypoxia on mRNA levels of Glut3 and Glut4 transporters, hypoxia inducible factor-1 and thyroid hormone receptors in developing rat brain. *Brain Res*. 2000;856(1-2):119-128. doi:10.1016/S0006-8993(99)02365-3

291. Semenza GL, Jiang BH, Leung SW, et al. Hypoxia response elements in the aldolase A, enolase 1, and lactate dehydrogenase a gene promoters contain essential binding sites for hypoxia-inducible factor 1. *J Biol Chem*. 1996;271(51):32529-32537. doi:10.1074/jbc.271.51.32529

292. Keith B, Johnson RS, Simon MC. HIF1 α and HIF2 α: sibling rivalry in hypoxic tumour growth and progression. *Nat Rev Cancer*. 2012;12(1):9-22. doi:10.1038/nrc3183

293. Tsai YP, Wu KJ. Hypoxia-regulated target genes implicated in tumor metastasis. *J Biomed Sci*. 2012;19(1). doi:10.1186/1423-0127-19-102

294. Giannoni E, Bianchini F, Calorini L, Chiarugi P. Cancer associated fibroblasts exploit reactive oxygen species through a proinflammatory signature leading to epithelial mesenchymal transition and stemness. *Antioxidants Redox Signal*. 2011;14(12):2361-2371. doi:10.1089/ars.2010.3727

295. Giannoni E, Bianchini F, Masieri L, et al. Reciprocal activation of prostate cancer cells and cancer-associated fibroblasts stimulates epithelial-mesenchymal transition and cancer stemness. *Cancer Res*. 2010;70(17):6945-6956. doi:10.1158/0008-5472.CAN-10-0785

296. Sun S, Ning X, Zhang Y, et al. Hypoxia-inducible factor-1α induces Twist expression in

tubular epithelial cells subjected to hypoxia, leading to epithelial-to-mesenchymal transition. *Kidney Int*. 2009;75(12):1278-1287. doi:10.1038/ki.2009.62

297. Widmann C, Gibson S, Johnson GL. Caspase-dependent cleavage of signaling proteins during apoptosis. A turn-off mechanism for anti-apoptotic signals. *J Biol Chem*. 1998;273(12):7141-7147. doi:10.1074/jbc.273.12.7141
298. Stoletov K, Kato H, Zardouzian E, et al. Visualizing extravasation dynamics of metastatic tumor cells. *J Cell Sci*. 2010;123(13):2332-2341. doi:10.1242/jcs.069443
299. Strell C, Entschladen F. Extravasation of leukocytes in comparison to tumor cells. *Cell Commun Signal*. 2008;6. doi:10.1186/1478-811X-6-10
300. Paget S. THE DISTRIBUTION OF SECONDARY GROWTHS IN CANCER OF THE BREAST. *Lancet*. 1889;133(3421):571-573. doi:10.1016/S0140-6736(00)49915-0
301. Leber MF, Efferth T. Molecular principles of cancer invasion and metastasis (Review). *Int J Oncol*. 2009;34(4):881-895. doi:10.3892/ijo_00000214
302. Fidler IJ. The pathogenesis of cancer metastasis: The "seed and soil" hypothesis revisited. *Nat Rev Cancer*. 2003;3(6):453-458. doi:10.1038/nrc1098
303. Dai CY, Haqq CM, Puzas JE. Molecular correlates of site-specific metastasis. *Semin Radiat Oncol*. 2006;16(2):102-110. doi:10.1016/j.semradonc.2005.12.005
304. Sipkins DA, Wei X, Wu JW, et al. In vivo imaging of specialized bone marrow endothelial microdomains for tumour engraftment. *Nature*. 2005;435(7044):969-973. doi:10.1038/nature03703
305. Ewing J. Neoplastics. *3rd Philadelphia Saunders*. 1928;(Metastasis):77–89.
306. Schlüter K, Gassmann P, Enns A, et al. Organ-specific metastatic tumor cell adhesion and extravasation of colon carcinoma cells with different metastatic potential. *Am J Pathol*. 2006;169(3):1064-1073. doi:10.2353/ajpath.2006.050566
307. Jeon JS, Zervantonakis IK, Chung S, Kamm RD, Charest JL. In Vitro Model of Tumor Cell Extravasation. *PLoS One*. 2013;8(2). doi:10.1371/journal.pone.0056910
308. Balic M, Lin H, Young L, et al. Most early disseminated cancer cells detected in bone marrow of breast cancer patients have a putative breast cancer stem cell phenotype. *Clin Cancer Res*. 2006;12(19):5615-5621. doi:10.1158/1078-0432.CCR-06-0169
309. Hermann PC, Huber SL, Herrler T, et al. Distinct Populations of Cancer Stem Cells Determine Tumor Growth and Metastatic Activity in Human Pancreatic Cancer. *Cell Stem Cell*. 2007;1(3):313-323. doi:10.1016/j.stem.2007.06.002
310. Mueller MM, Fusenig NE. Friends or foes - Bipolar effects of the tumour stroma in cancer. *Nat Rev Cancer*. 2004;4(11):839-849. doi:10.1038/nrc1477
311. Anderson ARA, Weaver AM, Cummings PT, Quaranta V. Tumor Morphology and

Phenotypic Evolution Driven by Selective Pressure from the Microenvironment. *Cell*. 2006;127(5):905-915. doi:10.1016/j.cell.2006.09.042

312. Psaila B, Lyden D. The metastatic niche: Adapting the foreign soil. *Nat Rev Cancer*. 2009;9(4):285-293. doi:10.1038/nrc2621
313. Kaplan RN, Rafii S, Lyden D. Preparing the "soil": The premetastatic niche. *Cancer Res*. 2006;66(23):11089-11093. doi:10.1158/0008-5472.CAN-06-2407
314. Joyce JA, Pollard JW. Microenvironmental regulation of metastasis. *Nat Rev Cancer*. 2009;9(4):239-252. doi:10.1038/nrc2618
315. Van Zijl F, Krupitza G, Mikulits W. Initial steps of metastasis: Cell invasion and endothelial transmigration. *Mutat Res - Rev Mutat Res*. 2011;728(1-2):23-34. doi:10.1016/j.mrrev.2011.05.002
316. Egeblad M, Werb Z. New functions for the matrix metalloproteinases in cancer progression. *Nat Rev Cancer*. 2002;2(3):161-174. doi:10.1038/nrc745
317. Abarrategi A, Tornin J, Lucia MC, et al. Osteosarcoma: Cells-of-Origin, Cancer stem cells, and targeted therapies. *Stem Cells Int*. 2016;2016. doi:10.1155/2016/3631764
318. Raymond AK, Jaffe N. Osteosarcoma multidisciplinary approach to the management from the pathologist's perspective. In: *Cancer Treatment and Research*. Vol 152. Cancer Treat Res; 2009:63-84. doi:10.1007/978-1-4419-0284-9_4
319. Visvader JE. Cells of origin in cancer. *Nature*. 2011;469(7330):314-322. doi:10.1038/nature09781
320. Luetke A, Meyers PA, Lewis I, Juergens H. Osteosarcoma treatment - Where do we stand? A state of the art review. *Cancer Treat Rev*. 2014;40(4):523-532. doi:10.1016/j.ctrv.2013.11.006
321. Gambera S, Abarrategi A, Rodríguez-Milla MA, et al. Role of Activator Protein-1 Complex on the Phenotype of Human Osteosarcomas Generated from Mesenchymal Stem Cells. *Stem Cells*. 2018;36(10):1487-1500. doi:10.1002/stem.2869
322. Mohseny AB, Hogendoorn PCW, Cleton-Jansen AM. Osteosarcoma models: From cell lines to zebrafish. *Sarcoma*. 2012;2012. doi:10.1155/2012/417271
323. Alfranca A, Martinez-Cruzado L, Tornin J, et al. Bone microenvironment signals in osteosarcoma development. *Cell Mol Life Sci*. 2015;72(16):3097-3113. doi:10.1007/s00018-015-1918-y
324. Klein MJ, Siegal GP. Osteosarcoma. *Am J Clin Pathol*. 2006;125(4):555-581. doi:10.1309/UC6K-QHLD-9LV2-KENN
325. Bielack SS, Kempf-Bielack B, Delling G, et al. Prognostic Factors in High-Grade Osteosarcoma of the Extremities or Trunk: An Analysis of 1,702 Patients Treated on

Neoadjuvant Cooperative Osteosarcoma Study Group Protocols. *J Clin Oncol*. 2002;20(3):776-790. doi:10.1200/jco.2002.20.3.776

326. Ozaki T, Flege S, Liljenqvist U, et al. Osteosarcoma of the spine: Experience of the Cooperative Osteosarcoma Study Group. *Cancer*. 2002;94(4):1069-1077. doi:10.1002/cncr.10258
327. Bielack S, Carrle D, Casali PG. Osteosarcoma: ESMO clinical recommendations for diagnosis, treatment and follow-up. *Ann Oncol*. 2009;20(SUPPL. 4). doi:10.1093/annonc/mdp154
328. Ottaviani G, Jaffe N. The epidemiology of osteosarcoma. In: *Cancer Treatment and Research*. Vol 152. Kluwer Academic Publishers; 2009:3-13. doi:10.1007/978-1-4419-0284-9_1
329. Kager L, Zoubek A, Dominkus M, et al. Osteosarcoma in very young children. *Cancer*. 2010;116(22):5316-5324. doi:10.1002/cncr.25287
330. Choong PFM, Broadhead ML, Clark JCM, Myers DE, Dass CR. The molecular pathogenesis of osteosarcoma: A review. *Sarcoma*. 2011;2011. doi:10.1155/2011/959248
331. Rani AS, Kumar S. Transformation of non-tumorigenic osteoblast-like human osteosarcoma cells by hexavalent chromates: Alteration of morphology, induction of anchorage-independence and proteolytic function. *Carcinogenesis*. 1992;13(11):2021-2027. doi:10.1093/carcin/13.11.2021
332. Paulino AC, Fowler BZ. Secondary neoplasms after radiotherapy for a childhood solid tumor. *Pediatr Hematol Oncol*. 2005;22(2):89-101. doi:10.1080/08880010590896459
333. Gelberg KH, Fitzgerald EF, Hwang SA, Dubrow R. Growth and development and other risk factors for osteosarcoma in children and young adults. *Int J Epidemiol*. 1997;26(2):272-278. doi:10.1093/ije/26.2.272
334. Osasan S, Zhang M, Shen F, Paul PJ, Persad S, Sergi C. Osteogenic sarcoma: A 21st century review. *Anticancer Res*. 2016;36(9):4391-4398. doi:10.21873/anticanres.10982
335. Botter SM, Neri D, Fuchs B. Recent advances in osteosarcoma. *Curr Opin Pharmacol*. 2014;16(1):15-23. doi:10.1016/j.coph.2014.02.002
336. David S. Geller and Richard Gorlick. Osteosarcoma: A Review of Diagnosis, Management, and Treatment Strategies – Hematology & Oncology. *Clin Adv Hema tol Oncol*. Published online 2010. Accessed November 11, 2020. https://www.hematologyandoncology.net/archives/october-2010/osteosarcoma-a-review-of-diagnosis-management-and-treatment-strategies/
337. Schwarz R, Bruland O, Cassoni A, Schomberg P, Bielack S. The Role of Radiotherapy in oseosarcoma. In: *Cancer Treatment and Research*. Vol 152. Cancer Treat Res; 2009:147-

164. doi:10.1007/978-1-4419-0284-9_7

338. Allison DC, Carney SC, Ahlmann ER, et al. A meta-analysis of osteosarcoma outcomes in the modern medical era. *Sarcoma*. 2012;2012. doi:10.1155/2012/704872

339. Erices A, Conget P, Minguell JJ. Mesenchymal progenitor cells in human umbilical cord blood. *Br J Haematol*. 2000;109(1):235-242. doi:10.1046/j.1365-2141.2000.01986.x

340. Fukuchi Y, Nakajima H, Sugiyama D, Hirose I, Kitamura T, Tsuji K. Human Placenta-Derived Cells Have Mesenchymal Stem/Progenitor Cell Potential. *Stem Cells*. 2004;22(5):649-658. doi:10.1634/stemcells.22-5-649

341. Ilancheran S, Moodley Y, Manuelpillai U. Human Fetal Membranes: A Source of Stem Cells for Tissue Regeneration and Repair? *Placenta*. 2009;30(1):2-10. doi:10.1016/j.placenta.2008.09.009

342. Mosna F, Sensebé L, Krampera M. Human bone marrow and adipose tissue mesenchymal stem cells: A user's guide. *Stem Cells Dev*. 2010;19(10):1449-1470. doi:10.1089/scd.2010.0140

343. Dominici M, Le Blanc K, Mueller I, et al. Minimal criteria for defining multipotent mesenchymal stromal cells. The International Society for Cellular Therapy position statement. *Cytotherapy*. 2006;8(4):315-317. doi:10.1080/14653240600855905

344. Roobrouck VD, Ulloa-Montoya F, Verfaillie CM. Self-renewal and differentiation capacity of young and aged stem cells. *Exp Cell Res*. 2008;314(9):1937-1944. doi:10.1016/j.yexcr.2008.03.006

345. Ajeian JN, Horton ER, Astudillo P, et al. Proteomic analysis of integrin-associated complexes from mesenchymal stem cells. *Proteomics - Clin Appl*. 2016;10(1):51-57. doi:10.1002/prca.201500033

346. Cuiffo BG, Karnoub AE. Mesenchymal stem cells in tumor development: Emerging roles and concepts. *Cell Adhes Migr*. 2012;6(3):220-230. doi:10.4161/cam.20875

347. Wagner W, Ho AD. Mesenchymal stem cell preparations-comparing apples and oranges. *Stem Cell Rev*. 2007;3(4):239-248. doi:10.1007/s12015-007-9001-1

348. Väänänen HK. Mesenchymal stem cells. *Ann Med*. 2005;37(7):469-479. doi:10.1080/07853890500371957

349. Menicanin D, Bartold PM, Zannettino ACW, Gronthos S. Genomic profiling of mesenchymal stem cells. *Stem Cell Rev Reports*. 2009;5(1):36-50. doi:10.1007/s12015-009-9056-2

350. Ringe J, Strassburg S, Neumann K, et al. Towards in situ tissue repair: Human mesenchymal stem cells express chemokine receptors CXCR1, CXCR2 and CCR2, and migrate upon stimulation with CXCL8 but not CCL2. *J Cell Biochem*. 2007;101(1):135-

146. doi:10.1002/jcb.21172

351. Sordi V, Malosio ML, Marchesi F, et al. Bone marrow mesenchymal stem cells express a restricted set of functionally active chemokine receptors capable of promoting migration to pancreatic islets. *Blood*. 2005;106(2):419-427. doi:10.1182/blood-2004-09-3507

352. Spaeth E, Klopp A, Dembinski J, Andreeff M, Marini F. Inflammation and tumor microenvironments: Defining the migratory itinerary of mesenchymal stem cells. *Gene Ther*. 2008;15(10):730-738. doi:10.1038/gt.2008.39

353. Dwyer RM, Potter-Beirne SM, Harrington KA, et al. Monocyte chemotactic protein-1 secreted by primary breast tumors stimulates migration of mesenchymal stem cells. *Clin Cancer Res*. 2007;13(17):5020-5027. doi:10.1158/1078-0432.CCR-07-0731

354. Gutova M, Najbauer J, Frank RT, et al. Urokinase Plasminogen Activator and Urokinase Plasminogen Activator Receptor Mediate Human Stem Cell Tropism to Malignant Solid Tumors. *Stem Cells*. 2008;26(6):1406-1413. doi:10.1634/stemcells.2008-0141

355. Xu W ting, Bian Z yu, Fan Q ming, Li G, Tang T ting. Human mesenchymal stem cells (hMSCs) target osteosarcoma and promote its growth and pulmonary metastasis. *Cancer Lett*. 2009;281(1):32-41. doi:10.1016/j.canlet.2009.02.022

356. Coffelt SB, Marini FC, Watson K, et al. The pro-inflammatory peptide LL-37 promotes ovarian tumor progression through recruitment of multipotent mesenchymal stromal cells. *Proc Natl Acad Sci U S A*. 2009;106(10):3806-3811. doi:10.1073/pnas.0900244106

357. Wang Y, Crisostomo PR, Wang M, Markel TA, Novotny NM, Meldrum DR. TGF-α increases human mesenchymal stem cell-secreted VEGF by MEK- and PI3-K- but not JNK- or ERK-dependent mechanisms. *Am J Physiol - Regul Integr Comp Physiol*. 2008;295(4). doi:10.1152/ajpregu.90383.2008

358. Lee DC, Fenton SE, Berkowitz EA, Hissong MA. Transforming growth factor alpha: expression, regulation, and biological activities. *Pharmacol Rev*. 1995;47(1).

359. Comito G, Giannoni E, Segura CP, et al. Cancer-associated fibroblasts and M2-polarized macrophages synergize during prostate carcinoma progression. *Oncogene*. 2014;33(19):2423-2431. doi:10.1038/onc.2013.191

360. Giannoni E, Bianchini F, Masieri L, et al. Reciprocal activation of prostate cancer cells and cancer-associated fibroblasts stimulates epithelial-mesenchymal transition and cancer stemness. *Cancer Res*. 2010;70(17):6945-6956. doi:10.1158/0008-5472.CAN-10-0785

361. Khakoo AY, Pati S, Anderson SA, et al. Human mesenchymal stem cells exert potent antitumorigenic effects in a model of Kaposi's sarcoma. *J Exp Med*. 2006;203(5):1235-1247. doi:10.1084/jem.20051921

362. Barcellos-de-Souza P, Gori V, Bambi F, Chiarugi P. Tumor microenvironment: Bone

marrow-mesenchymal stem cells as key players. *Biochim Biophys Acta - Rev Cancer*. 2013;1836(2):321-335. doi:10.1016/j.bbcan.2013.10.004

363. Belgiovine C, Frapolli R, Bonezzi K, et al. Reduced expression of the rock inhibitor rnd3 is associated with increased invasiveness and metastatic potential in mesenchymal tumor cells. *PLoS One*. 2010;5(11). doi:10.1371/journal.pone.0014154
364. Barcellos-de-Souza P, Comito G, Pons-Segura C, et al. Mesenchymal Stem Cells are Recruited and Activated into Carcinoma-Associated Fibroblasts by Prostate Cancer Microenvironment-Derived TGF-β1. *Stem Cells*. 2016;34(10):2536-2547. doi:10.1002/stem.2412
365. Tsukamoto S, Honoki K, Fuji H, et al. Mesenchymal stem cells promote tumor engraftment and metastatic colonization in rat osteosarcoma model. *Int J Oncol*. 2012;40(1):163-169. doi:10.3892/ijo.2011.1220
366. Yu FX, Hu WJ, He B, Zheng YH, Zhang QY, Chen L. Bone marrow mesenchymal stem cells promote osteosarcoma cell proliferation and invasion. *World J Surg Oncol*. 2015;13(1). doi:10.1186/s12957-015-0465-1
367. Chen Q, Sun W, Liao Y, et al. Monocyte chemotactic protein-1 promotes the proliferation and invasion of osteosarcoma cells and upregulates the expression of AKT. *Mol Med Rep*. 2015;12(1):219-225. doi:10.3892/mmr.2015.3375
368. Giner F, López-Guerrero JA, Machado I, García-Casado Z, Peydró-Olaya A, Llombart-Bosch A. The early stages of tumor angiogenesis in human osteosarcoma: a nude mice xenotransplant model. *Virchows Arch*. 2015;467(2):193-201. doi:10.1007/s00428-015-1791-y
369. Liu C, Ma M, Zhang J, Gui S, Zhang X, Xue S. Galangin inhibits human osteosarcoma cells growth by inducing transforming growth factor-β1-dependent osteogenic differentiation. *Biomed Pharmacother*. 2017;89:1415-1421. doi:10.1016/j.biopha.2017.03.030
370. Tu B, Peng ZX, Fan QM, Du L, Yan W, Tang TT. Osteosarcoma cells promote the production of pro-tumor cytokines in mesenchymal stem cells by inhibiting their osteogenic differentiation through the TGF-β/Smad2/3 pathway. *Exp Cell Res*. 2014;320(1):164-173. doi:10.1016/j.yexcr.2013.10.013
371. Boppana NB, Devarajan A, Gopal K, et al. Blockade of CXCR2 signalling: A potential therapeutic target for preventing neutrophil-mediated inflammatory diseases. *Exp Biol Med*. 2014;239(5):509-518. doi:10.1177/1535370213520110
372. Kansara M, Teng MW, Smyth MJ, Thomas DM. Translational biology of osteosarcoma. *Nat Rev Cancer*. 2014;14(11):722-735. doi:10.1038/nrc3838
373. Meyers PA, Healey JH, Chou AJ, et al. Addition of pamidronate to chemotherapy for the

treatment of osteosarcoma. *Cancer*. 2011;117(8):1736-1744. doi:10.1002/cncr.25744

374. Mishra PJ, Mishra PJ, Humeniuk R, et al. Carcinoma-associated fibroblast-like differentiation of human mesenchymal stem cells. *Cancer Res*. 2008;68(11):4331-4339. doi:10.1158/0008-5472.CAN-08-0943
375. Ottaviano L, Schaefer KL, Gajewski M, et al. Molecular characterization of commonly used cell lines for bone tumor research: A trans-European EuroBoNet effort. *Genes Chromosom Cancer*. 2010;49(1):40-51. doi:10.1002/gcc.20717
376. Lauvrak SU, Munthe E, Kresse SH, et al. Functional characterisation of osteosarcoma cell lines and identification of mRNAs and miRNAs associated with aggressive cancer phenotypes. *Br J Cancer*. 2013;109(8):2228-2236. doi:10.1038/bjc.2013.549
377. Perissinotto E, Cavalloni G, Leone F, et al. Involvement of Chemokine Receptor 4/Stromal Cell-Derived Factor 1 System during Osteosarcoma Tumor Progression. *Clin Cancer Res*. 2005;11(2):490-497.
378. Ponte AL, Marais E, Gallay N, et al. The In Vitro Migration Capacity of Human Bone Marrow Mesenchymal Stem Cells: Comparison of Chemokine and Growth Factor Chemotactic Activities. *Stem Cells*. 2007;25(7):1737-1745. doi:10.1634/stemcells.2007-0054
379. Karnoub AE, Dash AB, Vo AP, et al. Mesenchymal stem cells within tumour stroma promote breast cancer metastasis. *Nature*. 2007;449(7162):557-563. doi:10.1038/nature06188
380. Martin FT, Dwyer RM, Kelly J, et al. Potential role of mesenchymal stem cells (MSCs) in the breast tumour microenvironment: Stimulation of epithelial to mesenchymal transition (EMT). *Breast Cancer Res Treat*. 2010;124(2):317-326. doi:10.1007/s10549-010-0734-1
381. Tsai K, Yang S, Lei Y, et al. Mesenchymal stem cells promote formation of colorectal tumors in mice. *Gastroenterology*. 2011;141(3):1046-1056. doi:10.1053/j.gastro.2011.05.045
382. Cortini M, Massa A, Avnet S, Bonuccelli G, Baldini N. Tumor-activated mesenchymal stromal cells promote osteosarcoma stemness and migratory potential via IL-6 secretion. *PLoS One*. 2016;11(11). doi:10.1371/journal.pone.0166500
383. Schraufstatter IU, Chung J, Burger M. IL-8 activates endothelial cell CXCR1 and CXCR2 through Rho and Rac signaling pathways. *Am J Physiol - Lung Cell Mol Physiol*. 2001;280(6 24-6). doi:10.1152/ajplung.2001.280.6.l1094
384. Waugh DJJ, Wilson C. The interleukin-8 pathway in cancer. *Clin Cancer Res*. 2008;14(21):6735-6741. doi:10.1158/1078-0432.CCR-07-4843
385. Cai JP, Hudson S, Ye MW, Chin YH. The intracellular signaling pathways involved in

MCP-1-stimulated T cell migration across microvascular endothelium. *Cell Immunol*. 1996;167(2):269-275. doi:10.1006/cimm.1996.0035

386. Ma J, Wang Q, Fei T, Han JDJ, Chen YG. MCP-1 mediates TGF-β-induced angiogenesis by stimulating vascular smooth muscle cell migration. *Blood*. 2007;109(3):987-994. doi:10.1182/blood-2006-07-036400
387. Widera D, Holtkamp W, Entschladen F, et al. MCP-1 induces migration of adult neural stem cells. *Eur J Cell Biol*. 2004;83(8):381-387. doi:10.1078/0171-9335-00403
388. Mohseny AB, MacHado I, Cai Y, et al. Functional characterization of osteosarcoma cell lines provides representative models to study the human disease. *Lab Investig*. 2011;91(8):1195-1205. doi:10.1038/labinvest.2011.72
389. Taddei ML, Pietrovito L, Leo A, Chiarugi P. Lactate in Sarcoma Microenvironment: Much More than just a Waste Product. *Cells*. 2020;9(2):510. doi:10.3390/cells9020510
390. Zhang H, Wang J, Ren T, et al. Bone marrow mesenchymal stem cell-derived exosomal miR-206 inhibits osteosarcoma progression by targeting TRA2B. *Cancer Lett*. 2020;490:54-65. doi:10.1016/j.canlet.2020.07.008
391. Cai WT, Guan P, Lin MX, Fu B, Wu B, Wu J. MiRNA-206 suppresses the metastasis of osteosarcoma via targeting notch3. *J Biol Regul Homeost Agents*. 2020;34(3):775-783. doi:10.23812/20-72-A-26
392. Qin F, Tang H, Zhang Y, Zhang Z, Huang P, Zhu J. Bone marrow-derived mesenchymal stem cell-derived exosomal microRNA-208a promotes osteosarcoma cell proliferation, migration, and invasion. *J Cell Physiol*. 2020;235(5):4734-4745. doi:10.1002/jcp.29351
393. Cichorek M, Wachulska M, Stasiewicz A, Tymińska A. Skin melanocytes: Biology and development. *Postep Dermatologii i Alergol*. 2013;30(1):30-41. doi:10.5114/pdia.2013.33376
394. Michielin O, Atkins MB, Koon HB, Dummer R, Ascierto PA. Evolving impact of long-term survival results on metastatic melanoma treatment. *J Immunother Cancer*. 2020;8:948. doi:10.1136/jitc-2020-000948
395. Gandini S, Sera F, Cattaruzza MS, et al. Meta-analysis of risk factors for cutaneous melanoma: II. Sun exposure. *Eur J Cancer*. 2005;41(1):45-60. doi:10.1016/j.ejca.2004.10.016
396. Akbani R, Akdemir KC, Aksoy BA, et al. Genomic Classification of Cutaneous Melanoma. *Cell*. 2015;161(7):1681-1696. doi:10.1016/j.cell.2015.05.044
397. Hayward NK, Wilmott JS, Waddell N, et al. Whole-genome landscapes of major melanoma subtypes. *Nature*. 2017;545(7653):175-180. doi:10.1038/nature22071
398. Chiappetta C, Proietti I, Soccodato V, et al. BRAF and NRAS mutations are heterogeneous

and not mutually exclusive in nodular melanoma. *Appl Immunohistochem Mol Morphol*. 2015;23(3):172-177. doi:10.1097/PAI.0000000000000071

399. Griffin M, Scotto D, Josephs DH, et al. BRAF inhibitors: Resistance and the promise of combination treatments for melanoma. *Oncotarget*. 2017;8(44):78174-78192. doi:10.18632/oncotarget.19836
400. Campbell PJ, Getz G, Korbel JO, et al. Pan-cancer analysis of whole genomes. *Nature*. 2020;578(7793):82-93. doi:10.1038/s41586-020-1969-6
401. Amaral T, Sinnberg T, Meier F, et al. The mitogen-activated protein kinase pathway in melanoma part I – Activation and primary resistance mechanisms to BRAF inhibition. *Eur J Cancer*. 2017;73:85-92. doi:10.1016/j.ejca.2016.12.010
402. Palmieri G, Capone M, Ascierto ML, et al. Main roads to melanoma. *J Transl Med*. 2009;7. doi:10.1186/1479-5876-7-86
403. Uong A, Zon LI. Melanocytes in development and cancer. *J Cell Physiol*. 2010;222(1):38-41. doi:10.1002/jcp.21935
404. Williams PF, Olsen CM, Hayward NK, Whiteman DC. Melanocortin 1 receptor and risk of cutaneous melanoma: A meta-analysis and estimates of population burden. *Int J Cancer*. 2011;129(7):1730-1740. doi:10.1002/ijc.25804
405. Karim RZ, Li W, Sanki A, et al. Reduced p16 and Increased Cyclin D1 and pRb Expression Are Correlated with Progression in Cutaneous Melanocytic Tumors. *Int J Surg Pathol*. 2009;17(5):361-367. doi:10.1177/1066896909336177
406. Villares GJ, Dobroff AS, Wang H, et al. Overexpression of protease-activated receptor-1 contributes to melanoma metastasis via regulation of connexin 43. *Cancer Res*. 2009;69(16):6730-6737. doi:10.1158/0008-5472.CAN-09-0300
407. Hsu M, Wheelock M, Johnson K, Herlyn M. Shifts in cadherin profiles between human normal melanocytes and melanomas. *undefined*. Published online 1996.
408. Sviatoha V, Tani E, Kleina R, Sperga M, Skoog L. Immunohistochemical analysis of the S100A1, S100B, CD44 and Bcl-2 antigens and the rate of cell proliferation assessed by Ki-67 antibody in benign and malignant melanocytic tumours. *Melanoma Res*. 2010;20(2):118-125. doi:10.1097/CMR.0b013e3283350554
409. Alla V, Engelmann D, Niemetz A, et al. E2F1 in melanoma progression and metastasis. *J Natl Cancer Inst*. 2010;102(2):127-133. doi:10.1093/jnci/djp458
410. Khazaei Z, Ghorat F, Jarrahi AM, Adineh HA, Sohrabivafa M, Goodarzi E. *GLOBAL INCIDENCE AND MORTALITY OF SKIN CANCER BY HISTOLOGICAL SUBTYPE AND ITS RELATIONSHIP WITH THE HUMAN DEVELOPMENT INDEX (HDI); AN ECOLOGY STUDY IN 2018*.; 2019.

411. Matthews NH, Li WQ, Qureshi AA et al. pidemiology of Melanoma. In: Ward WH FJ, ed. *Cutaneous Melanoma: Etiology and Therapy*. ; 2017. https://www.ncbi.nlm.nih.gov/books/NBK481862/ doi: 10.15586/codon.cutaneousmelanoma.2017.ch1

412. Khazaei Z, Goodarzi E, Khazaei Z, et al. *EPIDEMIOLOGY AND POPULATION ATTRIBUTABLE FRACTION OF MELANOMA TO ULTRAVIOLET RADIATION IN ASIA: AN ECOLOGICAL STUDY WCRJ 2018; 5 (3): E1114*.; 2018.

413. V Radović-Kovacević, T Pekmezović, B Adanja, M Jarebinski, J Marinković RT. [Survival analysis in patients with cutaneous malignant melanoma]. *Srp Arh Celok Lek*. 1997;125, no. 5:132–137. https://pubmed.ncbi.nlm.nih.gov/9265233/

414. Bandarchi B, Ma L, Navab R, Seth A, Rasty G. From melanocyte to metastatic malignant melanoma. *Dermatol Res Pract*. 2010;2010(1). doi:10.1155/2010/583748

415. Erdei E, Torres SM. A new understanding in the epidemiology of melanoma. *Expert Rev Anticancer Ther*. 2010;10(11):1811-1823. doi:10.1586/era.10.170

416. Chang YM, Barrett JH, Bishop TD, et al. Sun exposure and melanoma risk at different latitudes: A pooled analysis of 5700 cases and 7216 controls. *Int J Epidemiol*. 2009;38(3):814-830. doi:10.1093/ije/dyp166

417. Zito CR, Kluger HM. Immunotherapy for metastatic melanoma. *J Cell Biochem*. 2012;113(3):725-734. doi:10.1002/jcb.23402

418. Houghton AN, Polsky D. Focus on melanoma. *Cancer Cell*. 2002;2(4):275-278. doi:10.1016/S1535-6108(02)00161-7

419. Corrie P, Hategan M, Fife K, Parkinson C. Management of melanoma. *Br Med Bull*. 2014;111(1):149-162. doi:10.1093/bmb/ldu019

420. Chapman PB, Hauschild A, Robert C, et al. Improved Survival with Vemurafenib in Melanoma with BRAF V600E Mutation. *N Engl J Med*. 2011;364(26):2507-2516. doi:10.1056/nejmoa1103782

421. Larkin J, Del Vecchio M, Ascierto PA, et al. Vemurafenib in patients with BRAFV600 mutated metastatic melanoma: An open-label, multicentre, safety study. *Lancet Oncol*. 2014;15(4):436-444. doi:10.1016/S1470-2045(14)70051-8

422. Hauschild A, Grob JJ, Demidov L V., et al. Dabrafenib in BRAF-mutated metastatic melanoma: A multicentre, open-label, phase 3 randomised controlled trial. *Lancet*. 2012;380(9839):358-365. doi:10.1016/S0140-6736(12)60868-X

423. Alcalá AM, Flaherty KT. BRAF inhibitors for the treatment of metastatic melanoma: Clinical trials and mechanisms of resistance. *Clin Cancer Res*. 2012;18(1):33-39. doi:10.1158/1078-0432.CCR-11-0997

424. Hodi FS, O'Day SJ, McDermott DF, et al. Improved Survival with Ipilimumab in Patients with Metastatic Melanoma. *N Engl J Med*. 2010;363(8):711-723. doi:10.1056/nejmoa1003466

425. Robert C, Thomas L, Bondarenko I, et al. Ipilimumab plus Dacarbazine for Previously Untreated Metastatic Melanoma. *N Engl J Med*. 2011;364(26):2517-2526. doi:10.1056/nejmoa1104621

426. Schadendorf D, Hodi FS, Robert C, et al. Pooled analysis of long-term survival data from phase II and phase III trials of ipilimumab in unresectable or metastatic melanoma. *J Clin Oncol*. 2015;33(17):1889-1894. doi:10.1200/JCO.2014.56.2736

427. Mason R, Au L, Ingles Garces A, Larkin J. Current and emerging systemic therapies for cutaneous metastatic melanoma. *Expert Opin Pharmacother*. 2019;20(9):1135-1152. doi:10.1080/14656566.2019.1601700

428. Luo L, Nong Wang J, Kong LD, Jiang QG, Tan RX. Antidepressant effects of Banxia Houpu decoction, a traditional Chinese medicinal empirical formula. *J Ethnopharmacol*. 2000;73(1-2):277-281. doi:10.1016/S0378-8741(00)00242-7

429. Ranaware AM, Banik K, Deshpande V, et al. Magnolol: A neolignan from the Magnolia family for the prevention and treatment of cancer. *Int J Mol Sci*. 2018;19(8). doi:10.3390/ijms19082362

430. Wu B, Fu S hong, Tang H, et al. Design, synthesis and antibacterial evaluation of honokiol derivatives. *Bioorganic Med Chem Lett*. 2018;28(4):834-838. doi:10.1016/j.bmcl.2017.06.022

431. Park J, Lee J, Jung E, et al. In vitro antibacterial and anti-inflammatory effects of honokiol and magnolol against Propionibacterium sp. *Eur J Pharmacol*. 2004;496(1):189-195. doi:10.1016/j.ejphar.2004.05.047

432. Chang B, Lee Y, Ku Y, Bae K, Chung CP. Antimicrobial activity of magnolol and honokiol against periodontopathic microorganisms. *Planta Med*. 1998;64(4):367-369. doi:10.1055/s-2006-957453

433. Ho KY, Tsai CC, Chen CP, Huang JS, Lin CC. Antimicrobial activity of honokiol and magnolol isolated from Magnolia officinalis. *Phyther Res*. 2001;15(2):139-141. doi:10.1002/ptr.736

434. Liou KT, Shen YC, Chen CF, Tsao CM, Tsai SK. Honokiol protects rat brain from focal cerebral ischemia-reperfusion injury by inhibiting neutrophil infiltration and reactive oxygen species production. *Brain Res*. 2003;992(2):159-166. doi:10.1016/j.brainres.2003.08.026

435. Kuribara H, Stavinoha WB, Maruyama Y. Behavioural pharmacological characteristics of

honokiol, an anxiolytic agent present in extracts of Magnolia bark, evaluated by an elevated plus-maze test in mice. *J Pharm Pharmacol*. 1998;50(7):819-826. doi:10.1111/j.2042-7158.1998.tb07146.x

436. Kuribara H, Kishi E, Kimura M, Weintraub ST, Maruyama Y. Comparative assessment of the anxiolytic-like activities of honokiol and derivatives. *Pharmacol Biochem Behav*. 2000;67(3):597-601. doi:10.1016/S0091-3057(00)00401-9
437. Qiang LQ, Wang CP, Wang FM, et al. Combined administration of the mixture of honokiol and magnolol and ginger oil evokes antidepressant-like synergism in rats. *Arch Pharm Res*. 2009;32(9):1281-1292. doi:10.1007/s12272-009-1914-6
438. Xu Q, Yi LT, Pan Y, et al. Antidepressant-like effects of the mixture of honokiol and magnolol from the barks of Magnolia officinalis in stressed rodents. *Prog Neuro-Psychopharmacology Biol Psychiatry*. 2008;32(3):715-725. doi:10.1016/j.pnpbp.2007.11.020
439. Tsai SK, Huang CH, Huang SS, Hung LM, Hong CY. Antiarrhythmic effect of magnolol and honokiol during acute phase of coronary occlusion in anesthetized rats: Influence of L-NAME and aspirin. *Pharmacology*. 1999;59(5):227-233. doi:10.1159/000028324
440. Zhao C, Liu ZQ. Comparison of antioxidant abilities of magnolol and honokiol to scavenge radicals and to protect DNA. *Biochimie*. 2011;93(10):1755-1760. doi:10.1016/j.biochi.2011.06.012
441. Eastham LL, Howard CM, Balachandran P, Pasco DS, Claudio PP. Eating Green: Shining Light on the Use of Dietary Phytochemicals as a Modern Approach in the Prevention and Treatment of Head and Neck Cancers. *Curr Top Med Chem*. 2018;18(3). doi:10.2174/1568026618666180112160713
442. Bai X, Cerimele F, Ushio-Fukai M, et al. Honokiol, a small molecular weight natural product, inhibits angiogenesis in vitro and tumor growth in vivo. *J Biol Chem*. 2003;278(37):35501-35507. doi:10.1074/jbc.M302967200
443. Hu J, Chen LJ, Liu L, et al. Liposomal honokiol, a potent anti-angiogenesis agent, in combination with radiotherapy produces a synergistic antitumor efficacy without increasing toxicity. *Exp Mol Med*. 2008;40(6):617-628. doi:10.3858/emm.2008.40.6.617
444. Lin YR, Chen HH, Lin YC, Ko CH, Chan MH. Antinociceptive actions of honokiol and magnolol on glutamatergic and inflammatory pain. *J Biomed Sci*. 2009;16(1). doi:10.1186/1423-0127-16-94
445. Hu H, Zhang XX, Wang YY, Chen SZ. Honokiol inhibits arterial thrombosis through endothelial cell protection and stimulation of prostacyclin. *Acta Pharmacol Sin*. 2005;26(9):1063-1068. doi:10.1111/j.1745-7254.2005.00164.x

446. Ko CH, Chen HH, Lin YR, Chan MH. Inhibition of smooth muscle contraction by magnolol and honokiol in porcine trachea. *Planta Med*. 2003;69(6):532-536. doi:10.1055/s-2003-40654

447. Alexeev M, Grosenbaugh DK, Mott DD, Fisher JL. The natural products magnolol and honokiol are positive allosteric modulators of both synaptic and extra-synaptic GABA A receptors. *Neuropharmacology*. 2012;62(8):2507-2514. doi:10.1016/j.neuropharm.2012.03.002

448. Amblard F, Delinsky D, Arbiser JL, Schinazi RF. Facile purification of honokiol and its antiviral and cytotoxic properties. *J Med Chem*. 2006;49(11):3426-3427. doi:10.1021/jm060268m

449. Chen S zhen. Research progress in anticancer effects and molecular targets of honokiol in experimental therapy. *Yao Xue Xue Bao*. 2016;51(2):202-207. Accessed November 11, 2020. https://europepmc.org/article/med/29856535

450. Prasad R, Katiyar SK. Honokiol, an active compound of Magnolia plant, inhibits growth, and progression of cancers of different organs. In: *Advances in Experimental Medicine and Biology*. Vol 928. Springer New York LLC; 2016:245-265. doi:10.1007/978-3-319-41334-1_11

451. Tang H, Zhang Y, Li D, et al. Discovery and synthesis of novel magnolol derivatives with potent anticancer activity in non-small cell lung cancer. *Eur J Med Chem*. 2018;156:190-205. doi:10.1016/j.ejmech.2018.06.048

452. Guo YB, Bao XJ, Xu SB, Zhang XD, Liu HY. Honokiol induces cell cycle arrest and apoptosis via p53 activation in H4 human neuroglioma cells. *Int J Clin Exp Med*. 2015;8(5):7168-7175. Accessed November 11, 2020. www.ijcem.com/

453. Yan B, Peng Z-Y. Honokiol induces cell cycle arrest and apoptosis in human gastric carcinoma MGC-803 cell line. *Int J Clin Exp Med*. 2015;8(4):5454-5461. Accessed November 11, 2020. http://www.ncbi.nlm.nih.gov/pubmed/26131123

454. Huang KJ, Kuo CH, Chen SH, Lin CY, Lee YR. Honokiol inhibits in vitro and in vivo growth of oral squamous cell carcinoma through induction of apoptosis, cell cycle arrest and autophagy. *J Cell Mol Med*. 2018;22(3):1894-1908. doi:10.1111/jcmm.13474

455. Hahm ER, Singh KB, Singh S V. c-Myc is a novel target of cell cycle arrest by honokiol in prostate cancer cells. *Cell Cycle*. 2016;15(17):2309-2320. doi:10.1080/15384101.2016.1201253

456. Wang Y, Zhu X, Yang Z, Zhao X. Honokiol induces caspase-independent paraptosis via reactive oxygen species production that is accompanied by apoptosis in leukemia cells. *Biochem Biophys Res Commun*. 2013;430(3):876-882. doi:10.1016/j.bbrc.2012.12.063

457. Xie L, Jiang F, Zhang X, et al. Honokiol sensitizes breast cancer cells to TNF-α induction of apoptosis by inhibiting Nur77 expression. *Br J Pharmacol*. 2016;173(2):344-356. doi:10.1111/bph.13375

458. Park EJ, Min HY, Chung HJ, et al. Down-regulation of c-Src/EGFR-mediated signaling activation is involved in the honokiol-induced cell cycle arrest and apoptosis in MDA-MB-231 human breast cancer cells. *Cancer Lett*. 2009;277(2):133-140. doi:10.1016/j.canlet.2008.11.029

459. Singh T, Gupta NA, Xu S, Prasad R, Velu SE, Katiyar SK. Honokiol inhibits the growth of head and neck squamous cell carcinoma by targeting epidermal growth factor receptor. *Oncotarget*. 2015;6(25):21268-21282. doi:10.18632/oncotarget.4178

460. Leeman-Neill RJ, Cai Q, Joyce SC, et al. Honokiol inhibits epidermal growth factor receptor signaling and enhances the antitumor effects of epidermal growth factor receptor inhibitors. *Clin Cancer Res*. 2010;16(9):2571-2579. doi:10.1158/1078-0432.CCR-10-0333

461. Yarden Y, Shilo BZ. SnapShot: EGFR Signaling Pathway. *Cell*. 2007;131(5):1018.e1-1018.e2. doi:10.1016/j.cell.2007.11.013

462. Sordella R, Bell DW, Haber DA, Settleman J. Gefitinib-sensitizing EGFR mutations in lung cancer activate anti-apoptotic pathways. *Science (80-)*. 2004;305(5687):1163-1167. doi:10.1126/science.1101637

463. Lynch TJ, Bell DW, Sordella R, et al. Activating Mutations in the Epidermal Growth Factor Receptor Underlying Responsiveness of Non–Small-Cell Lung Cancer to Gefitinib. *N Engl J Med*. 2004;350(21):2129-2139. doi:10.1056/nejmoa040938

464. Arora S, Singh S, Piazza GA, Contreras CM, Panyam J, Singh AP. Honokiol: A Novel Natural Agent for Cancer Prevention and Therapy. *Curr Mol Med*. 2012;12(10):1244-1252. doi:10.2174/156652412803833508

465. Avtanski DB, Nagalingam A, Bonner MY, Arbiser JL, Saxena NK, Sharma D. Honokiol inhibits epithelial-mesenchymal transition in breast cancer cells by targeting signal transducer and activator of transcription 3/Zeb1/E-cadherin axis. *Mol Oncol*. 2014;8(3):565-580. doi:10.1016/j.molonc.2014.01.004

466. Rajendran P, Li F, Shanmugam MK, et al. Honokiol inhibits signal transducer and activator of transcription-3 signaling, proliferation, and survival of hepatocellular carcinoma cells via the protein tyrosine phosphatase SHP-1. *J Cell Physiol*. 2012;227(5):2184-2195. doi:10.1002/jcp.22954

467. Liu H, Zang C, Emde A, et al. Anti-tumor effect of honokiol alone and in combination with other anti-cancer agents in breast cancer. *Eur J Pharmacol*. 2008;591(1-3):43-51. doi:10.1016/j.ejphar.2008.06.026

468. Crane C, Panner A, Pieper RO, Arbiser J, Parsa AT. Honokiol-mediated inhibition of PI3K/mTOR pathway: A potential strategy to overcome immunoresistance in glioma, breast, and prostate carcinoma without impacting T cell function. *J Immunother*. 2009;32(6):585-592. doi:10.1097/CJI.0b013e3181a8efe6

469. Sethi G, Sung B, Aggarwal BB. Nuclear factor-κB activation: From bench to bedside. *Exp Biol Med*. 2008;233(1):21-31. doi:10.3181/0707-MR-196

470. Ahn KS, Sethi G, Shishodia S, Sung B, Arbiser JL, Aggarwal BB. Honokiol potentiates apoptosis, suppresses osteoclastogenesis, and inhibits invasion through modulation of nuclear factor-κB activation pathway. *Mol Cancer Res*. 2006;4(9):621-633. doi:10.1158/1541-7786.MCR-06-0076

471. Lefranc F, Facchini V, Kiss R. Proautophagic Drugs: A Novel Means to Combat Apoptosis-Resistant Cancers, with a Special Emphasis on Glioblastomas. *Oncologist*. 2007;12(12):1395-1403. doi:10.1634/theoncologist.12-12-1395

472. Singh SS, Vats S, Chia AYQ, et al. Dual role of autophagy in hallmarks of cancer. *Oncogene*. 2018;37(9):1142-1158. doi:10.1038/s41388-017-0046-6

473. Huang K, Chen Y, Zhang R, et al. Honokiol induces apoptosis and autophagy via the ROS/ERK1/2 signaling pathway in human osteosarcoma cells in vitro and in vivo article. *Cell Death Dis*. 2018;9(2). doi:10.1038/s41419-017-0166-5

474. Li Z, Dong H, Li M, et al. Honokiol induces autophagy and apoptosis of osteosarcoma through PI3K/Akt/mTOR signaling pathway. *Mol Med Rep*. 2018;17(2):2719-2723. doi:10.3892/mmr.2017.8123

475. Luo LX, Li Y, Liu ZQ, et al. Honokiol induces apoptosis, G1 arrest, and autophagy in KRAS mutant lung cancer cells. *Front Pharmacol*. 2017;8(APR). doi:10.3389/fphar.2017.00199

476. Wu GJ, Lin CJ, Lin YW, Chen RM. Data analyses of honokiol-induced autophagy of human glioma cells in vitro and in vivo. *Data Br*. 2016;9:667-672. doi:10.1016/j.dib.2016.09.045

477. Yeh PS, Wang W, Chang YA, Lin CJ, Wang JJ, Chen RM. Honokiol induces autophagy of neuroblastoma cells through activating the PI3K/Akt/mTOR and endoplasmic reticular stress/ERK1/2 signaling pathways and suppressing cell migration. *Cancer Lett*. 2016;370(1):66-77. doi:10.1016/j.canlet.2015.08.030

478. Sánchez-Peris M, Murga J, Falomir E, Carda M, Marco JA. Synthesis of honokiol analogues and evaluation of their modulating action on VEGF protein secretion and telomerase-related gene expressions. *Chem Biol Drug Des*. 2017;89(4):577-584. doi:10.1111/cbdd.12880

479. Gong CY, Shi S, Wang XH, et al. Novel composite drug delivery system for honokiol delivery: Self-assembled poly(ethylene glycol)-poly(ε-caprolactone)-poly(ethylene glycol) micelles in thermosensitive poly(ethylene glycol)-poly(ε-caprolactone)-poly(ethylene glycol) hydrogel. *J Phys Chem B*. 2009;113(30):10183-10188. doi:10.1021/jp902697d

480. Zheng X, Wang X, Gou M, et al. A novel transdermal honokiol formulation based on Pluronic F127 copolymer. *Drug Deliv*. 2010;17(3):138-144. doi:10.3109/10717541003604874

481. Kumar A, Kumar Singh U, Chaudhary A. Honokiol analogs: A novel class of anticancer agents targeting cell signaling pathways and other bioactivities. *Future Med Chem*. 2013;5(7):809-829. doi:10.4155/fmc.13.32

482. Akamata K, Wei J, Bhattacharyya M, et al. SIRT3 is attenuated in systemic sclerosis skin and lungs, and its pharmacologic activation mitigates organ fibrosis. *Oncotarget*. 2016;7(43):69321-69336. doi:10.18632/oncotarget.12504

483. Benigni A, Perico L, Macconi D. Mitochondrial Dynamics Is Linked to Longevity and Protects from End-Organ Injury: The Emerging Role of Sirtuin 3. *Antioxidants Redox Signal*. 2016;25(4):185-199. doi:10.1089/ars.2016.6682

484. Bonner MY, Karlsson I, Rodolfo M, Arnold RS, Vergani E, Arbiser JL. Honokiol bis-dichloroacetate (Honokiol DCA) demonstrates activity in vemurafenib-resistant melanoma in vivo. *Oncotarget*. 2016;7(11):12857-12868. doi:10.18632/oncotarget.7289

485. Friedl P, Zänker KS, Bröcker EB. Cell migration strategies in 3-D extracellular matrix: Differences in morphology, cell matrix interactions, and integrin function. *Microsc Res Tech*. 1998;43(5):369-378. doi:10.1002/(SICI)1097-0029(19981201)43:5<369::AID-JEMT3>3.0.CO;2-6

486. Worthylake RA, Lemoine S, Watson JM, Burridge K. RhoA is required for monocyte tail retraction during transendothelial migration. *J Cell Biol*. 2001;154(1):147-160. doi:10.1083/jcb.200103048

487. Lehmann S, te Boekhorst V, Odenthal J, et al. Hypoxia Induces a HIF-1-Dependent Transition from Collective-to-Amoeboid Dissemination in Epithelial Cancer Cells. *Curr Biol*. 2017;27(3):392-400. doi:10.1016/j.cub.2016.11.057

488. Guillermo-Lagae R, Santha S, Thomas M, et al. Antineoplastic effects of honokiol on melanoma. *Biomed Res Int*. 2017;2017. doi:10.1155/2017/5496398

489. Chiu CS, Tsai CH, Hsieh MS, et al. Exploiting Honokiol-induced ER stress CHOP activation inhibits the growth and metastasis of melanoma by suppressing the MITF and β-catenin pathways. *Cancer Lett*. 2019;442:113-125. doi:10.1016/j.canlet.2018.10.026

490. Wang W die, Shang Y, Li Y, Chen S zhen. Honokiol inhibits breast cancer cell metastasis

by blocking EMT through modulation of Snail/Slug protein translation. *Acta Pharmacol Sin*. 2019;40(9):1219-1227. doi:10.1038/s41401-019-0240-x

491. Sadok A, McCarthy A, Caldwell J, et al. Rho kinase inhibitors block melanoma cell migration and inhibit metastasis. *Cancer Res*. 2015;75(11):2272-2284. doi:10.1158/0008-5472.CAN-14-2156
492. Noh KH, Kim BW, Song KH, et al. Nanog signaling in cancer promotes stem-like phenotype and immune evasion. *J Clin Invest*. 2012;122(11):4077-4093. doi:10.1172/JCI64057
493. Takahashi K, Yamanaka S. Induction of Pluripotent Stem Cells from Mouse Embryonic and Adult Fibroblast Cultures by Defined Factors. *Cell*. 2006;126(4):663-676. doi:10.1016/j.cell.2006.07.024
494. Perego M, Tortoreto M, Tragni G, et al. Heterogeneous phenotype of human melanoma cells with in vitro and in vivo features of tumor-initiating cells. *J Invest Dermatol*. 2010;130(7):1877-1886. doi:10.1038/jid.2010.69
495. Sabharwal SS, Schumacker PT. Mitochondrial ROS in cancer: Initiators, amplifiers or an Achilles' heel? *Nat Rev Cancer*. 2014;14(11):709-721. doi:10.1038/nrc3803
496. Zhao B, Qiang L, Joseph J, Kalyanaraman B, Viollet B, He YY. Mitochondrial dysfunction activates the AMPK signaling and autophagy to promote cell survival. *Genes Dis*. 2016;3(1):82-87. doi:10.1016/j.gendis.2015.12.002
497. Schaffer BE, Levin RS, Hertz NT, et al. Identification of AMPK Phosphorylation Sites Reveals a Network of Proteins Involved in Cell Invasion and Facilitates Large-Scale Substrate Prediction. *Cell Metab*. 2015;22(5):907-921. doi:10.1016/j.cmet.2015.09.009
498. Dasgupta B, Seibel W. Compound C/Dorsomorphin: Its use and misuse as an AMPK inhibitor. In: *Methods in Molecular Biology*. Vol 1732. Humana Press Inc.; 2018:195-202. doi:10.1007/978-1-4939-7598-3_12
499. Valastyan S, Weinberg RA. Tumor metastasis: Molecular insights and evolving paradigms. *Cell*. 2011;147(2):275-292. doi:10.1016/j.cell.2011.09.024
500. Friedl P, Gilmour D. Collective cell migration in morphogenesis, regeneration and cancer. *Nat Rev Mol Cell Biol*. 2009;10(7):445-457. doi:10.1038/nrm2720
501. Wilkinson S, Paterson HF, Marshall CJ. Cdc42-MRCK and Rho-ROCK signalling cooperate in myosin phosphorylation and cell invasion. *Nat Cell Biol*. 2005;7(3):255-261. doi:10.1038/ncb1230
502. Wyckoff JB, Pinner SE, Gschmeissner S, Condeelis JS, Sahai E. ROCK- and Myosin-Dependent Matrix Deformation Enables Protease-Independent Tumor-Cell Invasion In Vivo. *Curr Biol*. 2006;16(15):1515-1523. doi:10.1016/j.cub.2006.05.065

503. Orgazy JL, Herraizy C, Sanz-Moreno V. Rho GTPases modulate malignant transformation of tumor cells. *Small GTPases*. 2014;5(4). doi:10.4161/sgtp.29019

504. Misek SA, Appleton KM, Dexheimer TS, et al. Rho-mediated signaling promotes BRAF inhibitor resistance in de-differentiated melanoma cells. *Oncogene*. 2020;39(7):1466-1483. doi:10.1038/s41388-019-1074-1

505. ALISSA ROUTHIER, MICHELLE ASTUCCIO, DEANNA LAHEY, NICHOLAS MONFREDO AJ, WILLIAM CALLAHAN, AMY PARTINGTON, KELLY FELLOWS, LORI OUELLETTE SZ, CARRIE GOODROW, ALEXIS SMITH, KAITLYN SULLIVAN, PETER SIMONE, LEO LE BV, MICHELINE ZOHNI, ELIZABETH WEST DG and BB. Pharmacological inhibition of Rho-kinase signaling with Y-27632 blocks melanoma tumor growth. *Oncol Rep*. Published online 2010.

506. Ahn J, Sanz-Moreno V, Marshall CJ. The metastasis gene NEDD9 product acts through integrin β3 and Src to promote mesenchymal motility and inhibit amoeboid motility. *J Cell Sci*. 2012;125(7):1814-1826. doi:10.1242/jcs.101444

507. Trotta AP, Gelles JD, Serasinghe MN, Loi P, Arbiser JL, Chipuk JE. Disruption of mitochondrial electron transport chain function potentiates the pro-apoptotic effects of MAPK inhibition. *J Biol Chem*. 2017;292(28):11727-11739. doi:10.1074/jbc.M117.786442

508. Ruocco MR, Avagliano A, Granato G, et al. Metabolic flexibility in melanoma: A potential therapeutic target. *Semin Cancer Biol*. 2019;59. doi:10.1016/j.semcancer.2019.07.016

509. Ratnikov BI, Scott DA, Osterman AL, Smith JW, Ronai ZA. Metabolic rewiring in melanoma. *Oncogene*. 2017;36(2):147-157. doi:10.1038/onc.2016.198

510. Gayard M, Guilluy C, Rousselle A, et al. AMPK Alpha 1-induced RhoA phosphorylation mediates vasoprotective effect of estradiol. *Arterioscler Thromb Vasc Biol*. 2011;31(11):2634-2642. doi:10.1161/ATVBAHA.111.228304

511. Guo W, Wang H, Yang Y, et al. Down-regulated miR-23a contributes to the metastasis of cutaneous melanoma by promoting autophagy. *Theranostics*. 2017;7(8):2231-2249. doi:10.7150/thno.18835

512. Laurenzana A, Chillà A, Luciani C, et al. uPA/uPAR system activation drives a glycolytic phenotype in melanoma cells. *Int J Cancer*. 2017;141(6):1190-1200. doi:10.1002/ijc.30817

513. Coating 6-well or 12-well Plates with Collagen - Protocol Place. Accessed December 2, 2020. https://protocol-place.com/cell-culture/collagen-coating-protocol/

514. Pietrovito L, Comito G, Parri M, Giannoni E, Chiarugi P, Taddei ML. Zoledronic Acid Inhibits the RhoA-mediated Amoeboid Motility of Prostate Cancer Cells. *Curr Cancer Drug Targets*. 2019;19(10):807-816. doi:10.2174/1568009619666190115142858